Evaluation of quinazolin-4-piperidine sulfamides as inhibitors of human NPP1: relevance in the treatment of pathologic mineralization of valve interstitial cells

Mémoire

Elnur Elyar Shayhidin

Maîtrise en médecine moléculaire
Maîtrise ès sciences (M.Sc.)

Québec, Canada

© Elnur Elyar Shayhidin, 2016

Résumé

Le rétrécissement valvulaire aortique calcifié (RAC) est le trouble valvulaire le plus fréquent chez les personnes âgées des pays développés. La seule option de traitement possible le remplacement de la valve aortique. L'identification du rôle de l'enzyme ecto-nucleotidase NPP1 dans le processus de calcification suggère que cette enzyme pourrait être une cible potentielle pour le développement d'un inhibiteur pharmacologique contre la calcification de la valve aortique. Jusqu'à présent, les composés qui ont été développés en tant qu'inhibiteurs de NPP1 manquent de puissance et de spécificité. Dans la présente étude, nous avons démontré que les dérivés de sulfonamides quinazolin-4-pipéridine sont des inhibiteurs puissants, spécifiques, et non-compétitifs de NPP1. *In vitro*, dans des cellules isolées de valve aortique nous avons fourni des preuves que l'inhibition de NPP1 par ces dérivés bloque la minéralisation, l'apoptose et la transition ostéogénique des cellules interstitielles de valve aortique.

Abstract

Calcific aortic valve disease (CAVD) is the most common valvular disorder in the elderly population in the developed counties with the only valid treatment option today remains the aortic valve repair or replacement. The identification of the role of an ectonucleotidase enzyme NPP1 in the process of calcification shed new light into the development of a pharmacological inhibitor that may prevent the calcification of the aortic valve. By far, the compounds that have been developed as inhibitors of NPP1 lack potency and specificity. In the current study, we showed that the quinazolin-4-piperidin sulfamide derivatives to be a potent, specific, and non-competitive inhibitors of NPP1. We also provided evidence that by inhibiting NPP1 enzyme activity these derivatives are able to prevent phosphate-induced mineralization of valve interstitial cells (VICs), the main cellular component of the aortic valve, by preventing both apoptosis and osteoblastic transitions of VICs.

Table of contents

Résumé iii
Abstract v
List of tables ix
List of figures xi
Abbreviations xiii
Acknowledgements xv
Avant-Propos xvii
Chapter 1 Introduction 1
  Section 1 1
    1.1 Calcific Aortic Valve Disease (CAVD) 1
    1.2 Epidemiology 2
    1.3 Clinical evaluations 3
    1.4 Risk factors 4
  Section 2 5
    2.1 Structure of the heart and heart valves 5
    2.2 Architecture of the heart valves 6
  Section 3 9
    3.1 Molecular mechanism of CAVD 9
  Section 4 14
    3.1 Ectonucleotidsas enzymes 14
    3.2 Mechanisms of NPP1 in CAVD 20
    3.3 Inhibitors 24
  Section 5 28
    4.1 Hypothesis 28
    4.2 Objectives 28
Chapter 2 29
Quinazolin-4-piperidine sulfamides are specific inhibitors of human NPP1 and prevent pathologic mineralization of valve interstitial cells 29
Supplementary information 71
  General information 71
  Synthetic schemes 72
    Scheme 1. Synthesis of QPS1[a] 72
    Scheme 2. Synthesis of QPS2[a] 73
  Materials and methods 74
    Synthetic route for QPS1 74
    Synthetic route for QPS2 77
  NMR spectra of all the new compounds 83
Chapter 3 Conclusions and discussions 101
  3.1 Potency, specificity, and non-competitivity of QPS 1 101
  3.2 Implications 102
Chapter 4 limitations and future perspectives 105
  4.1 Impact on purinergic receptors 105

- 4.2 Interaction with hERG channel 105
- 4.3 Pharmacokinetics 106

Chapter 5 References 107

Appendix Enzyme Inhibitor Kinetics 113
- Types of inhibitors 113
  - *1) Competitive inhibitor* 113
  - *2) Non-competitive inhibitor* 113
  - *3) Uncompetitive inhibitor* 114
- Dixon plot 114

List of tables

Table 1. Guidelines for grading severity of CAVD. 4

List of figures

Figure 1. Severely calcified aortic valve. 2
Figure 2. Anatomy o the heart. 6
Figure 3. Cellular architecture of the aortic valve. 8
Figure 4. Domain structure of NPPs. 15
Figure 5. The role of the ectonucleotidase and purinergic signalling in calcific aortic valve disease (CAVD). 22
Figure 6. Schematic representation of the role of the cAMP/PKA signalling pathway on the NPP1-positive feedback regulation during mineralization.. 24
Figure 7. Chemical structure of ARL 67156 (6-N,N-Diethyl-D-β,γ-dibromomethylene adenosine triphosphate). 26

Abbreviations

ALP	Alkaline phosphatase
ApoE	Apolipoprotein E
BMP2	Bone morphogenic protein 2
CAVD	Calcific aortic valve disease
cAMP	Cyclic adenosine monophosphate
Cbfa1	Core-binding factor subunit alpha 1
CREB	cAMP response element-binding protein
CPPD	Calcium pyrophosphate dehydrate crystals
CT	Computed tomography
EnMT	Endothelial-mesenchymal transition
GAGs	Glycosaminoglycans
HACs	Hydroxyapatite crystals
hERG	human 'ether-a-go-go' channel
IIAC	Idiopathic infantile arterial calcification
IL-6	Interleukin-6
LDL	Low-density lipoprotein
Lp(a)	Lipoprotein a
Lp-PLA2	Lipoprotein-associated phospholipase A2
LPA	Lysophosphatidic acid
LPC	Lysophosphatidylcholine
Lrp5	Low-density lipoprotein receptor-related protein 5
Lyso-PLD	Lysophospholipase D
MMP	Matrix metalloprotease
NFκB	Nuclear factor-κB
NO	Nitric oxide
NPP	Ectonucleotide pyrophosphate/phosphodiesterase
NTPDase	Ectonucleoside triphosphate diphosphohydrolase
NT5E	5'-ectonucleotidase
OPLL	Ossification of the posterior longitudinal ligament
Ox-LDL	Oxidized low-density lipoprotein

PI3K	Phosphatidylinositol 3 kinase
Pi	Inorganic phosphate
PPi	Inorganic pyrophosphate
Pit1	TypeIII sodium-dependent Pi cotransporter
PKA	Phosphokinase A
QPS	Quinazolin-4-piperidin sulfamide
ROS	Reactive oxygen species
Runx2	Runt-related transcription factor 2
TNF	Tumor necrosis factor
VECs	Valve endothelial cells
VICs	Valve interstitial cells

Acknowledgements

I would like to thank Dr. Patrick Mathieu for giving me the opportunity to be part of his research team and Dr. Philippe Pibarot for supporting my study. Their guidance and advices helped me along the way of my entire mastery study. I also want to acknowledge Dominique Fournier and Marie-Chloé Boulanger for training and providing me with necessary laboratory techniques. Their patients and kindness supported me to achieve my objectives during this part of my life. I also want to thank all of the team members: Rihab Bouchareb, Ablajan Mahmut, Fayes Hadiji, Mohammed Nsaibia, Diala El Husseini, and Marie-Hélène Laflamme. Their support and advice made me a person, who can think critically about science.

I want to thank Dr. Patrick Lagüe, Dr. Jean Sévigny, Dr. Jean-François Paquin, and their team, especially Elsa Forcellini, Sébastien Dautrey, and Xavier Barbeau. They provided me with chemical, biochemical, computational biology, and bio-informatics knowledge and contributed significantly to our project.

I want to specially thank my husband Ablajan Mahmut and my baby girl Emily Shayhidin Abulajiang. They made my life easier with their love and kisses when I had to struggle with language difficulties in a place far away from home.

I want to thank my parents, Elyar Shayhidin and Qimangul Wushur, and my parent in-laws, Mahmut Tohti and Amina Mahmut, for their love and support even from a long distance. I also want to thank my grandparents, my brother and sister-in-law, my aunts and uncles, my cousins and nieces.

Avant-Propos

The present "mémoire" shows the results of a newly developed pharmacological compound in inhibiting ectonucleotidase pyrophosphate/phosphodiesterase-1 (NPP1) acitivity and its ability to inhibit mineralization in *in vitro* experiments. There are four chapters in this "mémoire". The first chapter provides an introduction to calcific aortic valve disease (CAVD), epidemiology, clinical evaluations, risk factors, molecular mechanisms, ectonucleotidase enzymes, association of NPP1 in CAVD and NPP1 inhibitors. This chapter summarizes currently knowledge about CAVD and provides hypothesis and objectives of the study. The second chapter is the scientific manuscript of the results of the current study. The manuscript was recently accepted and published in British Journal of Pharmacology (2015 Aug; 172(16):4189-99. License number: 3690930724944). In addition, the results of this study were presented at local scientific meetings and at national congress, Canadian Cardiovascular Congress that was held in Vancouver, BC, Canada on October 26th, 2014. They were also presented at the American Heart Association annual scientific session that was held in Chicago, Illinois, USA on November 16th, 2014. Chapter three provides a general conclusion and discussion to the study and chapter four brings the limitations and future perspectives.

The manuscript was written by Dr. Patrick Mathieu and Elnur Elyar Shayhidin with contributions of eight co-authors. The experimental design was conceived by Dr. Patrick Mathieu. The *in vitro* experiments on enzyme kinetics and in cell culture were performed by Elnur Elyar Shayhidin, Marie-Chloé Boulanger, and Ablajan Mahmut. Data analysis was performed by Elnur Elyar Shayhidin. Elsa Forcellini and Sébastien Dautrey synthesized compounds used in this study and Dr. Jean-François Paquin supervised the synthesis of the chemical compounds. Xavier Barbeau, Dr. Patrick Lagüe, and Dr. Jean Sévigny critically reviewed data. All authors critically reviewed the manuscript.

Dr. Patrick Mathieu has patent application for the use of the ectonucleotidase inhibitors and purinergic agonists in the treatment of CAVD.

Chapter 1 Introduction

Section 1

1.1 Calcific Aortic Valve Disease (CAVD)

Affecting 25% of the elderly population aged over 65 years old, calcific aortic valve disease (CAVD) is becoming the most common valvular heart disease in the developed world [1]. It is characterized by progressive mineral deposition at the aortic face of the aortic valve leading to rigidity of the valve leaflets and finally obstructed valve opening that requires surgical intervention. The progression of CAVD is generally divided into two categories: aortic valve sclerosis and aortic valve stenosis. Aortic valve sclerosis is termed by the first detectable calcification of the leaflet [2]. At this stage, valve leaflet is thickened but the hemodynamic functions remain normal. Histological examinations often reveal thickened subendothelial layer, lipid and calcium accumulation and infiltration of inflammatory cells including foam cell macrophages, non-foam cell macrophages and T lymphocytes [3]. The end stage, aortic stenosis is, however, characterized by the obstructed left ventricular outflow due to pathologically larger calcium nodules at the valve surface and impaired valve compliance (Figure 1). Histological examination of the later stage reveals bone morphogenic proteins 2 and 4.

Owing to limited therapeutic options beyond surgical repair and replacement of aortic valves and increased longevity as the result of medical advances, the health care burden continues to increase, from 2.5 million in 2000 [4]. In 2011, the National Heart, Lung, and Blood Institute gathered a group of scientists working on CAVD to review all available articles published on CAVD and redefined the calcifying process of the aortic valve, long thought as a “degenerative” event accumulated over the years by wear-and-tear mechanism, is actually an active and regulated disease process involving cellular mechanisms and signalling pathways that definitely required in depth attention [2]. This has shed light on many molecular biologists to think beyond the mechanical fatigue into more of the cellular regulations that has led to the calcifying process and opened window into identifying possible pathways that can be eventually targeted pharmacologically.

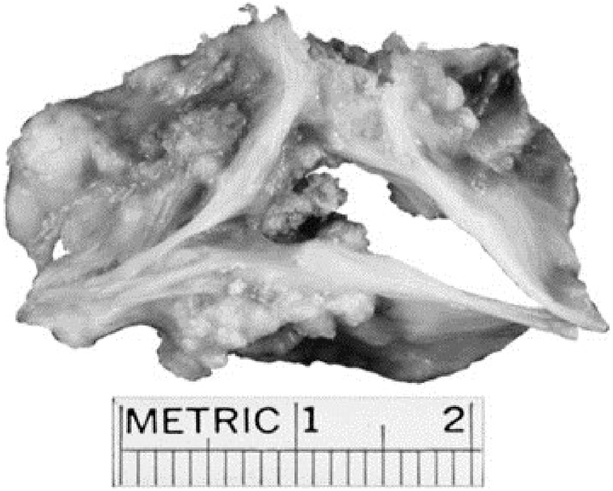

Figure 1. Severely calcified aortic valve. Excised tricuspid aortic valve showing severe nodular calcification and stenosis. License: 3683700554570.

1.2 Epidemiology

1) Aortic sclerosis

Aortic sclerosis is thought to be the initial stage of CAVD where hemodynamic property of the valve is intact even there are detectable phenotypic deteriorations of the valve. Sclerosis is quite common and present in about 25% of people aged over 65 [5]. The prevalence of it increases to almost 50% in elderly over 84 years old. Except that it is defined by echocardiography where the thickening of the valve is observed with normal leaflet mobility, there is no other clinical symptoms present in the patients. The transvalvular jet velocity across the valve is < 2.5m/s which represents a normal valve function (Table 1). Although asymptomatic, aortic sclerosis is largely associated with increased risk of myocardial infarction and cardiovascular deaths.

2) Aortic stenosis

Aortic stenosis is viewed as the advanced state of CAVD where large, extensive valvular calcification can be observed using echocardiography. At this stage, valve leaflets are stiffened and thus the transvalvular jet velocity across the valve increases to > 2.5m/s due to limited opening of the cusps following cardiac cycle. Between two and four percent of the aging population over 65 years old are diagnosed with calcific aortic stenosis. There is no clear boundary between sclerosis and stenosis expect that current medical protocol sets the cut-off point of hemodynamic ejection velocity of 2.5m/s (Table 1) [5].

3) Progression of sclerosis to stenosis

Even it is viewed that sclerosis is the early stage of CAVD whereas stenosis is the late stage, it is not clear that if sclerosis progresses to stenosis. There are very few studies investigating the hemodynamic progression of aortic sclerosis to calcific aortic stenosis. In a large study which included >2000 sclerotic patients, 16% of them developed stenosis in an average time interval of 8 years. Even though the portion is relatively small, it is quite apparent that the portion would increase if the years of follow-up prolonged [6]. Hence, there is a need for close follow-up studies in a long time period after diagnosing patients with aortic sclerosis.

1.3 Clinical evaluations

The principle and the most common method of diagnosing a patient with calcific aortic valve disease is measuring the magnitude of the systolic transvalvular pressure gradient, which is proportional to the aortic jet velocity measured by Doppler echocardiography. By principle (Table 1), aortic jet velocity $\leq$ 2.5m/s with thickening of the leaflets is defined as sclerosis, whereas the jet velocity $\geq$ 2.5m/s is diagnosed as stenosis. The severity of the stenosis is then evaluated by setting different cut-off points for the jet velocity. Echocardiography can not only distinguish sclerosis and stenosis with good precision, but can also evaluate the severity of stenosis based on the hemodynamic range given by Table 1. However, it is not a good method of choice to quantify anatomical calcium deposition due its low spatial resolution which makes it difficult to define boarders of calcium [1]. Cardiac computed tomography (CT) on the other hand can well overcome this limitation of the echocardiography and can not only identify the presence but also quantify calcium with high precision. Cardiac catheterization can also measure the transvalvular gradient but it is less frequently used, only in the cases of patients with non-diagnostic echocardiography or when clinical data is inconsistent with echocardiographic readings [5]. Coronary angiography is usually performed prior to surgery to assess whether or not a concurrent coronary artery bypass is needed.

Table 1. Guidelines for grading severity of CAVD. License: 3683690847992.

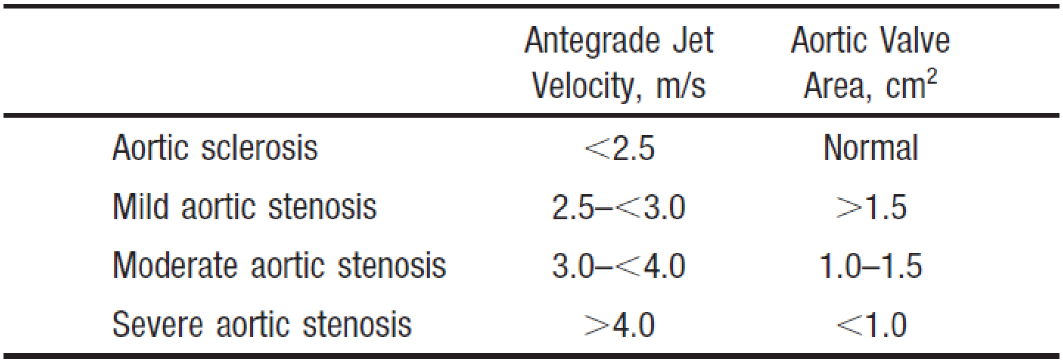

	Antegrade Jet Velocity, m/s	Aortic Valve Area, cm^2
Aortic sclerosis	<2.5	Normal
Mild aortic stenosis	$2.5–<3.0$	>1.5
Moderate aortic stenosis	$3.0–<4.0$	1.0–1.5
Severe aortic stenosis	>4.0	<1.0

1.4 Risk factors

Epidemiology studies have proposed many risk factors of CAVD that are commonly shared clinical risk factors with the vascular calcification such as age, male gender, smoking, diabetes mellitus, hypertension, and dyslipidemia [7]. Metabolic syndrome had also been shown to be associated with a faster progression to CAVD. Besides, genetic predispositions may also explain the cause of CAVD. In this regard, congenitally bicuspid aortic valve with presence in 1-2% of the population develop CAVD decades earlier than tricuspid valve [8]. Also a recent finding of a gene variant of *LPA* encoding for lipoprotein a (Lp(a)) results in elevated circulation Lp(a) level and is significantly associated with CAVD [9]. Despite the factors that are shared with atherosclerosis, many patients present only with either CAVD or atherosclerosis [5, 10]. This suggests that there may exist undetermined factors that contribute to the onset and progression of CAVD apart from those of atherosclerosis.

Section 2

2.1 Structure of the heart and heart valves

The normal heart of a human consists of four chambers: two atria and two ventricles (Figure 2). They are separated by four leaflets that allow unidirectional flow of blood. The locations and functions of the four heart valves are:

1) ***Tricuspid valve***

   Tricuspid valve, often referred to right atrioventricular valve, is located between the right atrium and the right ventricle. Deoxygenated blood fills back into the heart via the inferior and superior vena cava and collects into the right atrium and makes its way to the right ventricle though the tricuspid valve. It closes to prevent blood from regressing back into right atrium when the blood pumps out of the heart into the lungs to be re-oxygenated.

2) ***Pulmonary valve***

   The pulmonary valve is located between the right ventricle and the pulmonary artery. It opens when the pressure in the right ventricle increases during ventricular systole and pushes blood out into the pulmonary arteries and to the lungs to get it re-oxygenated.

3) ***Mitral valve***

   Oxygenated blood from lungs flows back into the heart through the mitral valve. It is located between the left atrium and the left ventricle. It opens during left ventricle expansion (diastole) and closes as it contracts (systole).

4) ***Aortic valve***

   Aortic valve is one of the tricuspid valves in the heart that is located between the left ventricle and the aorta. During systole, the heart contracts and pushes oxygenated blood out into aorta and to the whole body circulation through aortic valve. In most cases, the aortic valve is trileaflet where in some rare congenital conditions it is a bicuspid. The 2% of the people that has born with bicuspid aortic valves develop aortic stenosis decades earlier than those with tricuspid valves.

The valves open and shut in coordinates to respond to the contraction and relaxation of the heart muscles and complete the cardiac cycle.

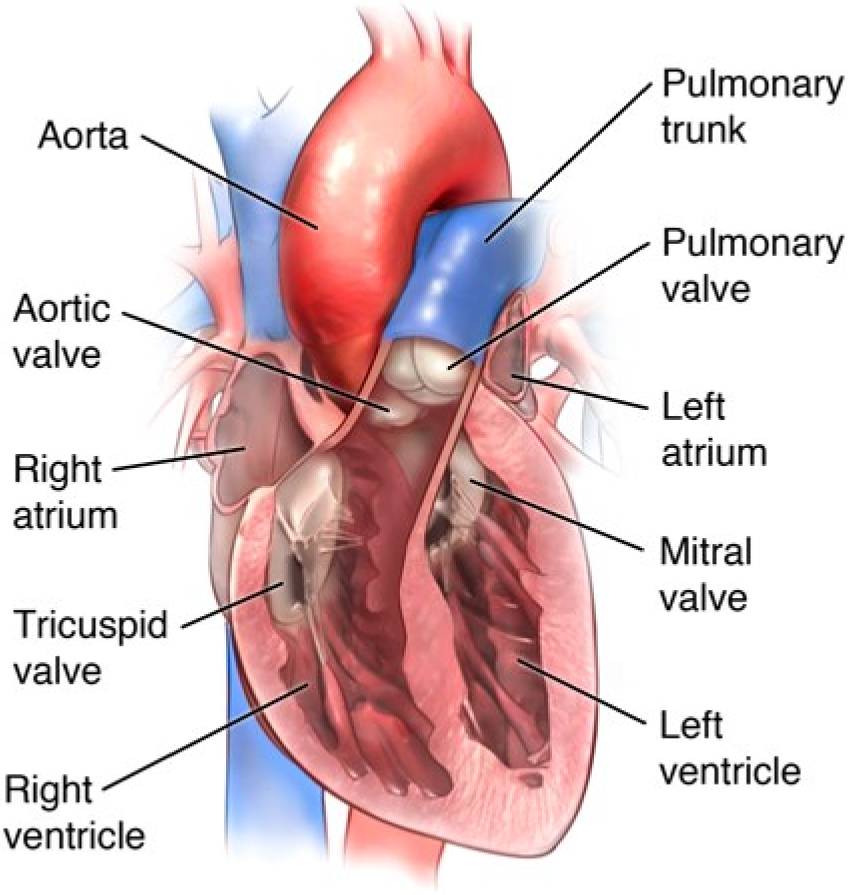
Aorta
Pulmonary trunk
Pulmonary valve
Aortic valve
Left atrium
Right atrium
Mitral valve
Tricuspid valve
Left ventricle
Right ventricle

Figure 2. Anatomy of the heart. Source: http://m.hopkinsmedicine.org/healthlibrary/conditions/cardiovascular_diseases/anatomy_and_function_of_the_heart_valves_90,P03059/.

2.2 Architecture of the heart valves

The normal functional aortic valve connects the left ventricle to the aorta, through which the unidirectional, unobstructed ejection of the cardiac output is permitted and feeds the entire body with nutrients and oxygen. The cardiac valves open and shut > 3 billion times for decades throughout a person's lifetime, hence, the architecture of the valve must accomplish the second-to-second movements required by the vigorous cardiac cycle.

All four valves share similar architectural layers of cells and extracellular matrix (Figure 3). Monolayered valve endothelial cells (VECs) line the surface of the valve and separate the valve interstitium from the circulation [11]. Like their roles elsewhere in the vasculature, VECs regulate the homeostasis of the valves by regulating leaflet permeability and by initiating and controlling inflammation. There is evidence showing that VECs can also, through paracrine signaling, regulate the contractility of the valve interstitial cells (VICs) by releasing endothelial NO [12, 13]. They also have ability to undergo endothelial-mesenchymal transition (EnMT) by losing some of the common endothelial markers and instead gaining contractile properties [14, 15].

Sandwiched in between the VECs are the three layers of matrix and cells. The layer closest to the aorta side is fibrosa which contains fibroblasts and collagen laying in a circumferential orientation and providing strength to the valve. On the opposite side, closest to the left ventricle is the ventricularis. This layer is filled with elastin-rich fibers arranged in a radial direction to allow for maximum opening of the valves. In between fibrosa and ventricularis is the spongiosa. It is a loose connective tissue layer rich in glycosaminoglycans (GAGs) and resides fibroblasts and mesenchymal stem cells.

VICs are filled in all three layers of the valve where they synthesize valvular extracellular matrix, constantly regulate matrix turnover by expressing matrix metalloproteases (MMPs) and their inhibitors. VICs are activated during embryogenesis and in the fetal heart corresponding to the developmental progress, whereas in adult heart, they are relatively quiescent. However, they can be re-activated and can differentiate into many cell lines including myofibroblasts and osteoblasts in a diseased state by increasing expressions of smooth muscle cell and osteoblastic markers.

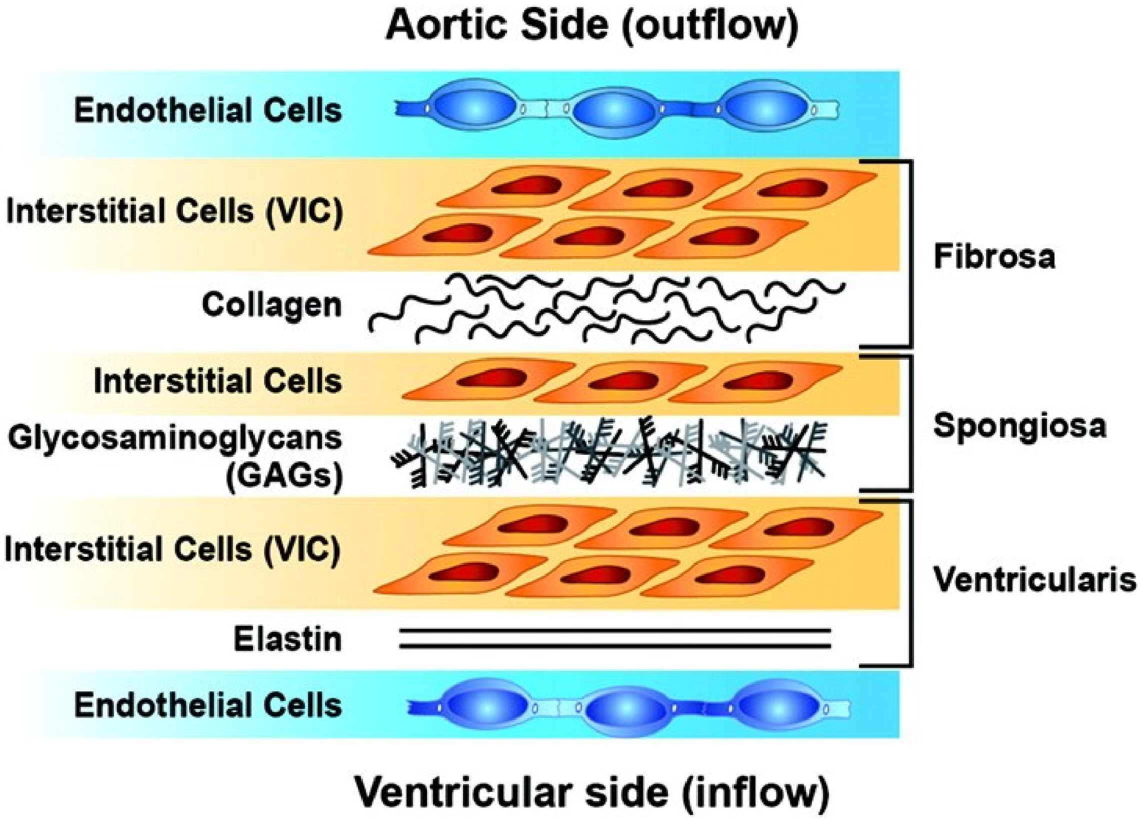
Aortic Side (outflow)
Endothelial Cells
Interstitial Cells (VIC)
Collagen
Fibrosa
Interstitial Cells
Glycosaminoglycans (GAGs)
Spongiosa
Interstitial Cells (VIC)
Ventricularis
Elastin
Endothelial Cells
Ventricular side (inflow)

Figure 3. Cellular architecture of the aortic valve. Demonstration of the cellular architecture of a normal aortic valve**.** The aortic valve leaflets are outlined by monolayers of valve endothelial cells (VECs) which separate the blood circulation from the valve interstitium. Sandwiched in between the VECs are three layers of matrix and cells. The layer closest to aorta side is fibrosa whereas the layer closest to left ventricle is ventricularis. Spongiosa layer is in between the fibrosa and ventricularis. License: 3683701362056.

Section 3

3.1 Molecular mechanism of CAVD

CAVD is a multifactorial disorder. In other words, there are many mechanisms involved at the onset and progression of the disease. These factors work in concert and ultimately lead to the calcification of the aortic valve leaflets.

1) Lipid retention

Histological analysis of explanted CAVD valve leaflets showed a high level of infiltration of oxidized lipids and lipoproteins in the areas of mineralization [16]. Epidemiological studies also emphasizing that low-density lipoprotein (LDL) being a risk factor for the development of CAVD [7]. These findings lead us to think that lowering circulating lipid by statins may have a beneficial effect to prevent the progression of CAVD. As such, retrospective studies showed a significant slower progression rate of aortic stenosis [17-20]. However, in another 3 randomized, well controlled trials including more patients, statins failed to demonstrate beneficial effect on the progression of aortic stenosis. In these trials, statins did not reduce either CAVD-associated events or the number of required aortic valve replacement surgeries compared to placebo [21-23]. Also, in a SEAS study follow-up, statins did not prevent CAVD events even in the patients with mild stenosis suggesting that they shouldn't be used as treatment for CAVD even in the early stages [24].

Considering the lipid species present in the CAVD tissue, why statins failed to show any beneficial effect? There have been some arguments regarding this issue: first, it's said that may be statins were introduced too late where calcification is already irreversible [25]. Second, the molecular target of statins in the aortic valve is unclear [10]. Statins are known for their ability to reduce morbidity and mortality resulting from atherosclerosis-associated cardiovascular events by lowering cholesterol-lipid and enhancing plaque stability through anti-inflammatory effects. However, one pleiotropic effect of statin is to enhance the expression of osteogenic markers that could actually lead to progression of CAVD [26]. Lastly, part of the answers may lie in the specific process of lipid retention in CAVD [25, 26]. In this regard, high proportion of small, dense LDL was documented in patients with metabolic syndrome and was associated with a faster progression to aortic valve stenosis [27]. Of note, small dense LDL particles have greater ability to infiltrate tissue and are prone to oxidation. It has been shown that high amount of oxidized LDLs derived from small, dense LDLs are present in the CAVD tissues and are associated with aortic valve inflammation [28]. Statins do not affect the proportion of small, dense LDL. Recently, it has been shown that lipoprotein-associated phospholipase A2 (Lp-PLA2), the enzyme that converts ox-LDL to lysophosphatidylcholine (LPC), is elevated in CAVD. LPC is also present in the explanted CAVD tissue and it has been shown to promote mineralization through cAMP/PKA pathway in isolated VICs [29].

2) Inflammation

Despite the high level of lipid retention, inflammatory cells also infiltrated explanted CAVD tissues in pathological samples [30]. The density of these cells in the tissue is associated with a faster progression of mineralization process [31]. Also, about 15% of the genes that are differentially regulated in CAVD are related to inflammation [32]. These evidences suggest that inflammation has involvement in both the development and the progression of CAVD. In this regard, the nuclear factor-κB (NFκB) appears to be at the center stage of inflammation. It is regulated by several factors: first, it is suspected that the reactive oxygen species (ROS) that are generated in mineralized aortic valves promote the expression of osteogenic genes by acting through canonical pathway of NFκB in which ROS act as a cofactor in protein kinase A (PKAc)-mediated phosphorylation of p65 [33, 34]. Second, intracellular channeling of extracellular inorganic phosphate generated by ectonucleotidases activities is associated with a lower level of Akt kinase [35]. Akt is a kinase involved in cell survival that negatively regulates NFκB activation and represses interleukin-6 (IL-6) production in VICs [36]. IL-6 expression is one important target of NFκB cascade and it is highly expressed in mineralized aortic valves. Silencing of IL-6 in cell culture model prevented the mineralizing effect of phosphate medium by abrogating the rise of osteogenic gene expressions [36]. Also, antagonist of BMP2 prevented IL-6-induced mineralization. Considering these, IL-6 production induces osteoblastic transition of VICs through a BMP2-dependent pathway. Lastly, TNF family of cytokines are also shown to activate NFκB and promotes mineralization of VIC by activation of the apoptotic pathway [37, 38]. In this regard, the apoptotic bodies promote the nucleation of hydroxyapatite. Taken together, inflammatory responses are involved and play crucial roles in regulating the mineralization process by modulating genes that have osteogenic properties.

3) Osteoblastic transition

One study showed that 36 out of 288 valves with dystrophic calcification had mature lamellar bones with hematopoietic elements and active bone remodelling [39]. This suggests that, at least in subsets of patients with CAVD, complete transition of VICs to osteoblastic phenotype occurred. Studies also demonstrated the up-regulation of osteoblastic markers including osteocalcin, osteopontin, and Runx2 in mineralized human aortic valves [40, 41]. In this regard, BMP2 activated by atherogenic factors and inflammation in CAVD exerts osteogenic signalling in two ways: first, BMP2 activates Runx2/Cbfa1 pathway, which is the master transcription regulator of osteoblasts. Runx2/Cbfa1 is present in human aortic valve lesions and its activation promotes calcification via BMP2-dependent pathway [42, 43]. Second, BMP2 is also shown to be an activator of the transcription factor Msx2 which promotes signaling through Wnt. In this case, Rajamannan et al. suggested the involvement of Wnt/low-density lipoprotein receptor-related protein 5 (Lrp5)/β-catenin pathway in the process of valvular calcification [44].

In addition, new findings in the investigation of osteoblastic transition involved Notch1 signaling. Notch signalling has been demonstrated to play an important role in the embryonic developmental process of many organisms. Proper organisations of tissue and determinations of cell fates were achieved by cell-cell communications through interactions of Notch receptors and their ligands. This interaction results in the release of Notch intracellular domain (NICD) by γ-secretase complex. NICD is then translocated to the nucleus where it regulates many genes expressions [45]. In VICs, translocation of NICD activates expression of Hairy family of repressors that prevents the expression Runx2 and BMP2. Hence, disturbance in Notch signalling resulted in pro-osteogenic response of VICs [25].

4) Phosphate

In a community-based cohort, higher serum level of phosphate was associated with the development of valvular calcification [46]. End-stage renal disease patients have high levels of circulating phosphate and vascular calcification is a common complication in these patients [47]. The calcium nodules present on the valves of CAVD patients are in the form of hydroxyapatite that is formed by calcium and inorganic phosphate (Pi). All these findings suggest that phosphate is a crucial regulator of soft-tissue mineralization.

Calcium and phosphate are readily present in human at almost any tissue, any site. However, the presences of proteins that interfere with the nucleation of calcium-Pi crystals prevent mineralization of soft tissues under normal conditions. For instance, liver secreted fetuin A is an abundant plasma protein that prevents formation of calcium-Pi crystals. A cross-sectional study showed that a low concentration of fetuin A was associated with cardiovascular mortality in patients on dialysis [48]. Matrix Gla protein is another inhibitor of mineralization in the vascular system and aortic valve [49, 50]. It has been shown to prevent the process of mineralization in a vitamin K-dependent manner.

In the aortic valve tissue, phosphate is generated by a class of ectonucleotidase enzymes expressed on the cell membrane at the cost of extracellular nucleotides and nucleosides. It is then transported back into the cells by a type III sodium-dependent Pi cotrasnporter (Pit1) which was found to be overexpressed in stenotic aortic valves [35]. *In vitro*, phosphate induced the mineralization of VICs by increasing the expression of Pit1 and the inhibition of this transporter prevented phosphate-induced mineralization. In this study, entering of phosphate into the VICs caused a loss of mitochondrial membrane potential which ultimately lead to activation of caspase-3 and thus induced apoptosis-mediated mineralization.

Section 4

4.1 Ectonucleotidsas enzymes

Ecto-enzymes are a collection of catalytic membrane enzymes that respond to wide variety of hormones and cytokines in mediating many cellular functions. By general concepts, ecto-enzymes are large glycoproteins with a short intracellular amino-terminal, a single transmembrane domain that is transiently adenylated and/or phosphorylated during catalytic cycle, and a large extracellular carboxy-terminal which usually contains the catalytic domain [51]. They are commonly involved in the control of cell growth, differentiation and movements, and also in the modulation of adjacent cell activities. There are many classes of enzymes that are grouped into ecto-enzymes and ectonucleotidases are just one of those. The ectonucleotidases includes four families of genes that modulate extracellular nucleotides and nucleosides and by doing so, regulate the levels and ratio of extracellular inorganic phosphate (Pi) and pyrophosphate (PPi) [52]. The four families of ectonucleotidase enzymes include: ectonucleotide pyrophosphate/phosphodiesterases (NPPs), ectonucleoside triphosphate diphosphohydolases (NTPDases), 5'-ectonucleotidase (NT5E), and alkaline phosphatase (ALP).

4.1.1 Ectonucleotide pyrophosphate/phosphodiesterases (NPPs)

There are seven structurally related members in the family of ectonucleotide pyrophosphate/phosphodiesterases (NPPs) (Figure 4) [53]. They are found as membrane proteins that are either type I or type II, but are also found as secreted or shedded enzymes. NPP1-3 are relatively well understood and less is known about the roles of NPP4-7.

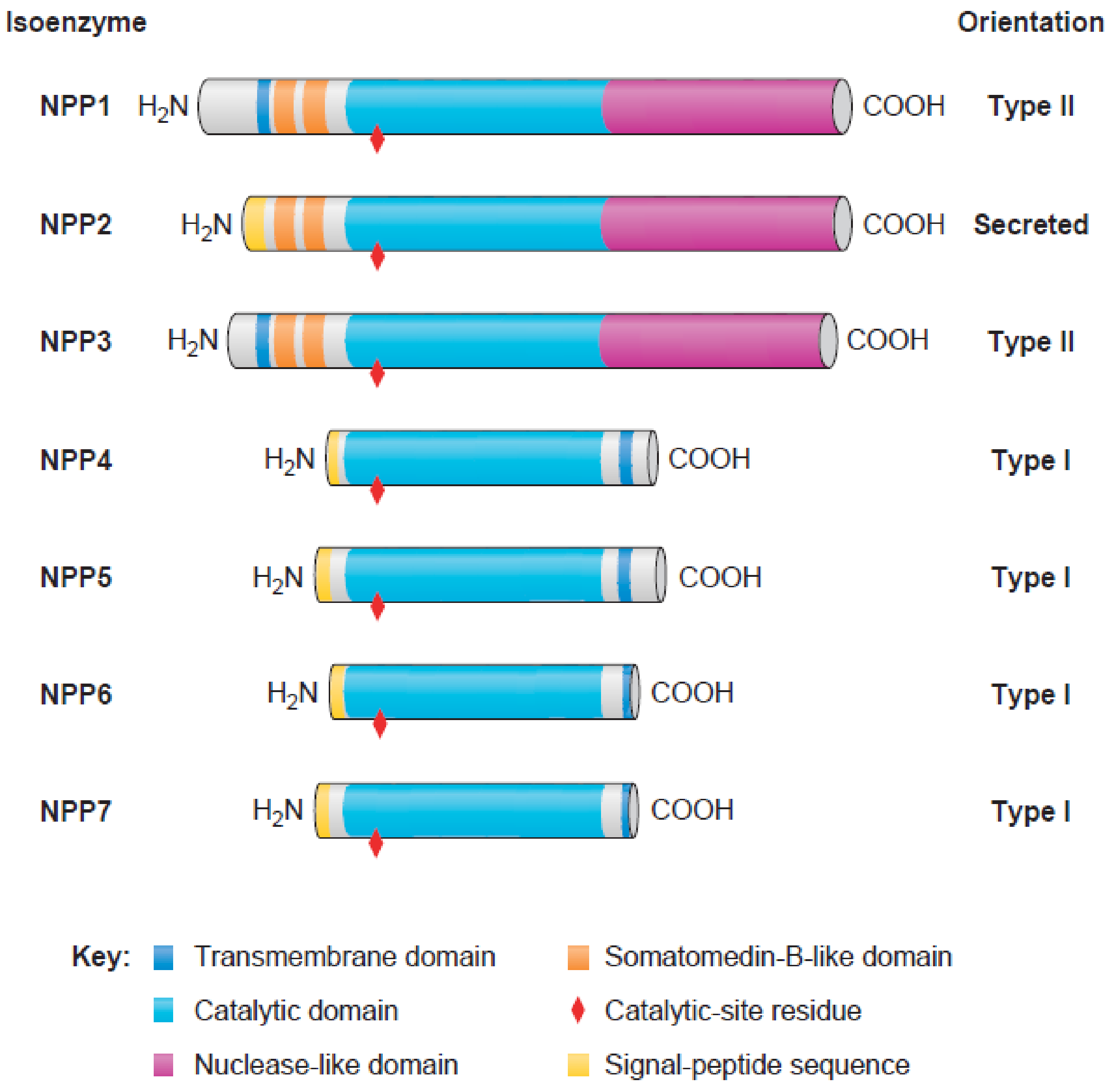
Isoenzyme
Orientation
NPP1
H_2N
COOH
Type II
NPP2
H_2N
COOH
Secreted
NPP3
H_2N
COOH
Type II
NPP4
H_2N
COOH
Type I
NPP5
H_2N
COOH
Type I
NPP6
H_2N
COOH
Type I
NPP7
H_2N
COOH
Type I
Key:
Transmembrane domain
Somatomedin-B-like domain
Catalytic domain
Catalytic-site residue
Nuclease-like domain
Signal-peptide sequence

Figure 4. Domain structure of NPPs. The seven NPP-type ectophosphodiesterases have a structurally related catalytic domain. Catalysis occurs via a covalent catalytic intermediate with a conserved threonine residue (serine for NPP6) in the catalytic site. NPP1 and NPP3 contain an N-terminal transmembrane domain and have a type-II orientation. The N-terminal hydrophobic sequence of NPP2 and NPP4–7 is a signal peptide, rather than a transmembrane domain, that mediates uptake in the endoplasmic reticulum during translation. This sequence is removed co-translationally by the signal peptidase, and, therefore, is not part of the mature polypeptides. In contrast to NPP2, which enters the secretory pathway, NPP4–7 contain a C-terminal transmembrane domain that retains them at the plasma membrane with a type-I orientation. Thus, except for NPP2, all NPPs are membrane-bound ecto-enzymes. NPP1–3 contain two N-terminal somatomedin-B like domains and a C-terminal nuclease-like domain, but the exact function of these domains is not yet known. The structures are drawn to scale. License: 3683710165950.

1) NPP1

The main function of the NPP1 is to hydrolyze the phosphodiester and/or pyrophosphate bonds of extracellular nucleotides to generate extracellular pyrophosphate (PPi) and/or inorganic phosphate (Pi), and by doing so, it liberates anti-mineralizing or pro-mineralizing effects of extracellular matrix. Mineralization process often begins with the formation and transportation of matrix vesicles that contains hydroxyapatite crystals (HACs) to the plasma membrane where they grow further by incorporating more and more Pi that are readily available at the extracellular milieu. It is noted that Pi is a pro-mineralization agent and PPi, on the contrary, inhibits mineralization by binding to nascent HACs and prevent Pi from incorporating into these crystals [53].

Owing to its ability to generate PPi, NPP1 was viewed as an anti-calcifying enzyme for a long period of time. In support of this view, a *ttw* (tiptoe walking) mouse which is caused by a nonsense point mutation in NPP1 suffered from extensive calcification in the peri-articular tissues and ligaments that lead to joint fusion [54]. Murine fibroblasts transfected with *ENPP1* recombinant adenovirus to overexpress NPP1 protein showed 80-90% less HAC deposition compared to cells transfected with empty vector or inactivated *ENPP1* [55]. In human, *ENPP1* mutation is shown to be associated with not only the susceptibility, but also the severity of the ossification of the posterior longitudinal ligament (OPLL) [56]. Analysis of idiopathic infantile arterial calcification (IIAC) from 11 unrelated kindreds also showed association to inactive mutant of *ENPP1* [57]. Similar results were also reported that loss of function mutation of *ENPP1* causes general arterial calcification of infancy in another two independent studies [58, 59].

On the other hand, however, overexpressing NPP1 does not necessarily attenuate the calcifying process. Instead, it has been reported to promote mineralization in many ectopic calcifying diseases. Two groups independently reported in 2001 that NPP1 expression was robust at sites of apoptotic cells and is associated with increased matrix vesicles in degenerative arthritis [60, 61]. It implicated that the increased NPP1 is both a marker and a potential pathogenic factor for knee meniscal cartilage matrix calcification. NPP1 also promoted vascular calcification in ApoE knockout mice [62]. Cote N, et.al and Mahmut A, et.al reported an increased NPP1 expression and activity in the human calcified aortic valves explanted from patients undergoing replacement surgeries [63, 64].

Hence, these findings together suggest a U-shaped effect of NPP1 in the process of calcification. In other word, it suggests that a certain amount of PPi production is necessary to prevent ectopic calcification which requires a tightly controlled amount and activity of NPP1 present. Too much or too little would ultimately lead to undesired mineral production and deposition.

2) NPP2

NPP2, also known as autotaxin, is a special member in the NPP family of enzymes. Despite the structural similarities shared with other members of the family, it has very weak phosphodiesterase/pyrophosphatase activity. Instead, it is best characterized by its lysophospholipase D (lyso PLD) activity by which it catalyzes lysophospholipids into lysophosphatidic acid (LPA). LPA binds to specific G protein-coupled receptors (at least LPA_{1-6} [65]) to elicit different signaling pathways leading to cell survival, proliferation, contraction, migration, and motility [53, 65]. It is secreted by a large variety of cell lines and exerts effects through autocrine and paracrine manner to many targets. For example, NPP2 was first discovered a tumor-motility stimulating factor in melanoma cells [53]. It has now established roles in many other cancer cell lines, both in the initiation and the progression. Its major property has been implicated in the metastasis of cancer cells by enhancing migratory of cancer cells and forming new vascular structures [65-67]. NPP2, by generating LPA, is implicated in the liver fibrosis [68]. In brief, LPA promotes fibrotic response of liver satellite cells by inhibiting apoptosis, stimulating proliferation and contraction of these cells. It also has many other implications during embryonic development in terms of neuronal development, vascular formation, and regulation of left-right symmetry

[69]. More recently, autotaxin derived from lipoprotein(a) (Lp(a)) and valve interstitial cells has been documented to promote inflammation and mineralization of the aortic valve through a NFκB/IL-6/BMP pathway [70].

3) NPP3

NPP3 possesses a similar structural architecture and enzymatic activity as NPP1. It is a transmembrane enzyme which hydrolyzes ectonucleotides and nucleosides. It has been shown to be present in bone, prostate and uterus. The most prominent function of it would be in the allergic reactions [71, 72]. NPP3 is the commonly defined marker of basophils and mast cells and it is not present in other blood cells.

4.1.2 Ecto-nucleoside triphosphate diphosphohydrolase (NTPDs)

The ecto-nucleoside triphosphate diphosphohydrolase (NTPDases) are a family of ectoenzymes that primarily hydrolyze extracellular nucleosides. There are eight *ENTPD* genes encode for eight NTPDases1-8 [73]. Among them, NTPDase1-3 and 8 are typical membrane enzymes with their active sites facing the extracellular milieu. NTPDase5 and 6 are cytosolic proteins and NTPDase4 and 7 are on the membranes of intracellular organelles and facing their lumen. All membrane-located NTPDases require Ca^{2+} or Mg^{2+} for their activity [74]. These enzymes play important roles in controlling vascular function, thrombosis and inflammation. To this effect, a knockdown of NTPDase1 in mice exhibited vasodilation induced by nucleotides suggesting that it contributes to the local regulation of vascular tone by nucleotides [75]. Of note, NTPDase1 is the major ectonucleotidase expressed on the vascular endothelium. Furthermore, NTPDase1 and 2 also exert control over platelet function. For instance, NTPDase1 preferentially hydrolyze ADP and by deleting extracellular ADP it abrogates platelet activation. On the other hand, NTPDase2 has a preference in hydrolyzing ATP to generate and supply ADP to promote aggregation of platelets [76].

4.1.3 5’-ectonucleotidase (NT5E)

To date, there have been seven human 5’-nucleotidases isolated and characterized [77]. Among them, five are located in the cytosol, one in the mitochondrial matrix and one on the plasma membrane. The nucleotidases located in the intracellular region are mainly involved in salvage pathways and/or nucleotide de novo synthesis [78]. The intracellular nucleotidases dephosphorylate 5’-ribonucleoside monophosphates (5’NMPs) with low affinity having Km > 10^{-3} M. The membrane-located 5’-ectonucleotidase (NT5E) hydrolyzes 5’AMP with a high efficiency (Km = 3-50 μM) and generates adenosine. Thus, NT5E exerts control over purinergic receptors by modulating the level of extracellular adenosine. NT5E has been shown to be expressed in a variety of tissues, with most abundant expressions in the colon, kidney, brain, liver, heart and lung [77]. Recently, it has been shown to be expressed by aortic valve interstitial cells (VICs), and together with NPP1 it promotes mineralization of VICs in cell culture model [63, 79].

4.1.4 Alkaline phosphatase (ALP)

Alkaline phosphatase (ALP) is a ubiquitous enzyme showing expressions in many organisms from bacteria to human [77]. There are three isozymes that are tissue specific and one that is abundantly expressed in bones, liver, kidney, and many other tissues. ALP displays a wide spectrum of substrates specificity ranging from phosphomonoesters to other phosphate compounds. In bones, ALP contributes to ensure a proper bone mineralization by hydrolyzing PPi and maintain an optimal concentration of this mineralization inhibitor [80]. ALP activity is also implicated in the calcification process of isolated VICs in cell culture [81]. In this regard, a missense mutation in the human ALP leads to human disorder, hypophosphatasia, which is characterized by poorly mineralized cartilage (rickets) and bones (osteomalacia) [82, 83]. The ALP-deficient mice models were also characterized by marked bone and cartilage abnormalities that phenotypically mimicked the infantile hypophosphatasia [84, 85].

4.2 Mechanisms of NPP1 in CAVD

It has been documented that the expression level of NPP1 in terms of both mRNA and proteins was overexpressed in explanted CAVD valves [63, 79]. The phosphodiesterase activity of NPP1 by which inorganic phosphates are generated was also significantly elevated when compared to normal valve. It was only recently that the mechanism of NPP1 in inducing mineralization was elucidated.

First, overexpression of NPP1 in the aortic valve promotes production and accumulation of extracellular inorganic phosphate (Figure. 5) [63]. In this regard, although less appreciated, NPP1 also possesses a phosphatase activity by which ATP is converted to ADP with a release of phosphate. ADP can in turn be used by NPP1 to further hydrolysis to generate AMP and phosphate. Experiment using recombinant NPP1 with incubation along with ATP showed that phosphate is generated about 2 times more than pyrophosphate [52]. On the other hand, ALP is often expressed in the aortic valves where it further hydrolyzes the pyrophosphate to phosphate and together with NPP1 it contributes to the build-up of extracellular phosphates. In this scheme of things, extracellular Pi is then channeled back into the cells via Pit1 sodium-phosphate cotransporter. Intracellular channeling of Pi has been shown to have several pro-mineralization effects. First, it increases the expression NPP1 in a vicious cycle to expand the extracellular phosphate pool [35]. Second, it also contributes to increase the expression of phosphate transporter and calcium channel, Pit1 and annexin V, respectively and thus promote intracellular formation of hydroxyapatite crystals by allowing both phosphate and calcium to enter the cells [86]. Furthermore, increased phosphate also promotes expression of some osteogenic genes including osteopontin [86]. Taken together, NPP1 overexpression induces mineralization by increasing the level of inorganic phosphates.

Second, elevated expression of NPP1 also depletes extracellular ATP and in turn, reduces survival signalling through P2Y2 receptors (Figure. 5) [25, 36, 63]. Cells express wide range of purinergic receptors and there are a total of 19 genes encoding for these receptors and they are adenosine-sensitive (P1) or ATP, ADP-sensitive (P2).

P2 receptors can be further classified as ion channel receptors (P2X) and G protein-coupled receptors (P2Y). These receptors along with different ectonucleotidases regulate many cellular events. A dysregulation in any member of this network would result in modified cellular signaling and responses. In VICs, ATPs signal through P2Y2 receptor to deliver survival signal by activating phosphatidylinositol 3-kinase/Akt (PI3K/Akt) pathway [36, 63]. However, when NPP1 is overexpressed, ATP is depleted from the extracellular milieu and thus reduced signaling through P2Y2 receptor. Reduced PI3K/Akt activation as a result of decreased P2Y2 receptor signaling induces apoptosis-mediated mineralization through activation of caspase 3. Reduced PI3K/Akt also leads to production of IL-6 which is a pro-mineralizing agent through BMP2-dependent pathway.

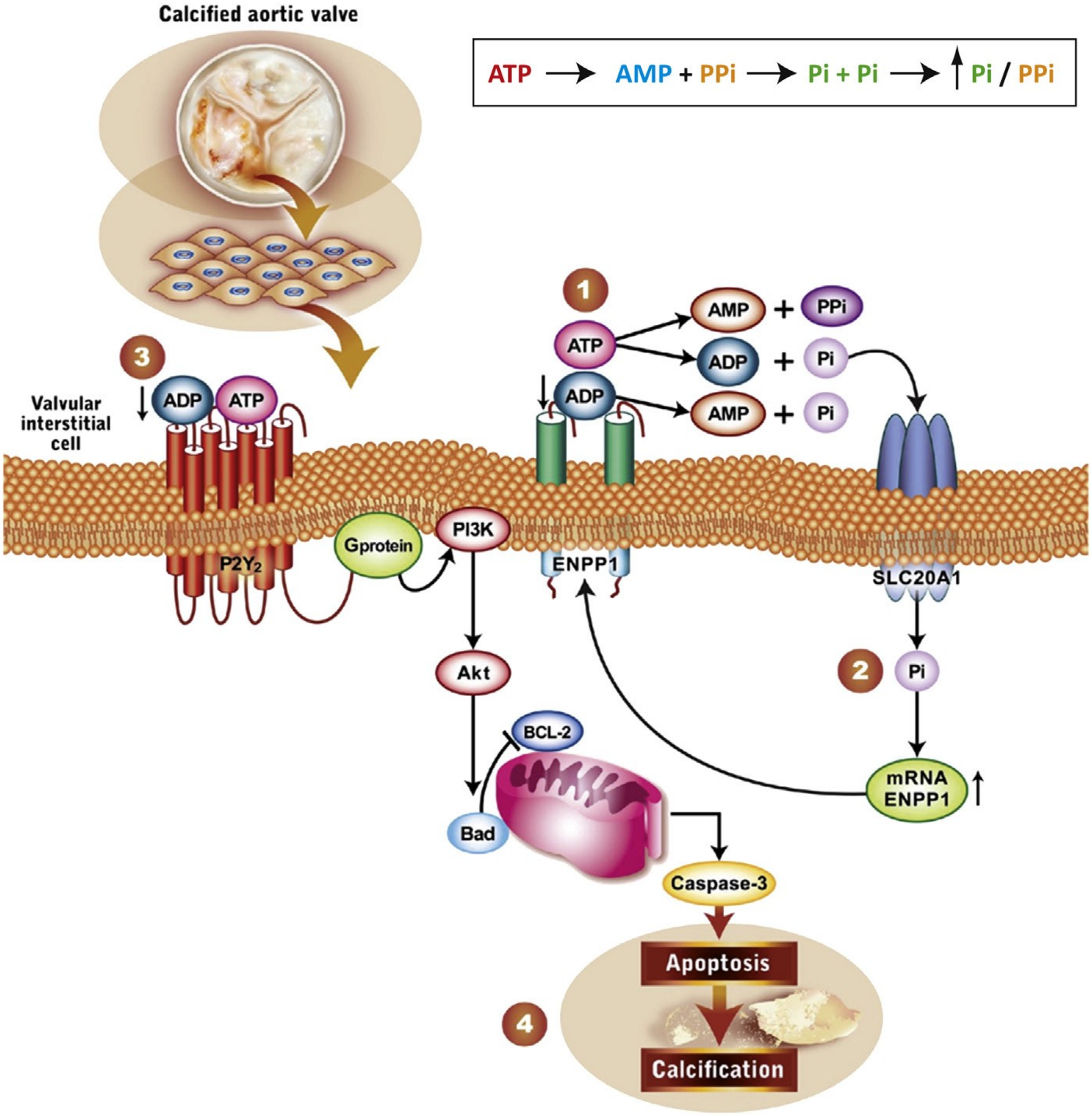
Calcified aortic valve
ATP → AMP + PPi → Pi + Pi → ↑ Pi / PPi
1
ATP
AMP
PPi
ADP
Pi
ADP
AMP
Pi
3
ADP
ATP
Valvular interstitial cell
P2Y2
Gprotein
PI3K
ENPP1
SLC20A1
Akt
2
Pi
BCL-2
mRNA ENPP1
Bad
Caspase-3
Apoptosis
4
Calcification

Figure 5. The role of the ectonucleotidase and purinergic signalling in calcific aortic valve disease (CAVD). Nucleotides are secreted by VICs and hydrolyzed by ENPP1 and alkaline phosphatase (ALP), which increases the level of phosphate (Pi) (1). Pi enters cells through the Pi transporter Pit1/SLC20A1, which increases the expression of ENPP1 in a positive feedback loop (2). A high level of ectonucleotidases in CAVD contributes to deplete the extracellular levels of nucleotides (3). In turn, decreased signalling through the P2Y2 receptor decreases Akt and promotes apoptosis-mediated mineralization (4). License: 3683710686942

Lastly, 5'-ectonucleotidase is found to be overexpressed and co-localized with NPP1 in the CAVD tissue to hydrolyze AMP and generate phosphate and adenosine

(Figure. 6) [25, 79]. Adenosine acts through A2a receptor to promote mineralization of VICs via cAMP/PKA-dependent pathway. There are four P1 adenosine receptors: A1 and A3 that are coupled to Gαi and exert an inhibitory effect in terms of cAMP level whereas A2a and A2b receptors are coupled to Gαs that stimulates cAMP production. In VICs, adenosine derived from ectonucleotidases acts on A2a receptor and lead to activation of PKA by increasing cAMP production. Activated PKA then phosphorylates cAMP response element-binding protein (CREB) and allow its binding to *ENPP1* promoter that leads to a further expression of NPP1.

Considering all these evidence, NPP1 seems to be at the central stage in inducing and promoting mineralization of the aortic valve.

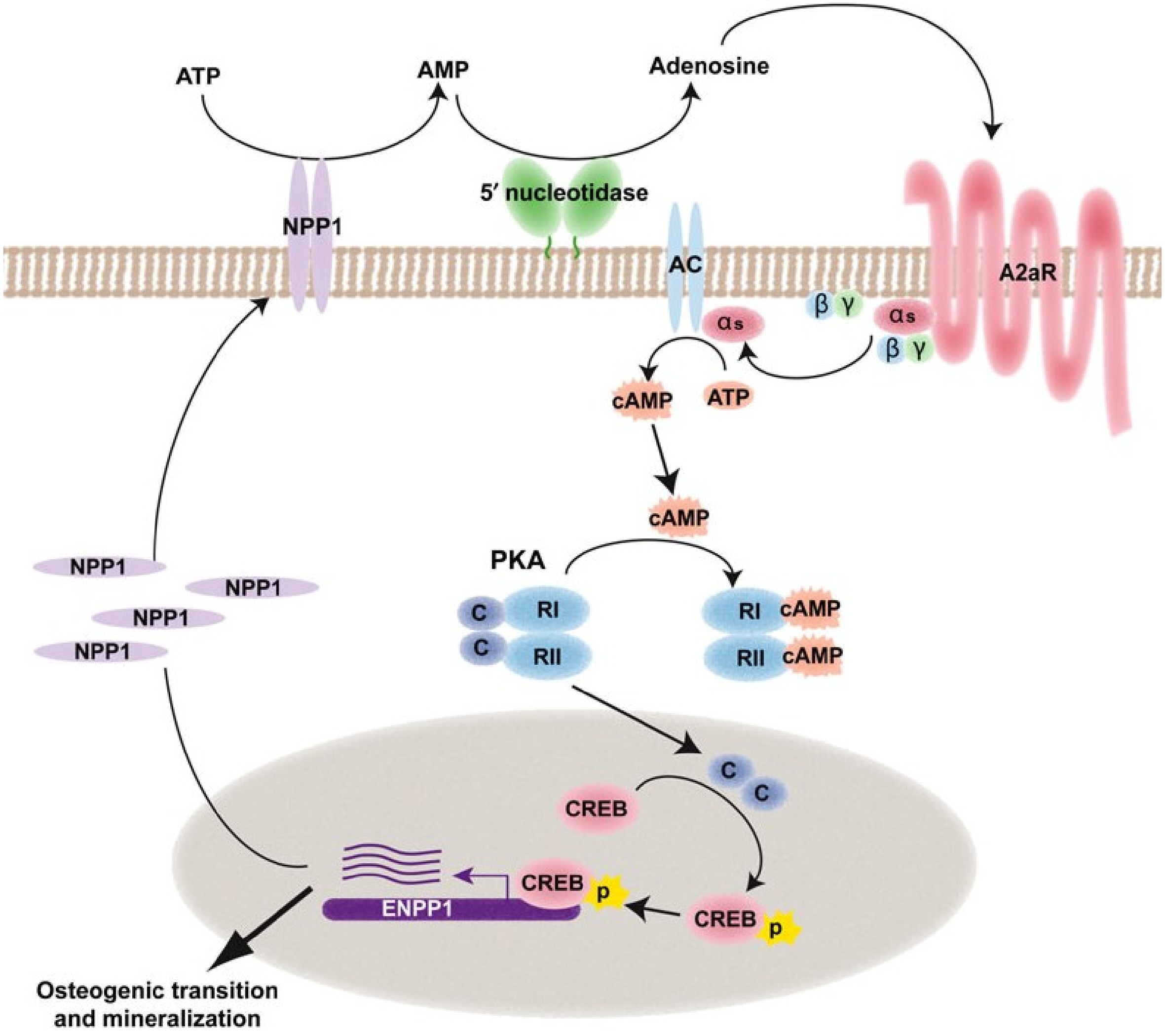
ATP
AMP
Adenosine
5′ nucleotidase
NPP1
AC
A2aR
αs
β γ
αs
β γ
cAMP
ATP
cAMP
PKA
C
RI
C
RII
RI cAMP
RII cAMP
NPP1
NPP1
NPP1
NPP1
C
C
CREB
CREB
p
ENPP1
CREB
p
Osteogenic transition
and mineralization

Figure 6. Schematic representation of the role of the cAMP/PKA signalling pathway on the NPP1-positive feedback regulation during mineralization. Coupling of NPP1 and 5'-nucleotidase promotes the production of adenosine. Adenosine is then acts on A2aR which is coupled with Gas and activates cAMP/PKA/CREB pathway that results in the physical binding of CREB to NPP1 promoter and positively regulates its function in a positive feedback loop. License: 3683710863271

4.3 Inhibitors

There are many natural or synthesized compounds that have been proposed in the aim of inhibiting NPP1. However, none of these made its way to the treatment of human disease due to the fact that these compounds either lack the potency or the specificity making that these drugs have to be either administered in large quantities or there is large off-target effects associated with them.

1) ARL 67156 (6-N,N-Diethyl-D-β,γ-dibromomethylene ATP)

6-N,N-Diethyl-D-β,γ-dibromomethylene adenosine triphosphate (ARL 67156) is a nucleotide analogue produced by AstraZeneca (Loughborough, UK) in the need to develop specific tools to study nucleotide receptors and their functions without interference of cell surface ectonucleotidases (Figure 7 [87]). It is the only commercially available ectonucleotidase inhibitor and was first described by Crack et al. (1995) as an inhibitor of ecto-ATPases in blood cells [88]. Decades following its first discovery, several members of the ecto-nucleotidase family of enzymes had been identified, cloned and characterized. Among these, are four NTPDases (1-3 and 8) and two NPPs (1 and 3).

It has been shown that ARL 67156 inhibits NPP1, but also significantly inhibits NTPDase 1 and 3 [89]. To a lesser extent, it also inhibits NPP3, NTPDase 2 and 8. Cote et al. (2012) has demonstrated that subcutaneously administrated ARL 67156 prevented development of CAVD in warfarin-treated rats [87]. However, the same group described that ARL 67156 was poorly absorbed by the digestive tract and must be administrated alternatively when using in animal models [52].

The non-specificity of ARL 67156 makes it difficult to develop into pharmacological treatment in the fact that it may produce larger off-target effects than benefits. For instance, inhibiting NTPDase1 may worsen inflammation as it is the enzyme that is largely associated with inflammation [75].

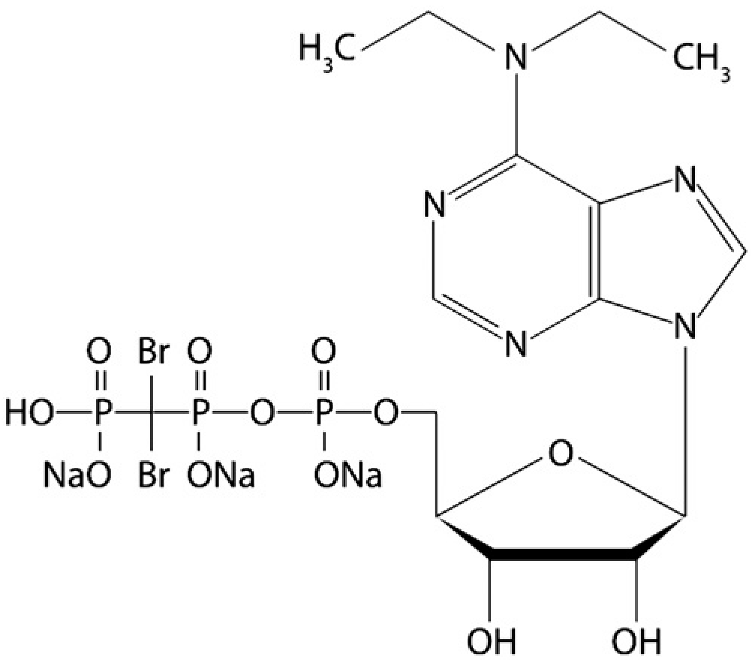

Figure 7. Chemical structure of ARL 67156 (6-N,N-Diethyl-D-β,γ-dibromomethylene adenosine triphosphate). License: 3683711082370.

2) Derivatives of the 1,3,4-oxadiazole-2(3H)-thione

1,3,4-oxadiazole-2(3H)-thione derivatives have been reported to have many biological activities including anti-inflammatory, anti-bactericidal, and anti-fungicidal [90-92]. Some of them have also been shown to be inhibitors of ATP-dependent membrane protein, P-glycoprotein [93]. Recently, Khan et al. (2009) have reported that 1,3,4-oxadiazole-2(3H)-thione and its analogues to be non-competitive inhibitors of NPP1 [94]. However, the potency of these inhibitors was relatively low having Ki value around 360 μM for human recombinant NPP1 enzymes.

3) QPS derivatives

Quinazolin-4-piperidin sulfamide (QPS) compounds were described by Patel et al. (2009) as potent inhibitors of NPP1 [95]. Among the different compounds in this category, their lead compound had been shown to be the most potent derivative with a Ki value of 36 nM. Unfortunately, it is also a potent ligand for the human ‘ether-a-go-go’ (hERG) channel, measuring 601 nM in the tritiated dofetilide binding assay. hERG channel is important in regulating cardiac rhythm. Therefore, compounds that have high affinity to this channel may result in undesired QT interval prolongation and, in some cases, this prolonged QT interval may cause drug-induced ventricular fibrillation and even sudden death. Despite the predicted side-effect that it may cause, the biological effects of these derivatives in cellular model were not assessed. In addition, the specificity and the mode of inhibition of these derivatives, which are the major concerns in drug design, were not determined.

Section 5

5.1 Hypothesis

Calcific aortic valve disease (CAVD) is the most common valvular disorder in the developed world. Despite numerous studies trying to develop alternative treatments to prevent and/or slow the progression of the mineralization of the aortic valve leaflets, surgical replacement and/or repair still remains the only existing treatment. In the large time window from the initial detection of early lesions to obstructions of left ventricular output, patients suffer from gradually decreased quality of life. Molecular biology studies recently identified the elevated presence and activity of ectonucleotide pyrophosphate/phosphodiesterase-1 (NPP1) in aortic valves explanted from CAVD patients. The mechanisms of NPP1 in promoting mineralization of isolated VICs makes it a viable target for pharmacology. The existing inhibitors for NPP1 either lack the potency or the specificity.

In this current study, we hypothesized that derivatives of quinazolin-4-piperidin sulfamide (QPS) are a class of specific and non-competitive inhibitors of NPP1. We also hypothesized that by inhibiting NPP1 enzyme activity, QPS derivatives can inhibit phosphate-induced mineralization of human valve interstitial cells (VICs) in cell culture model.

5.2 Objectives

To study the pharmacological natures of QPS derivatives, our objectives are: to document the efficacies of two QPS compounds, QPS1 and 2; to determine the mode of inhibitions of these drugs; and also to evaluate the specificity of QPS1. To study the biological effect of these derivatives in cell culture models, the objectives are: to evaluate the ability of QPS1 to prevent phosphate-induced mineralization of human primary VICs; also to evaluate the ability of this compound to prevent apoptosis and osteoblastic transitions of VICs.

Chapter 2

Quinazolin-4-piperidine sulfamides are specific inhibitors of human NPP1 and prevent pathologic mineralization of valve interstitial cells

Objectif: Dans la présente série d'expériences, nous avons évalué l'efficacité de deux dérivés, QPS1 -2, pour inhiber la NPP1 humaine, dont le plus puissant (QPS1) a été évalué sur d'autres ectonucléotidases, ainsi que son aptitude à empêcher l'induction de la minéralisation par le phosphate des cellules interstitielles des valves (VICs). **Background:** L'ectonucléotide pyrophosphatase / phosphodiestérase 1 (NPP1) est une ectoenzyme, qui joue un rôle dans plusieurs maladies, dont celle de la valve aortique calcifiée (CAVD). Jusqu'à présent, les composés qui ont été développés en tant qu'inhibiteurs de NPP1 manque de puissance et de spécificité. Les dérivés Quinazolin-4- pipéridin sulfamide (QPS) ont été décrits comme des inhibiteurs puissants de NPP1. Toutefois, leur mode d'inhibition, ainsi que leur sélectivité et la capacité de modifier les processus biologiques n'ont pas été étudiés. **Méthodes:** Nous avons étudié l'activité et la sélectivité des dérivés QPS dans l'inhibition de NPP1 par l'activité enzymatique. L'effet biologique des dérivés QPS a été documenté sur la minéralisation des cultures de cellules interstitielles de valve, la mesure du niveau d'apoptose, ainsi que l'expression des gènes ostéoblastiques par q-PCR. **Résultats:** Nous avons démontré que le dérivé QPS1 est un inhibiteur puissant (Ki 70.2 ± 6.2 nM), sélectif et non compétitif de la NPP1 humaine. En outre, le dérivé QPS1 inhibe également de manière significative la variante du gène NPP1 K121Q (Ki 73.4 ± 14.7 nM), qui est très répandue dans la population. QPS1 n'a pas modifié de façon significative l'activité d'autres enzymes exprimés à la surface cellulaire métabolisant les nucléotides, à savoir, NPP3, NTPDases (1-3), ecto -5'-nucléotidase et ALP. À de faible concentration (≤ 10 uM) QPS1 a empêché la minéralisation et l'apoptose des VICs induite par le phosphate et a réduit la hausse des gènes ostéogéniques. **Conclusion:** Par conséquent, QPS1 est un inhibiteur non compétitif puissant et sélectif de NPP1 qui empêche la minéralisation pathologique dans un modèle cellulaire.

Quinazolin-4-piperidine sulfamides are specific inhibitors of human NPP1 and prevent pathologic mineralization of valve interstitial cells

Elnur Elyar Shayhidin, HBSc[1*]; Elsa Forcellini, MSc[2*]; Marie-Chloé Boulanger, PhD[1]; Ablajan Mahmut, MD, MSc[1]; Sébastien Dautrey, PhD[2]; Xavier Barbeau, MSc[3]; Patrick Lagüe, PhD[3]; Jean Sévigny, PhD[4,5]; Jean-François Paquin, PhD[2]; Patrick Mathieu, MD[1]

[1] Laboratoire d'Études Moléculaires des Valvulopathies (LEMV), Groupe de Recherche en Valvulopathies (GRV), Quebec Heart and Lung Institute/Research Center, Department of Surgery, Université Laval, Quebec, Canada

[2] Canada Research Chair in Organic and Medicinal Chemistry, PROTEO, Department of Chemistry, Université Laval, Canada

[3] Department of Biochemistry, PROTEO, Laval University, Canada

[4] Department of Microbiology, Infectious Diseases and Immunology, Université Laval, Québec, QC, Canada.

[5] Centre de recherche du CHU de Québec, Québec, QC, Canada.

* Both authors contributed equally to this work

Address for correspondence:

Dr. Patrick Mathieu,
Institut de Cardiologie et de Pneumologie de Québec/Quebec Heart and Lung Institute, 2725 Chemin Ste-Foy, Québec, QC, Canada, G1V-4G5 Phone number: 418-656-4717
Fax number: 418-656-4707
E-mail address: patrick.mathieu@chg.ulaval.ca

Running head: Quinazolin derivatives as inhibitors of NPP1

Keywords: NPP1, ENPP1, inhibitor, ectonucleotidase, PC-1, valve interstitial cells, calcific aortic valve disease, aortic stenosis, ectopic mineralization

Competing interests: P. Mathieu has patent applications for the use of ectonucleotidase inhibitors and purinergic agonists in the treatment of CAVD.

Abstract

Background and purpose: Ectonucleotide pyrophosphatase/phosphodiesterase 1 (NPP1) is an ectoenzyme, which plays a role in several disorders including calcific aortic valve disease (CAVD). So far, compounds that have been developed as inhibitors of NPP1 lack potency and specificity. Quinazolin-4-piperidine sulfamides (QPS) have been described as potent inhibitors of NPP1. However, their mode of inhibition as well as their selectivity and capacity to modify biological processes have not been investigated. **Experimental approach:** In the present series of experiments, we have evaluated the efficacy of two derivatives, QPS1-2, in inhibiting human NPP1, and we have evaluated the effect of the most potent derivative (QPS1) on other ectonucleotidases as well as on the ability of this compound to prevent phosphate-induced mineralization of human primary aortic valve interstitial cells (VICs). **Key results:** We documented that QPS1 derivative is a potent (K_i 59.3±5.4 nM) and selective non-competitive inhibitor of human NPP1. Moreover, QPS1 also significantly inhibited the K121Q NPP1 gene variant (K_i 59.2±14.5 nM), which is prevalent in the general population. QPS1 did not significantly alter the activity of other nucleotide metabolizing ectoenzymes expressed at the cell surface, namely NPP3, NTPDases (1-3), ecto-5’-nucleotidase and ALP. Importantly, QPS1 in the low micromolar range (≤10 μM) prevented phosphate-induced mineralization of VICs and lowered the rise of osteogenic genes as expected for NPP1 inhibition. **Conclusions and implications:** Hence, we provide evidence that QPS1 is a potent and selective non-competitive inhibitor of NPP1 and that it prevents pathologic mineralization in a cellular model.

Keywords and Abbreviations

Keywords: NPP1, ENPP1, inhibitor, ectonucleotidase, PC-1, valve interstitial cells, calcific aortic valve disease, aortic stenosis, ectopic mineralization

Abbreviations:

CAVD: Calcific aortic valve disease

VICs: valve interstitial cells

NPP1/PC-1: ectonucleotide pyrophosphatase/phosphodiesterase-1

ALP/TNAP: alkaline phosphatase

NTPDases: ectonucleotide triphosphate diphosphohydrolases

NT5E/CD73: ecto-5’-nucleotidase

QPS: Quinazolin-4-piperidine sulfamides

Introduction

Studies have documented that ectonucleotide pyrophosphatase/PDE-1 (NPP1/PC-1) is involved in different disorders including diabetes, osteoarthritis and atherosclerosis (Goding *et al.*, 2003). We recently found that NPP1 promotes the mineralization of the aortic valve and that it is highly expressed during the development of calcific aortic valve disease (CAVD) (Cote *et al.*, 2012b). It is worth emphasizing that NPP1 is an enzyme that hydrolyses nucleotides such as ATP and produces AMP and pyrophosphate (PPi), the latter being a potent inhibitor of ectopic mineralization. On one hand, knockout mice for NPP1 show ectopic mineralization of tendons (Okawa *et al.*, 1998). On the other hand, when NPP1 is overexpressed it promotes pathologic mineralization of chondrocytes and valve interstitial cells (VICs) of the aortic valve (Johnson *et al.*, 2001a), (Cote *et al.*, 2012a). The mechanism by which NPP1 promotes pathologic mineralization is twofold. First, pathologic mineralization is often accompanied by the expression of alkaline phosphatase (ALP), which uses PPi to produce the pro-mineralizing phosphate (Pi) (Towler, 2005). Hence, a high level of NPP1 and ALP will promote a build-up of Pi, which triggers calcification of soft tissues. Second, a high level of NPP1 contributes to the depletion of the extracellular level of ATP, which reduces purinergic signalling. In turn, a decreased purinergic signalling triggers apoptosis-mediated mineralization.

The ectonucleotidase family of enzymes encompasses the ectonucleoside triphosphate diphosphohydrolases (NTPDases), which catalyze the conversion of ATP into ADP and also ADP into AMP. Ecto-5'-nucleotidase (NT5E/CD73) promotes the conversion of AMP into adenosine, whereas alkaline phosphatase (ALP/TNAP) uses a wide variety of substrates (Goding, 2000). So far, the compounds that have been used to probe the role of different ectonucleotidases lack specificity and potency. For instance, ARL67156 (6-*N, N*-Diethyl-D-β, γ-dibromomethylene ATP trisodium salt) inhibits NPP1 but also significantly affects other ectonucleotidases (Levesque *et al.*, 2007). Quinazolin-4-piperidine sulfamides (QPS) have been described as potent inhibitors of NPP1 (Patel *et al.*, 2009). However, it is presently unknown whether these compounds are specific and have biological activities in cell culture models. Furthermore, the mode of inhibition has not been described. In this work, we have evaluated QPS compounds as inhibitors of NPP1 and also determined whether it impacts on NPP3, NTPDase1-3, NT5E and ALP. Furthermore, we evaluated the capacity of QPS1 to inhibit *in vitro* phosphate-induced mineralization of human primary VICs.

Materials and methods

Chemicals and reagents

Dulbecco's Modified Eagle's Medium (DMEM) and fetal bovine serum (FBS) were purchased from Invitrogen (Grand Island, NY, USA). Quinazolin-4-piperidine sulfamides (QPS1 and QPS2) were synthesized (see supporting information for details). Para-nitrophenyl thymidine 5'-monophosphate (pnp-TMP), adenosine 5'-monophosphate sodium salt (AMP), adenosine 5'-triphosphate sodium salt hydrate (ATP), and phosphatase substrate were purchased from Sigma Aldrich (Oakville, ON, Canada).

Cell transfection with vectors

Cos-7 cells were seeded in 10 cm cell culture dishes. At 80-90% confluence, cells were transected with 10 µg of NPP1, NPP3, NTPDase1-3, CD73, ALP human cDNA. ENPP1 ORF clone incorporated into the vector pCMV6-AC-GFP was purchased from Origene (Rockville, MD, USA). Vectors for NPP3, NTPDase1, 2, 3, CD73 and ALP were described previously (Jin-Hua *et al.*, 1997) (Kaczmarek *et al.*, 1996; Chiang & Knowles, 2008; Smith & Kirley, 1998; Lecka *et al.*, 2010). The transfection was done using NanoJuice transfection reagent from Novagen (Darmstadt, Germany). After 24 hours, cells were harvested for enzymatic activities.

For the preparation of protein extracts, transfected cells were washed three times with Tris-saline buffer at 4 °C, collected by scraping in the harvesting buffer containing 95 mM NaCl, 0.1 mM phenylmethylsulphonyl floride (PMSF), 45 mM Tris at pH 7.5 and 10 µg/ml aprotinin and sonicated. Nucleus and cellular debris were discarded by centrifugation at 300 g for 10 min at 4 °C and the supernatant was collected and stored at -80 °C until used for the activity assays. Protein concentration was estimated by the Bradford microplate assay using bovine serum albumin (BSA) as a standard.

Enzymatic assays

NPPs

Evaluation of the effect of QPS1 or QPS2 on human NPP1, NPP1 K121Q and NPP3 activity was carried out with para-nitrophenyl thymidine 5'-monophosphate (pnp-TMP). The reactions were carried out at 37 °C in 0.2 ml of the following incubation mixture, 1 mM $CaCl_2$, 140 mM NaCl, 5 mM KCl and 50 mM Tris, pH 8.5, with or without QPS1 or QPS2 (50, 100, 500 and 1000 nM). Reaction was initiated by adding human NPP1, NPP1 K121Q or NPP3 cell extracts to the pre-incubated reaction mixture containing pnp-TMP (25, 50, 100 and 200 μM). The production of paranitrophenol was measured at 410 nm, 60 min after the initiation of the reaction. Results were normalized for protein content. The type of inhibition was determined by competition assay and the level of inhibition was reported as percent inhibition. K_i was calculated by plotting the data of independent experiments using Sigma Plot 12.3 (Systat Software Inc., CA, USA). Results were presented using Dixon plots.

NTPDases

Activity was measured in 96-well plate in 0.2 ml of incubation medium (5 mM $CaCl_2$ and 80 mM Tris, pH 7.4) at 37 °C with or without QPS1 (50, 100, 500 and 1000 nM). The reaction was initiated by adding NTPDase protein extracts to the pre-incubated reaction mixture containing 100 μM ATP (Sigma Aldrich, Oakville, ON, Canada) and stopped after 15 min with 50 μl of malachite green reagent. The released inorganic phosphate (Pi) was measured at 630 nm (Baykov *et al.*, 1988). Results were normalized to protein contents and reported as percent changes.

NT5E

Activity was measured at 37 °C for 15 min in 0.2 ml of incubation solution (5 mM $CaCl_2$ and 80 mM Tris, pH 7.4) containing AMP (25, 50, 100 and 200 μM) with or without QPS1 (50, 100, 500 and 1000 nM). Reaction was started by the addition of NT5E cell extracts and stopped with 50 μl malachite green reagent after 15 min. Released inorganic phosphate was measured as described above for NTPDases. Results were normalized to protein contents and reported as percent changes.

ALP

Activity was assayed using p-nitrophenyl phosphate as a substrate (PNPP) (Sigma, Oakville, ON, Canada). Samples were incubated in the presence of substrate for 30 min at 37 °C. The alkaline phosphatase activity was then measured by absorbance reading at 410 nm. The assay was carried out in triplicates. Results were normalized to protein contents and reported as percent changes.

Valve interstitial cells isolation and in vitro analyses of calcification

Human VICs were isolated from non-mineralized aortic leaflets, by collagenase digestion. Cells were isolated from non-calcified aortic valves obtained during heart transplant procedures. Patients with a history of rheumatic disease, endocarditis, and inflammatory diseases were excluded. Aortic valves with sclerosis/stenosis or moderate to severe regurgitation (grade >2) were excluded. The protocol was approved by the local ethical committee and informed consent was obtained from the subjects. To promote calcification, cells were incubated for 7 days with a pro-calcifying medium containing: DMEM + 5% FBS, 10^{-7} M insulin, 50 µg/ml ascorbic acid and NaH_2PO_4 at 2 mM. In some experiments, QPS1 (0.1-10 µM) (dissolved in DMSO) was added as specified. The calcium content was determined by the Arsenazo III method (Synermed, Monterey Park, CA, USA), which relies on the specific reaction of Arsenazo III with calcium to produce a blue complex. The results were measured at 650 nm on the Roche Diagnostics Modular P800 Elecsys (Roche Diagnostics, Laval, QC, Canada). This reaction is specific to calcium. Magnesium is prevented from forming a complex with the reactive. The results were normalized for protein contents and reported as percent changes.

Alizarin red staining

To visualize the calcium formation, cells were stained with 2% Alizarin red solution. Alizarin red solution was prepared by dissolving 2 g of Alizarin red (Sigma, Oakville, ON, Canada) in 100 ml distilled water, well mixed, and pH was adjusted to 4.1-4.3 with 0.1% NH_4OH. The solution was filtered before use. Human VICs were incubated for 7 days with pro-calcifying media as stated above to promote calcification. The medium was changed every 2 days. After 7 days, cells were washed once with PBS and fixed with 4% formaldehyde (Sigma, Oakville, ON, Canada) for 30 min, and then washed once with distilled water. Filtered 2% alizarin red solution was added to the cells for 2-3 min and washed with distilled water four times.

Detection of apoptosis

Apoptosis was documented in mouse VIC culture by the caspase 3/7 detection reagent (Invitrogen, Toronto, ON, Canada) according to manufacturer's instructions. After treatment with or without QPS1 (0.1-10 μM), cells were labelled with 2 μM CellEventTM caspase-3/7 green detection reagent in complete medium for 30 min at 37 °C, 5% CO_2 in the dark. Cells were fixed in 3.7% formaldehyde for 20 min at room temperature, then treated with 50 mM ammonium chloride for 15 min at room temperature and samples were mounted in DAPI containing mounting media (Sigma, Oakville, ON, Canada). Caspase-3/7 stained cells were counted over total population using an Olympus IX81 inverted microscope.

Quantitative real-time PCR

RNA was extracted from cells during *in vitro* experiments. Total RNA was isolated with RNeasy micro kit from Qiagen (Mississauga, ON, Canada). The RNA extraction protocol was performed according to the manufacturer's instructions. The quality of total RNA was monitored by capillary electrophoresis (Experion, Biorad, Mississauga, ON, Canada). One μg of RNA was reverse transcribed using the Quantitec Reverse Transcription Kit from Qiagen. Quantitative real-time PCR (q-PCR) was performed with Quantitec SYBR Green PCR kit from Qiagen on the Rotor-Gene 6000 system (Corbett Robotics Inc, San Francisco, CA, USA). Primers for runx2, osteopontin, osteocalcin, ALP and COL1A1 were obtained from Qiagen (Mississauga, ON, Canada). Cycling conditions were as follows: 2 min denaturation at 94 °C, and 40 amplification cycles consisting of 15 s at 94 °C and 1 min at 60 °C. The expression of HPRT was used as a reference gene to normalize the results.

ATP measurements

Cells were incubated for 7 days with a pro-calcifying medium containing: DMEM + 5% FBS, 10^{-7} M insulin, 50 mg/ml ascorbic acid and NaH_2PO4 at 2 mM. In some experiments, QPS1 was added as specified. At day 7 the medium was changed for a phenol free medium and ATP level was determined after an incubation of 1 hour. The level of ATP released by cells in supernatants was measured using the ATP SL luminescent kit from BioThema (Cedarlane, ON, Canada) according to manufacturer's instructions.

Statistical analyses

For the comparisons of groups the results were expressed as means ± SEM. For continuous data, values were compared between groups with Student t-test or ANOVA when two or more than two groups were compared, respectively. Post hoc Tukey analyses were done when the p value of the ANOVA was < 0.05. A p value < 0.05 was considered as statistically significant. Statistical analyses were performed with a commercially available software package JMP IN 8.1.

Results

Quinazolin-4-piperidine sulfamides are potent and selective inhibitors of human NPP1

Quinazolin-4-piperidine sulfamides (QPS) have been shown to be potent inhibitors of NPP1. However, their mode of inhibition as well as their specificity over other members of the ectonucleotidase family is unknown. The following two QPS compounds (1-2) were synthesized (> 95% purity estimated by 1H NMR; suppl. materials) and used in enzyme kinetic assays (Figure 1). QPS1 inhibited NPP1 (pANOVA < 0.0001) in a concentration-dependent manner (Figure 2A and B). The maximal rate of inhibition was 84% with 1000 nM QPS1 concentration. The inhibition rate did not vary significantly when increasing the concentration of substrate, suggesting that QPS1 is a non-competitive inhibitor of NPP1. Analyses of NPP1 activity in the Dixon plot indicated that QPS1 inhibited NPP1 with a K_i of 59.3 ± 5.4 nM (Figure 2C and G). Inhibited and uninhibited NPP1 had different *y*-intercepts, confirming a non-competitive inhibition (Figure 2C). We next documented that QPS2 is less potent than QPS1. The maximal inhibition rate of NPP1 activity achieved with 1000 nM QPS2 was 77% (pANOVA < 0.0006) (Figure 2D and E). The K_i obtained for QPS2 was 110.4 ± 22.7 nM (Figure 2F and G).

Considering that QPS1 was more potent, the next series of experiments was carried out with this compound. We tested QPS1 on the K121Q NPP1 variant, which is expressed in ~ 15% of the population and associated with diabetes. Similarly to the results obtained with wild type NPP1, QPS1 provided a strong inhibition of the K121Q NPP1 variant. The maximal rate of inhibition on NPP1 activity was 77% (pANOVA = 0.0035) (Figure 3A and B) with a K_i of 59.2 ± 14.5 nM (Figure 3C and D). Taken together, these findings indicate that QPS1 is a potent inhibitor of NPP1 including its common variant K121Q.

Specificity of quinazolin-4 sulfamide (QPS1)

The specificity of QPS1 inhibition was tested on the most important ectonucleotidases. Among the NPP family of enzymes, NPP2 has a poor pyrophosphatase activity and has instead a lysophospholipase D activity. On the other hand, NPP3 has a pyrophosphatase activity. Hence, we next tested QPS1 on NPP3. In these experiments we documented that QPS1 did not significantly inhibit NPP3 with a maximal inhibition rate of 7% on enzyme specific activity (Figure 4A). Ecto-5'-nucleotidase (NT5E; CD73) converts AMP into adenosine. We next verified the activity of ecto-5'-nucleotidase by using the malachite green technique and AMP as a substrate. In this series of experiments, we observed that QPS1 did not significantly impact on ecto-5'-nucleotidase activity, with a maximal inhibition rate of 5% (Figure 4B).We next tested the activity of QPS1 on human NTPDases, which catalyze the hydrolysis of ATP into ADP and also ADP into AMP. Enzyme activity of NTPDases was tested with the malachite green technique with ATP as a substrate. In experiments with human NTPDase1,-2,-3, QPS1 did not produce a significant inhibition, with a maximal inhibition rate of 12% for NTPDase2 (Figure 4C). Alkaline phosphatase or tissue non-specific alkaline phosphatase (ALP; TNAP) is a phosphatase with a wide spectrum of substrates. We used the p-nitrophenyl phosphate (PNPP) in cells transfected with a human vector encoding ALP. QPS1 yielded non-significant inhibition on ALP activity with a maximal inhibition rate of 6% (Figure 4C). Hence, QPS1 is specific for NPP1 and does not significantly affect NPP3, NTPDases (1-3), ALP and NT5E.

Blockade of NPP1 prevents calcification of isolated valve interstitial cells in response to phosphate

We previously showed that NPP1 is highly expressed in calcific aortic valve disease and that it promotes the mineralization of VICs. Hence, we used QPS1 in isolated human VICs exposed to a mineralizing medium (phosphate-containing medium) to document the biological activity of QPS1. Human primary VICs were isolated from 7 patients who had undergone heart transplantation (Table 1). A treatment of VICs with the mineralizing medium increased the level of calcium measured in cell culture after 7 days. A treatment of VIC cultures with QPS1 reduced in a dose-dependent manner the amount of calcium measured biochemically and normalized to the protein content (pANOVA<0.0001) (Figure 5A). These findings were corroborated by using alizarin red staining of cell cultures, which showed that QPS prevented the mineralization of VIC cultures (Figure 5B). Phosphate-induced mineralization relies on apoptosis and osteoblastic transition of cells. Phosphate induces the expression of NPP1, which contributes to depleting the extracellular level of ATP. In turn, a lower purinergic signalling in VICs promotes the mineralization through osteogenic and apoptotic mechanisms (Cote *et al*., 2012b). After 7 days of culture we measured the level of ATP in VIC supernatants. We found in osteogenic medium (containing phosphate) that the level of extracellular ATP was decreased, whereas a treatment with QPS1 (0.5 μM) significantly increased the level of nucleotides (pANOVA<0.0001) (Figure 5C). We next measured the level of apoptosis in VIC cultures treated with the phosphate-containing medium by using the caspase 3/7 activity assay. While a treatment with PO_4 increased apoptosis by a factor of 3.1, QPS1 negated this effect (pANOVA=0.0003) (Figure 5D). We next measured the level of osteoblastic genes following stimulation with the mineralizing medium with or without QPS1 at 10 μM. After a treatment with phosphate, the following osteoblastic genes were increased: runx2, osteopontin and osteocalcin (pANOVA<0.03) (Figure 5E). The mRNA encoding for ALP was not significantly modulated by a phosphate treatment (Figure 5E). QPS1 prevented the rise of runx2, osteopontin and osteocalcin, whereas it did not impact on the expression of ALP (Figure 5E). In addition, phosphate-induced expression of collagen alpha 1 chain type 1 (COL1A1) was also reduced by QPS1 (pANOVA=0.0001) (Figure 5F). These findings indicate that QPS1 has biological activities in the low micromolar range and prevents pathologic mineralization/fibrosis in an *in vitro* model.

Discussion

In this work, we highlighted that QPS compounds are specific and potent non-competitive inhibitors of human NPP1. Specifically, we found that QPS1 did not significantly inhibit NPP3, NTPDases (1-3), ecto-5'-nucleotidase and ALP. Furthermore, we found that QPS1 prevented phosphate-induced mineralization of human VICs. QPS1 was efficient, in the low micromolar range, to prevent phosphate-induced apoptosis of VICs. Also, the rise of osteoblastic gene markers induced by phosphate-containing medium was prevented by QPS1. Taken together, these findings indicate that QPS1 prevents the pathologic mineralization of VICs by specifically inhibiting NPP1.

Inhibitors of NPP1

ARL67156, a non-hydrolyzable competitive inhibitor of ectonucleotidases, is widely used in cell experiments. A report showed that ARL67156 inhibits NPP1 with a K_i of 12 ± 3 µM (Levesque *et al.*, 2007). The effect of ARL67156 is relatively non-specific and impacts significantly on the activity of NTPDase1 and NTPDase3 with K_i of 11 ± 3 µM and 18 ± 4 µM respectively. Also, derivatives of oxadiazole-2(3h)-thione have been described as inhibitors of NPP1 (Khan *et al.*, 2009). However, the potency of these compounds is low with $K_i \sim 100$ µM. More recently, novel diadenosine polyphosphonate derivatives have been described as inhibitors of NPP1 with K_i varying between 9 and 51 µM (Eliahu *et al.*, 2010). Diadenosine polyphosphonate compounds also significantly inhibited NPP2 and NPP3. In the present series of experiments, we documented that QPS1 and QPS2 were potent inhibitors of NPP1 with K_i of 0.06 µM (59.3 nM) and 0.11 µM (110.4 nM) respectively. Patel *et al.* (2009) reported K_i of 0.036 µM and 0.061 µM respectively for QPS1 and QPS2, which is similar to the present findings. Hence, the present study confirmed the potency of QPS derivatives as significant inhibitors of NPP1.

Specificity of QPS1

The first report on QPS derivatives neither addressed the specificity of this class of compounds on other ectonucleotidases, nor their efficacy in a biological system such as in cell culture models. In the present study, we underlined that QPS1 did not significantly impact on NPP3, NTPDases (1-3), ecto-5'-nucleotidase and ALP. It is worth emphasizing that it is, to our knowledge, the first description of a compound that is both a potent and a specific inhibitor of NPP1. Therefore, QPS1 could be used in biological assays where different ectonucleotidases are expressed. Hence, QPS1 could help to discriminate between the respective role of NPP1 and that of other ectonucleotidases in different biological assays. In this regard, different ectonucleotidases are expressed by cell populations and exert a powerful control over purinergic signalling and several biological functions (Mathieu, 2012).

QPS1 inhibits pathologic mineralization of isolated human cells

NPP1 has both anti and pro-mineralizing properties. Mice with deletion of NPP1 develop extensive mineralization of tendons and soft tissues owing to the absence of PPi (Okawa *et al.*, 1998). On the other hand, the expression of NPP1 is increased considerably in human pathologic specimens of CAVD. We documented that overexpression of NPP1 promotes the mineralization of VICs by depleting the level of extracellular ATP. In turn, a low level of ATP triggers apoptosis of cell cultures whereby mineralization is promoted. Human VICs express NPP1, NPP2, ecto-5'-nucleotidase and ALP (Cote *et al.*, 2012b). In this work, the use of QPS1, a potent and selective inhibitor of NPP1, prevented both apoptosis and mineralization of VIC cultures induced by phosphate. Phosphate-induced expression of osteogenic genes relies on the sodium/phosphate co-transporter Pit1 (*SLC20A1*), which is highly expressed during ectopic vascular/valvular mineralization (El Husseini *et al.*, 2013). However, the molecular mechanism by which intracellular phosphate mediates gene expression is still unknown. QPS1 prevented the rise of several osteogenic markers induced by phosphate, indicating that QPS1 has strong anti-mineralizing properties on VICs. Whether QPS can also inhibit the mineralization of vascular smooth muscle cells remains to be explored. It should be stressed that expression of osteogenic genes is increased in human specimens of CAVD (Bosse *et al.*, 2009). Furthermore, phosphate is a strong promoter of the expression of several osteoblastic genes (El Husseini *et al.*, 2013). Therefore, the present findings suggest that QPS1 has strong biological activities in the low micromolar range ($\leq$ 10 μM), which prevents both apoptosis and osteoblastic transition of VICs. Notably, COL1A1 was the most up-regulated gene following exposure of VICs to phosphate. QPS1 significantly decreased the rise of COL1A1 in VICs, suggesting that this derivative may prevent fibrotic processes. It is worthwhile to highlight that the expression of genes related to fibrosis is elevated in human CAVD tissues (Chen & Simmons, 2011).

Clinical implications

NPP1 is suspected of playing a role in several disorders. As previously described, expression of NPP1 is elevated during the development of CAVD. Moreover, a high level of NPP1 has been shown to promote the pathologic mineralization of meniscal cells. Blocking NPP1 has been suggested as a means to prevent the formation of calcium pyrophosphate dehydrate (CPPD) crystal and as such could be used in the treatment of chondrocalcinosis and osteoarthritis (Johnson *et al.*, 2001b). In apoE$^{-/-}$ NPP1$^{-/-}$ and apoE$^{-/-}$ NPP1$^{+/-}$ mice the level of vascular atherosclerosis is reduced. Notably, vascular mineralization was not significantly increased in haploinsufficient apoE$^{-/-}$ NPP1$^{+/-}$ compared to ApoE$^{-/-}$ mice. Hence, NPP1 promotes atherosclerosis and a certain amount is required to prevent ectopic vascular mineralization (Nitschke *et al.*, 2011). Also, studies have stressed that overexpression of NPP1 could play a role in the pathogenesis of diabetes. In this regard, overexpression of NPP1 in the liver promotes insulin resistance. Expression of NPP1 is increased in fibroblast of patients with type 2 diabetes (T2D) (Maddux *et al.*, 1995). It is suspected that interaction of NPP1 with the insulin receptor could impede insulin signalling. However, whether enzyme activity of NPP1 is necessary to hinder insulin signalling is still a matter of debate (Grupe *et al.*, 1995), (Chin *et al.*, 2009). The K121Q variant of NPP1, prevalent in the population, has been associated in different studies with T2D (Abate *et al.*, 2005). Considering the prevalence of this gene variant in the general population, we tested the QPS1 compound on the K121Q NPP1 variant. Of interest, we documented that QPS1 was efficient at inhibiting the variant K121Q with a K_i of 0.06 µM (59.2 nM). Hence, the development of novel inhibitors for NPP1, which are specific and potent, is desperately needed to probe the role of NPP1 in different disorders. As a result, this study may have important implications as it underlines that QPS1 may be used, at least *in vitro,* to investigate the pathogenic role of NPP1.

Limitations

Though potent and selective, the QPS derivatives have not been validated *in vivo*. The *in vivo* kinetics and resistance to hydrolysis of QPS derivatives remain to be investigated. Some of the QPS derivatives bind to the hERG potassium channel and thus may induce prolongation of the QT interval (Patel *et al.*, 2009). QPS1 is a potent ligand of hERG, whereas QPS2 has the best ratio of NPP1 inhibition to hERG binding. Hence, further development of these compounds will require voltage clamp experiments to assess properly this class of compounds on hERG function. Also, their transmembrane kinetics and their impact on intracellular enzymes remain to be established. Nonetheless, the present series of investigations have cast some light on this novel class of NPP1 inhibitors. We have identified that QPS1 is potent, selective and efficient in a cellular model to inhibit pathologic mineralization.

Conclusion

In this study, we have provided evidence that quinazolin-4-piperidine sulfamides (QPS) are a novel class of non-competitive inhibitors of NPP1. Furthermore, we found that QPS1 is selective and prevents phosphate-induced apoptosis and mineralization of human VICs. Moreover, we identified that this selective inhibitor negated the osteogenic transition of VICs induced by mineralizing medium, thus highlighting its potential role to prevent ectopic mineralization.

AUTHOR CONTRIBUTIONS

E.E.S, M.C.B, and A.M. conducted *in vitro* experiments on enzyme kinetics and in cell culture. E.E.S. performed data analyses. E.F. and S.D. synthesized compounds used in this study. J.F.P. supervised synthesis of chemical compounds. X.B., J.S. and P.L. critically reviewed data. P.M. supervised *in vitro* experiments and wrote the manuscript. All the authors critically reviewed the manuscript.

ACKNOWLEDGEMENTS

This work was supported by grants from the Heart and Stroke Foundation of Canada (HSFC) (P.M.), the Canadian Institutes of Health Research (CIHR) P.M (MOP245048), and the Fonds de recherche du Québec – Nature et technologies (FRQNT) (P.M.). P.M. and J.S. are recipients of a Scholarship from the Fonds de recherche du Québec – Santé (FRQS). The Canada Research Chair Program (J.F.P.), the Natural Sciences and Engineering Research Council of Canada (J.F.P.), the Canada Foundation for Innovation (J.F.P.) (P.M.), PROTEO and Université Laval are also acknowledged.

Reference List

Abate, N, Chandalia, M, Satija, P, Adams-Huet, B, Grundy, SM, Sandeep, S, Radha, V, Deepa, R & Mohan, V. (2005). ENPP1/PC-1 K121Q polymorphism and genetic susceptibility to type 2 diabetes. *Diabetes*, **54**, 1207-1213.

Baykov, AA, Evtushenko, OA & Avaeva, SM. (1988). A malachite green procedure for orthophosphate determination and its use in alkaline phosphatase-based enzyme immunoassay. *Anal Biochem*, **171**, 266-270.

Bosse, Y, Miqdad, A, Fournier, D, Pepin, A, Pibarot, P & Mathieu, P. (2009). Refining molecular pathways leading to calcific aortic valve stenosis by studying gene expression profile of normal and calcified stenotic human aortic valves. *Circ Cardiovasc Genet*, **2**, 489-498.

Chen, JH & Simmons, CA. (2011). Cell-matrix interactions in the pathobiology of calcific aortic valve disease: critical roles for matricellular, matricrine, and matrix mechanics cues. *Circ Res*, **108**, 1510-1524.

Chiang, WC & Knowles, AF. (2008). Transmembrane domain interactions affect the stability of the extracellular domain of the human NTPDase 2. *Arch Biochem Biophys*, **472**, 89-99.

Chin, CN, Dallas-Yang, Q, Liu, F, Ho, T, Ellsworth, K, Fischer, P, Natasha, T, Ireland, C, Lu, P, Li, C, Wang, IM, Strohl, W, Berger, JP, An, Z, Zhang, BB & Jiang, G. (2009). Evidence that inhibition of insulin receptor signaling activity by PC-1/ENPP1 is dependent on its enzyme activity. *Eur J Pharmacol*, **606**, 17-24.

Cote, N, El Husseini D, Pepin, A, Bouvet, C, Gilbert, LA, Audet, A, Fournier, D, Pibarot, P, Moreau, P & Mathieu, P. (2012a). Inhibition of ectonucleotidase with ARL67156 prevents the development of calcific aortic valve disease in warfarin-treated rats. *Eur J Pharmacol*, **689**, 139-146.

Cote, N, El Husseini D, Pepin, A, Guauque-Olarte, S, Ducharme, V, Bouchard-Cannon, P, Audet, A, Fournier, D, Gaudreault, N, Derbali, H, McKee, MD, Simard, C, Despres, JP, Pibarot, P, Bosse, Y & Mathieu, P. (2012b). ATP acts as a survival signal and prevents the mineralization of aortic valve. *J Mol Cell Cardiol*, **52**, 1191-1202.

El Husseini D, Boulanger, MC, Fournier, D, Mahmut, A, Bosse, Y, Pibarot, P & Mathieu, P. (2013). High expression of the Pi-transporter SLC20A1/Pit1 in calcific aortic valve disease promotes mineralization through regulation of Akt-1. *PLoS One*, **8**, e53393.

Eliahu, S, Lecka, J, Reiser, G, Haas, M, Bigonnesse, F, Levesque, SA, Pelletier, J, Sevigny, J & Fischer, B. (2010). Diadenosine 5',5''-(boranated) polyphosphonate analogues as selective nucleotide pyrophosphatase/phosphodiesterase inhibitors. *J Med Chem*, **53**, 8485-8497.

Goding, JW. (2000). Ecto-enzymes: physiology meets pathology. *J Leukoc Biol*, **67**, 285-311.

Goding, JW, Grobben, B & Slegers, H. (2003). Physiological and pathophysiological functions of the ecto-nucleotide pyrophosphatase/phosphodiesterase family. *Biochim Biophys Acta*, **1638**, 1-19.

Grupe, A, Alleman, J, Goldfine, ID, Sadick, M & Stewart, TA. (1995). Inhibition of insulin receptor phosphorylation by PC-1 is not mediated by the hydrolysis of adenosine triphosphate or the generation of adenosine. *J Biol Chem*, **270**, 22085-22088.

Jin-Hua, P, Goding, JW, Nakamura, H & Sano, K. (1997). Molecular cloning and chromosomal localization of PD-Ibeta (PDNP3), a new member of the human phosphodiesterase I genes. *Genomics*, **45**, 412-415.

Johnson, K, Hashimoto, S, Lotz, M, Pritzker, K, Goding, J & Terkeltaub, R. (2001a). Up-regulated expression of the phosphodiesterase nucleotide pyrophosphatase family member PC-1 is a marker and pathogenic factor for knee meniscal cartilage matrix calcification. *Arthritis Rheum*, **44**, 1071-1081.

Johnson, K, Pritzker, K, Goding, J & Terkeltaub, R. (2001b). The nucleoside triphosphate pyrophosphohydrolase isozyme PC-1 directly promotes cartilage calcification through chondrocyte apoptosis and increased calcium precipitation by mineralizing vesicles. *J Rheumatol*, **28**, 2681-2691.

Kaczmarek, E, Koziak, K, Sevigny, J, Siegel, JB, Anrather, J, Beaudoin, AR, Bach, FH & Robson, SC. (1996). Identification and characterization of CD39/vascular ATP diphosphohydrolase. *J Biol Chem*, **271**, 33116-33122.

Khan, KM, Fatima, N, Rasheed, M, Jalil, S, Ambreen, N, Perveen, S & Choudhary, MI. (2009). 1,3,4-Oxadiazole-2(3H)-thione and its analogues: a new class of non-competitive nucleotide pyrophosphatases/phosphodiesterases 1 inhibitors. *Bioorg Med Chem*, **17**, 7816-7822.

Lecka, J, Rana, MS & Sevigny, J. (2010). Inhibition of vascular ectonucleotidase activities by the pro-drugs ticlopidine and clopidogrel favours platelet aggregation. *Br J Pharmacol*, **161**, 1150-1160.

Levesque, SA, Lavoie, EG, Lecka, J, Bigonnesse, F & Sevigny, J. (2007). Specificity of the ecto-ATPase inhibitor ARL 67156 on human and mouse ectonucleotidases. *Br J Pharmacol*, **152**, 141-150.

Maddux, BA, Sbraccia, P, Kumakura, S, Sasson, S, Youngren, J, Fisher, A, Spencer, S, Grupe, A, Henzel, W, Stewart, TA & . (1995). Membrane glycoprotein PC-1 and insulin resistance in non-insulin-dependent diabetes mellitus. *Nature*, **373**, 448-451.

Mathieu, P. (2012). Pharmacology of ectonucleotidases: relevance for the treatment of cardiovascular disorders. *Eur J Pharmacol*, **696**, 1-4.

Nitschke, Y, Weissen-Plenz, G, Terkeltaub, R & Rutsch, F. (2011). Npp1 promotes atherosclerosis in ApoE knockout mice. *J Cell Mol Med*, **15**, 2273-2283.

Okawa, A, Nakamura, I, Goto, S, Moriya, H, Nakamura, Y & Ikegawa, S. (1998). Mutation in Npps in a mouse model of ossification of the posterior longitudinal ligament of the spine. *Nat Genet*, **19**, 271-273.

Patel, SD, Habeski, WM, Cheng, AC, de la Cruz, E, Loh, C & Kablaoui, NM. (2009). Quinazolin-4-piperidin-4-methyl sulfamide PC-1 inhibitors: alleviating hERG interactions through structure based design. *Bioorg Med Chem Lett*, **19**, 3339-3343.

Smith, TM & Kirley, TL. (1998). Cloning, sequencing, and expression of a human brain ecto-apyrase related to both the ecto-ATPases and CD39 ecto-apyrases1. *Biochim Biophys Acta*, **1386**, 65-78.

Towler, DA. (2005). Inorganic pyrophosphate: a paracrine regulator of vascular calcification and smooth muscle phenotype. *Arterioscler Thromb Vasc Biol*, **25**, 651-654.

Table 1. Clinical characteristics of patients

	Aortic valves for VIC isolation (n=7)
Age	45 ± 3
Male (%)	71
Smoking (%)	29
Hypertension (%)	29
Diabetes (%)	14
BMI (kg/m^2)	30.2 ± 2.10
Triglycerides (mmol/L)	1.40 ± 0.34
LDL (mmol/L)	2.36 ± 0.68
HDL (mmol/L)	1.39 ± 0.11
Creatinine (µmol/L)	90.3 ± 9.55

BMI: body mass index; LDL: Low-density lipoprotein;

HDL: High-density lipoprotein; Values are mean ± SEM or %

Figure Legend

Figure 1: Molecular structure of NPP1 inhibitors QPS1 (A) and QPS2 (B).

Figure 2: Inhibition of NPP1 by QPS1 (A and B) (n = 5) and Dixon plot representation (C). Inhibition of NPP1 by QPS2 (D and E) (n = 4) and Dixon plot representation (F). G) Characteristics of inhibition by QPS1 and QPS2. S: substrate. Data are mean ± SEM.*$p < 0.05$ compared to control (no QPS); # $p < 0.05$ compared to 50 nM dose; ‡ $p < 0.05$ compared to 100 nM dose.

Figure 3: Inhibition of NPP1 K121Q by QPS1 (A and B) (n = 5), Dixon plot representation (C) and characteristics of inhibition (D). Data are mean ± SEM. *$p < 0.05$ compared to control (no QPS).

Figure 4: Percentage of enzyme inhibition by QPS1 for NPP3 (A) (n = 4) with pnp-TMP as the substrate, NT5E (B) (n = 5) with AMP as the substrate, NTPDases1-3 (C) (n = 5) (ATP as the substrate) and ALP (C) (n = 4) with PNPP as the substrate. Data are mean ± SEM. pANOVA = NS

Figure 5: A) Concentration-dependent inhibition of PO_4-induced VICs mineralization by QPS1 (n = 7). B) Alizarin red staining of VIC cultures. C) Percentage of ATP in VIC supernatants (n = 4). D) QPS1 prevented PO_4-induced apoptosis of VICs as evaluated with the caspase3/7 assay (n = 4). E and F) QPS1 (10 μM) significantly reduced the rise of osteogenic/fibrotic markers following a treatment of VICs with PO_4 (n = 3). Data are mean ± SEM. In panels A and D: *$p < 0.05$ compared to control (CTL), # $p < 0.05$ compared to CTL with QPS, ‡ $p < 0.05$ compared to PO4; in panels E and F: *$p < 0.05$ compared to control (CTL), # $p < 0.05$ compared to PO4 without QPS.

Figure 1.

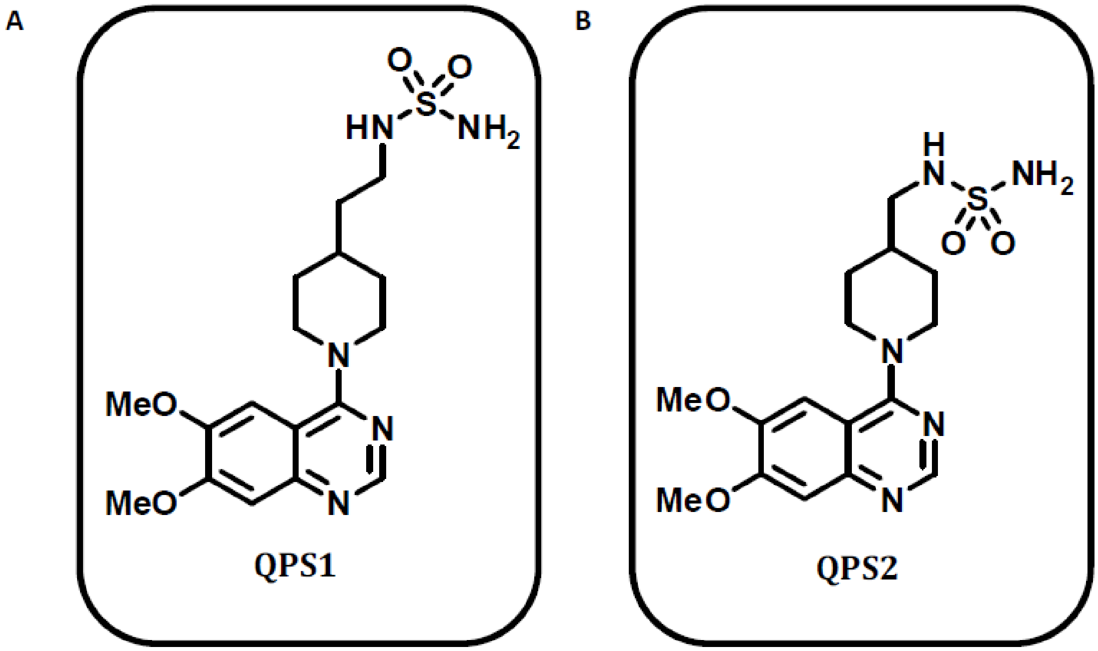
A
B
HN
NH2
MeO
MeO
N
QPS1
QPS2

Figure 2.

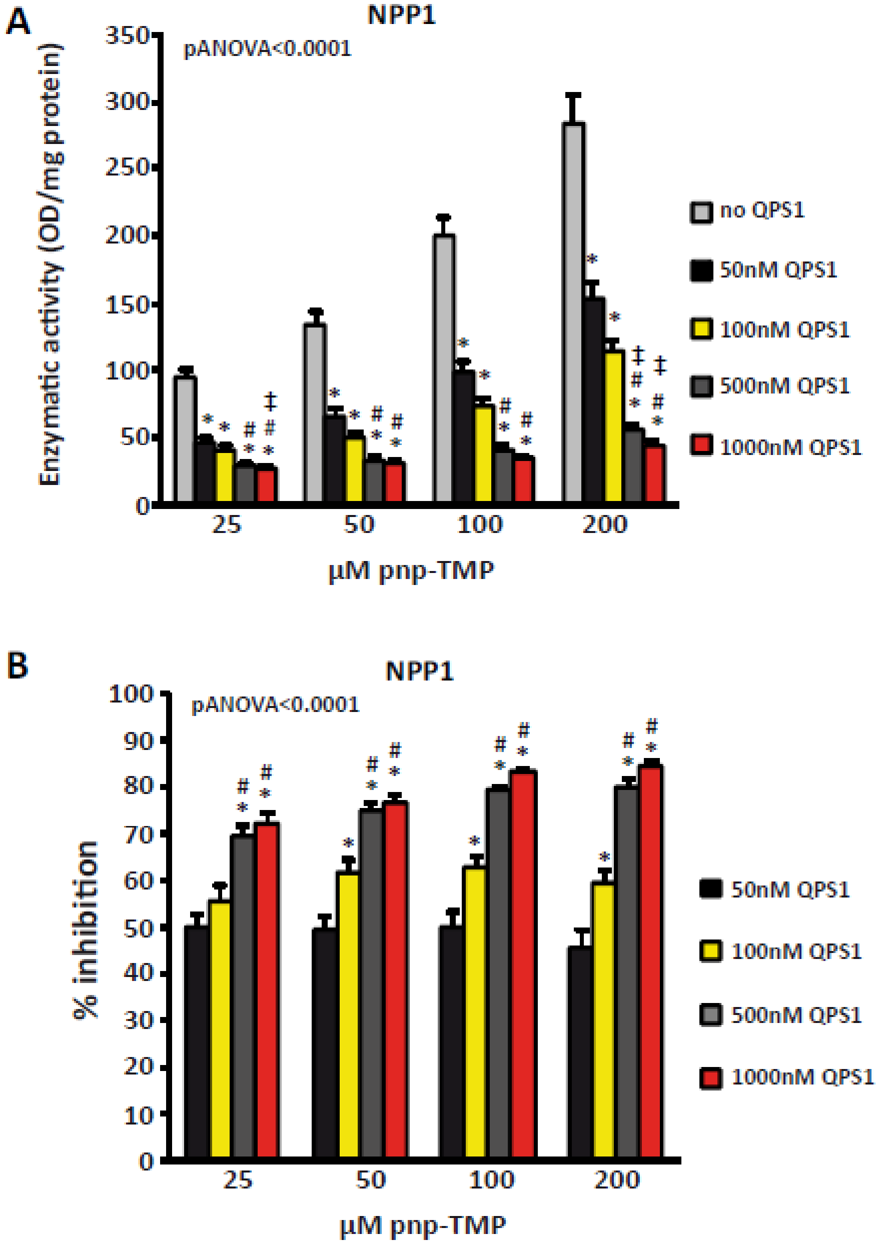
A
NPP1
pANOVA<0.0001
Enzymatic activity (OD/mg protein)
350
300
250
200
150
100
50
0
25
50
100
200
µM pnp-TMP
no QPS1
50nM QPS1
100nM QPS1
500nM QPS1
1000nM QPS1
*
#
‡
B
NPP1
pANOVA<0.0001
% inhibition
100
90
80
70
60
50
40
30
20
10
0
25
50
100
200
µM pnp-TMP
50nM QPS1
100nM QPS1
500nM QPS1
1000nM QPS1
*
#

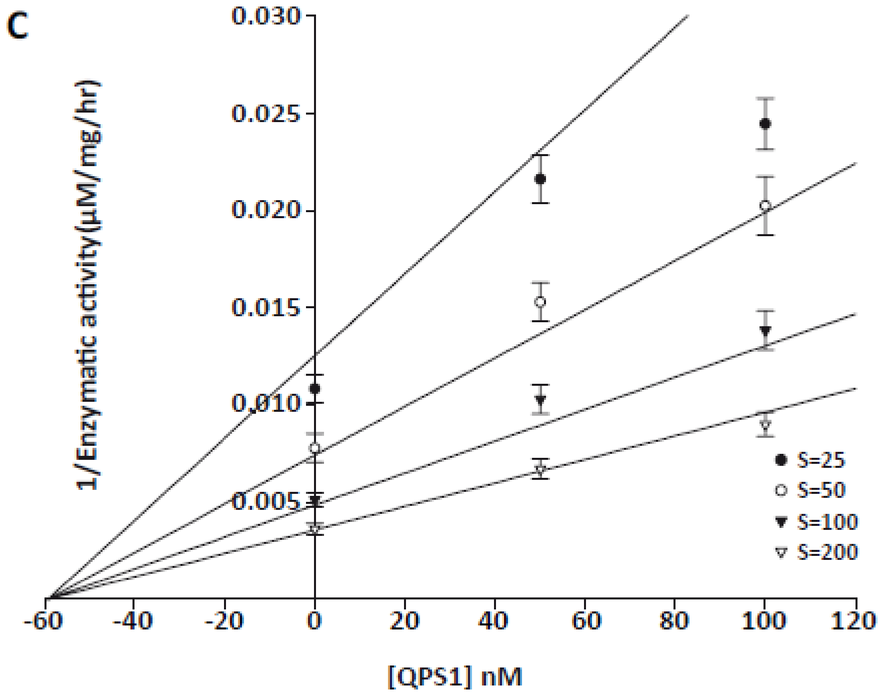
C
0.030
0.025
0.020
0.015
0.010
0.005
1/Enzymatic activity(µM/mg/hr)
-60
-40
-20
0
20
40
60
80
100
120
[QPS1] nM
● S=25
○ S=50
▼ S=100
▽ S=200

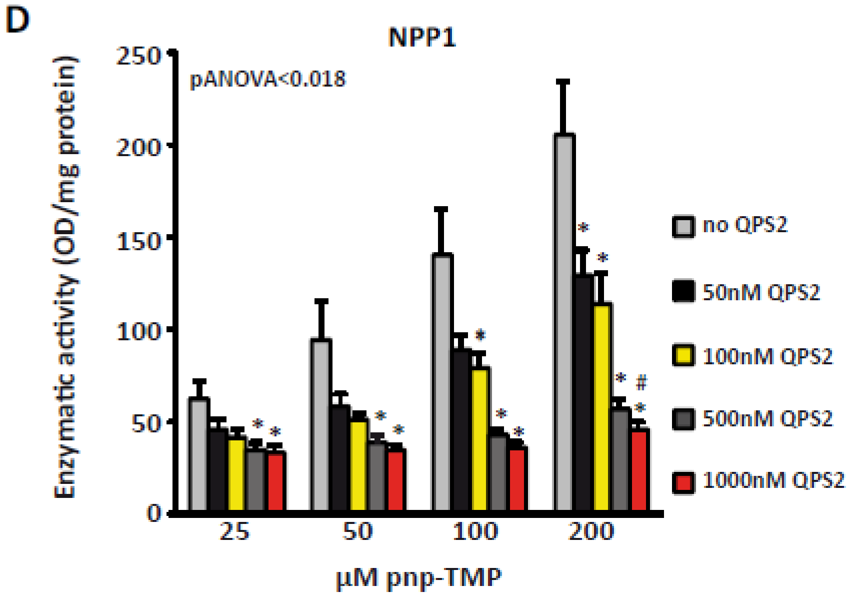
D
NPP1
pANOVA<0.018
250
200
150
100
50
0
Enzymatic activity (OD/mg protein)
25
50
100
200
µM pnp-TMP
*
#
no QPS2
50nM QPS2
100nM QPS2
500nM QPS2
1000nM QPS2

E

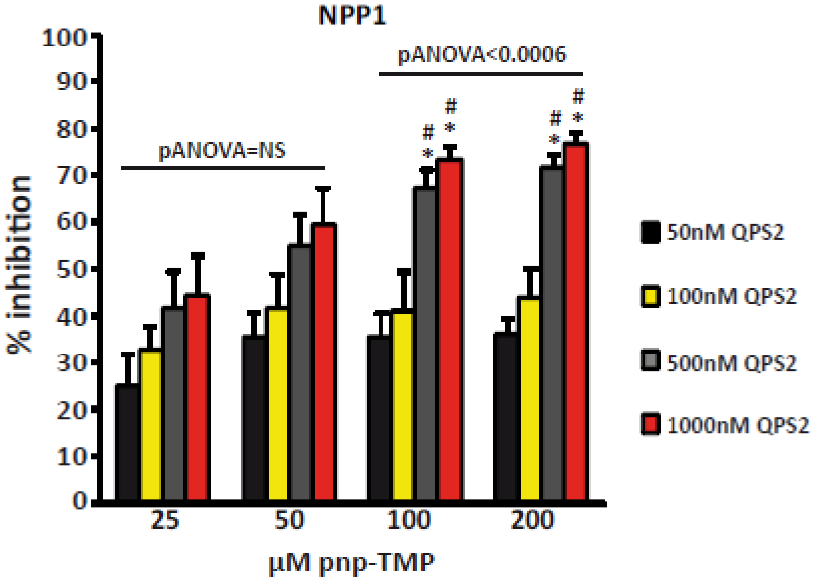
NPP1
% inhibition
100
90
80
70
60
50
40
30
20
10
0
pANOVA=NS
pANOVA<0.0006
#
*
25
50
100
200
µM pnp-TMP
50nM QPS2
100nM QPS2
500nM QPS2
1000nM QPS2

F

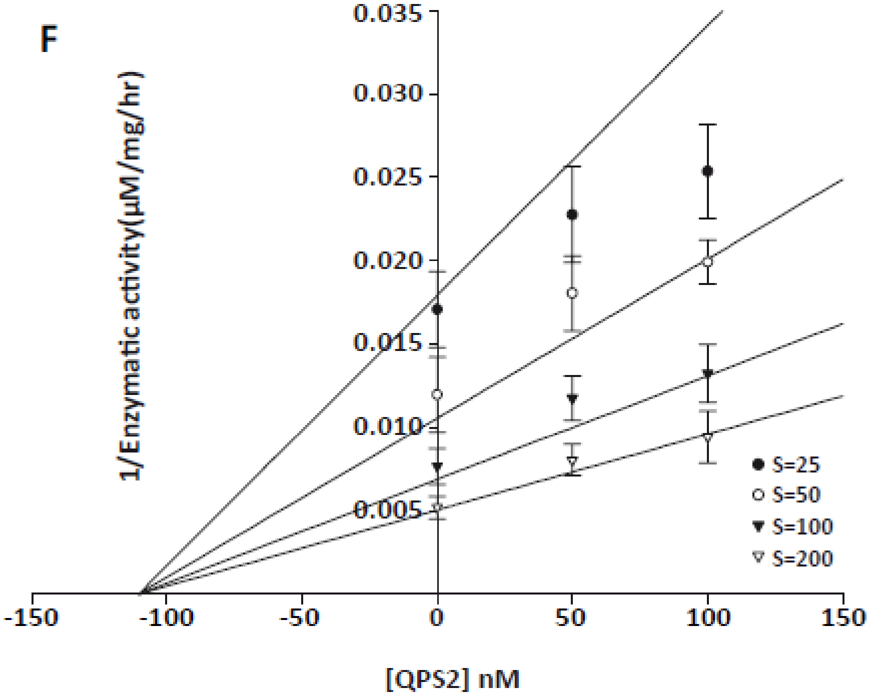
1/Enzymatic activity(µM/mg/hr)
0.035
0.030
0.025
0.020
0.015
0.010
0.005
-150
-100
-50
0
50
100
150
[QPS2] nM
S=25
S=50
S=100
S=200

G

NPP1 inhibitor	Type of inhibition	Ki ± SEM
QPS1	Non-competitive	59.3 ± 5.4 nM
QPS2	Non-competitive	110.4 ± 22.7 nM

Figure 3.

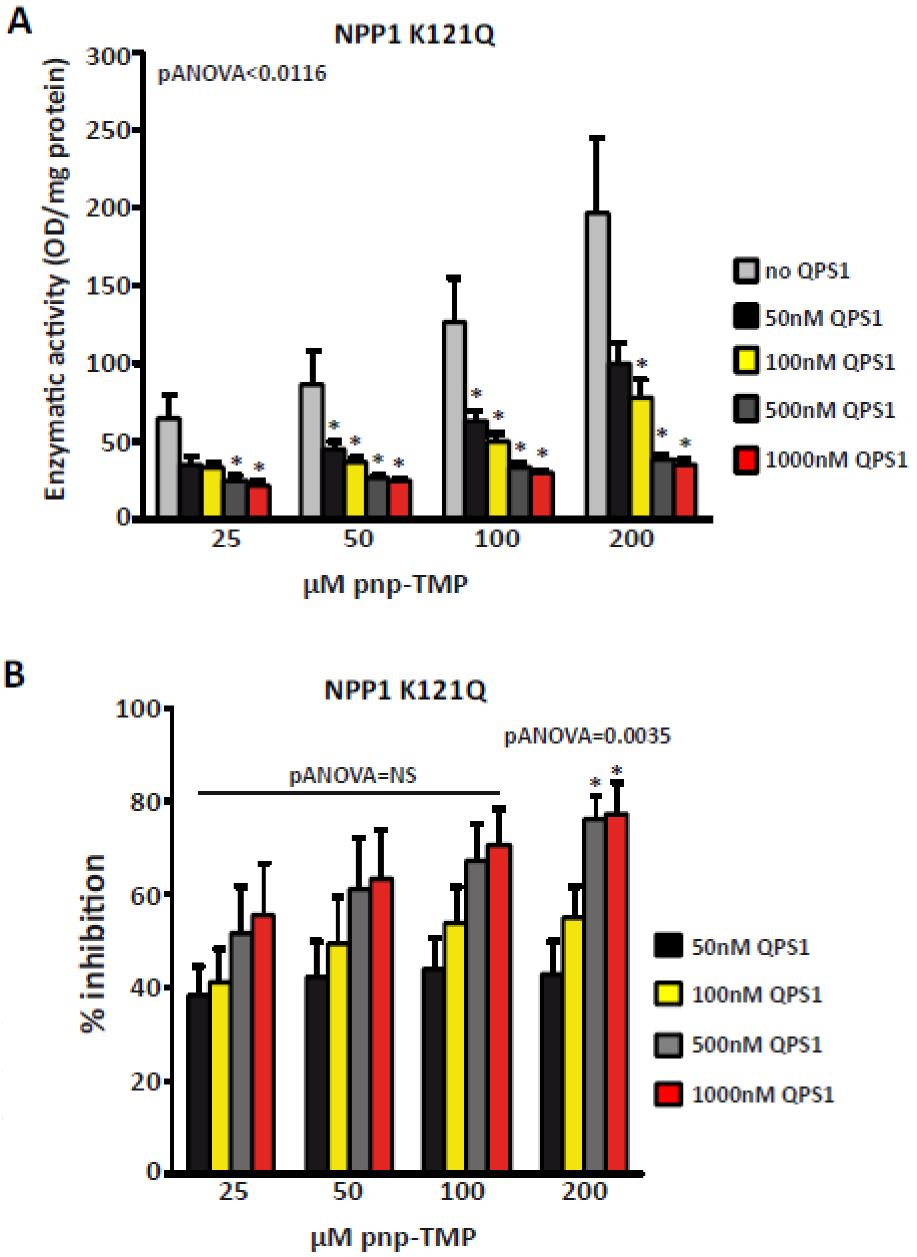
A
NPP1 K121Q
pANOVA<0.0116
Enzymatic activity (OD/mg protein)
300
250
200
150
100
50
0
25
50
100
200
µM pnp-TMP
no QPS1
50nM QPS1
100nM QPS1
500nM QPS1
1000nM QPS1
*
B
NPP1 K121Q
pANOVA=0.0035
pANOVA=NS
% inhibition
100
80
60
40
20
0
25
50
100
200
µM pnp-TMP
50nM QPS1
100nM QPS1
500nM QPS1
1000nM QPS1
*

C

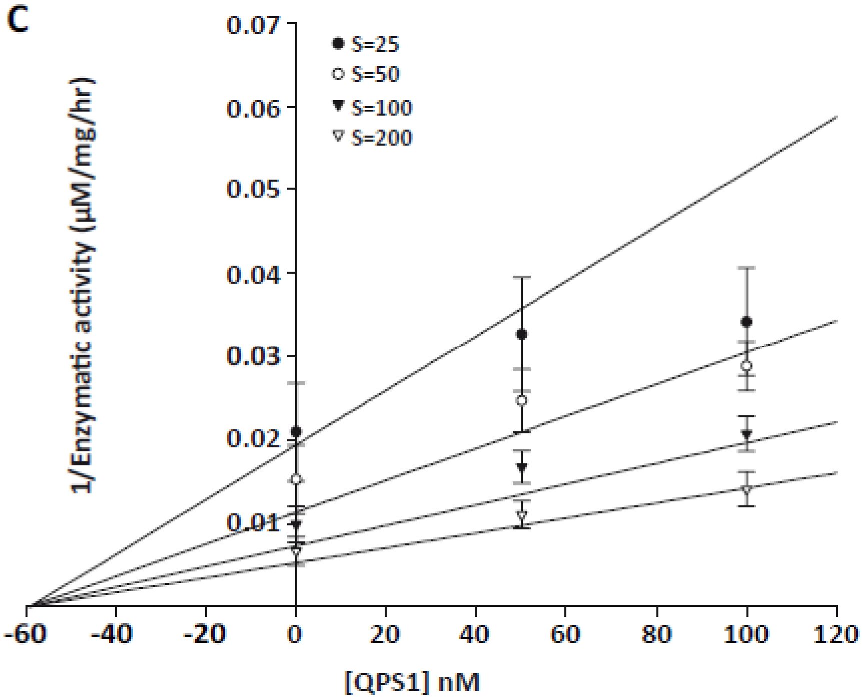

D

	Type of inhibition	Ki ± SEM
NPP1 K121Q	Non-competitive	59.2 ± 14.5nM

Figure 4.

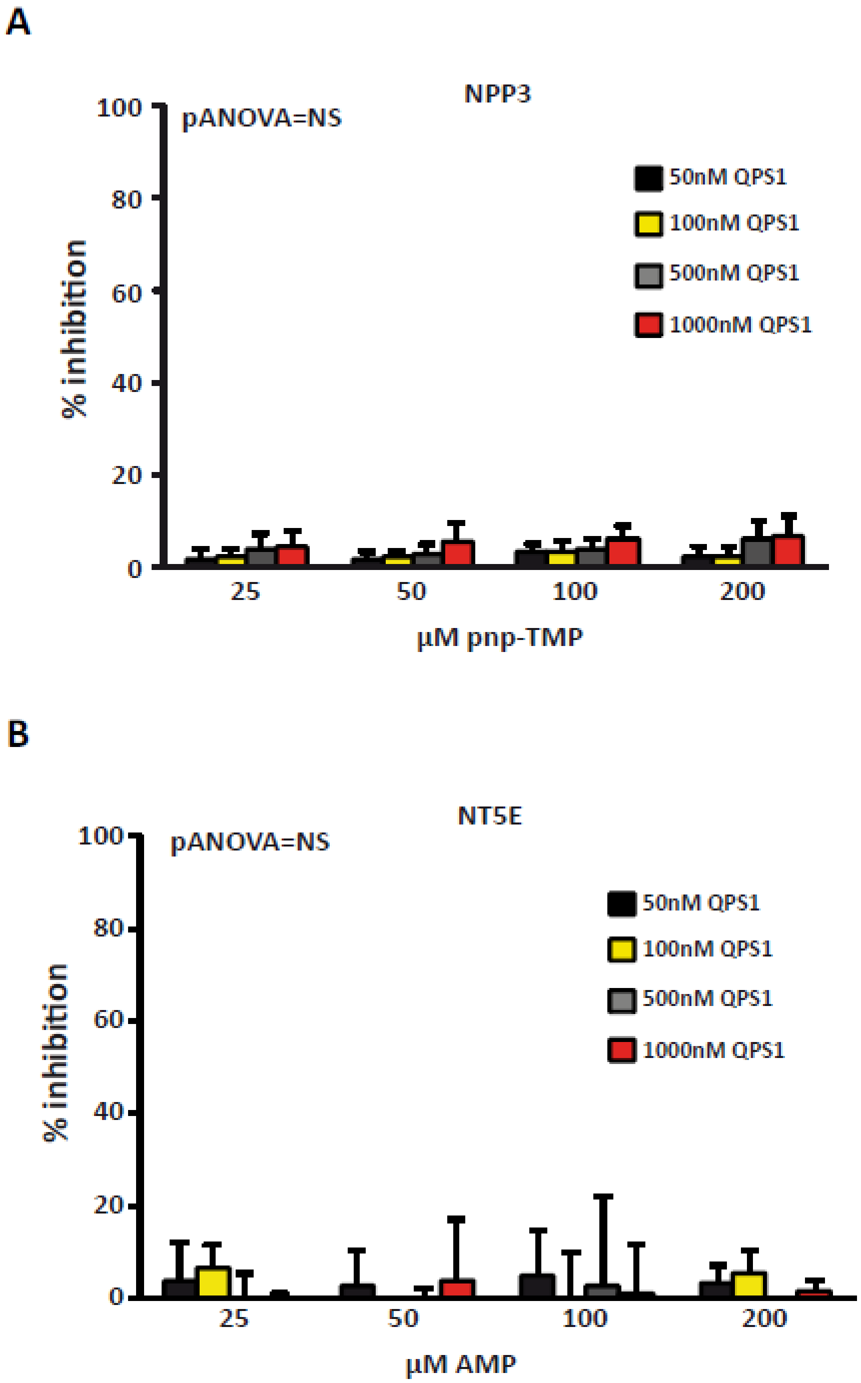
A
NPP3
pANOVA=NS
100
80
60
40
20
0
% inhibition
50nM QPS1
100nM QPS1
500nM QPS1
1000nM QPS1
25
50
100
200
µM pnp-TMP
B
NT5E
pANOVA=NS
100
80
60
40
20
0
% inhibition
50nM QPS1
100nM QPS1
500nM QPS1
1000nM QPS1
25
50
100
200
µM AMP

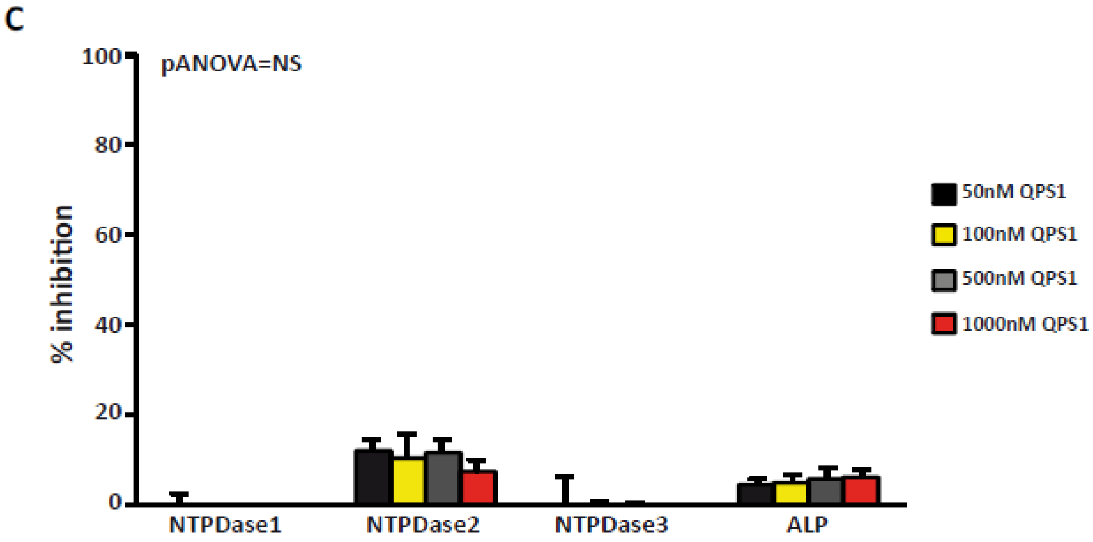
C
pANOVA=NS
% inhibition
100
80
60
40
20
0
NTPDase1
NTPDase2
NTPDase3
ALP
50nM QPS1
100nM QPS1
500nM QPS1
1000nM QPS1

Figure 5.

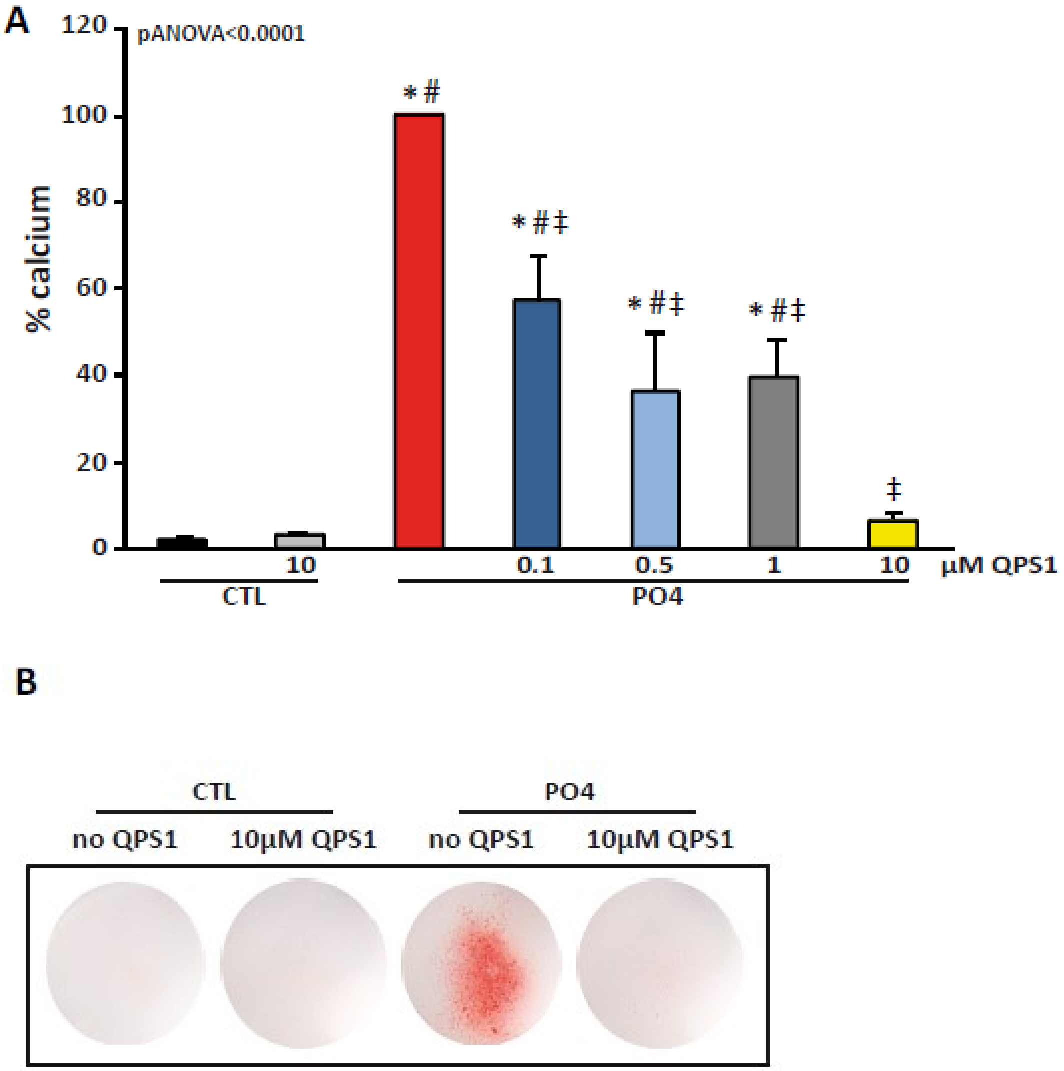
A
120
100
80
60
40
20
0
% calcium
pANOVA<0.0001
* #
* # ‡
* # ‡
* # ‡
‡
10
0.1
0.5
1
10
µM QPS1
CTL
PO4
B
CTL
PO4
no QPS1
10µM QPS1
no QPS1
10µM QPS1

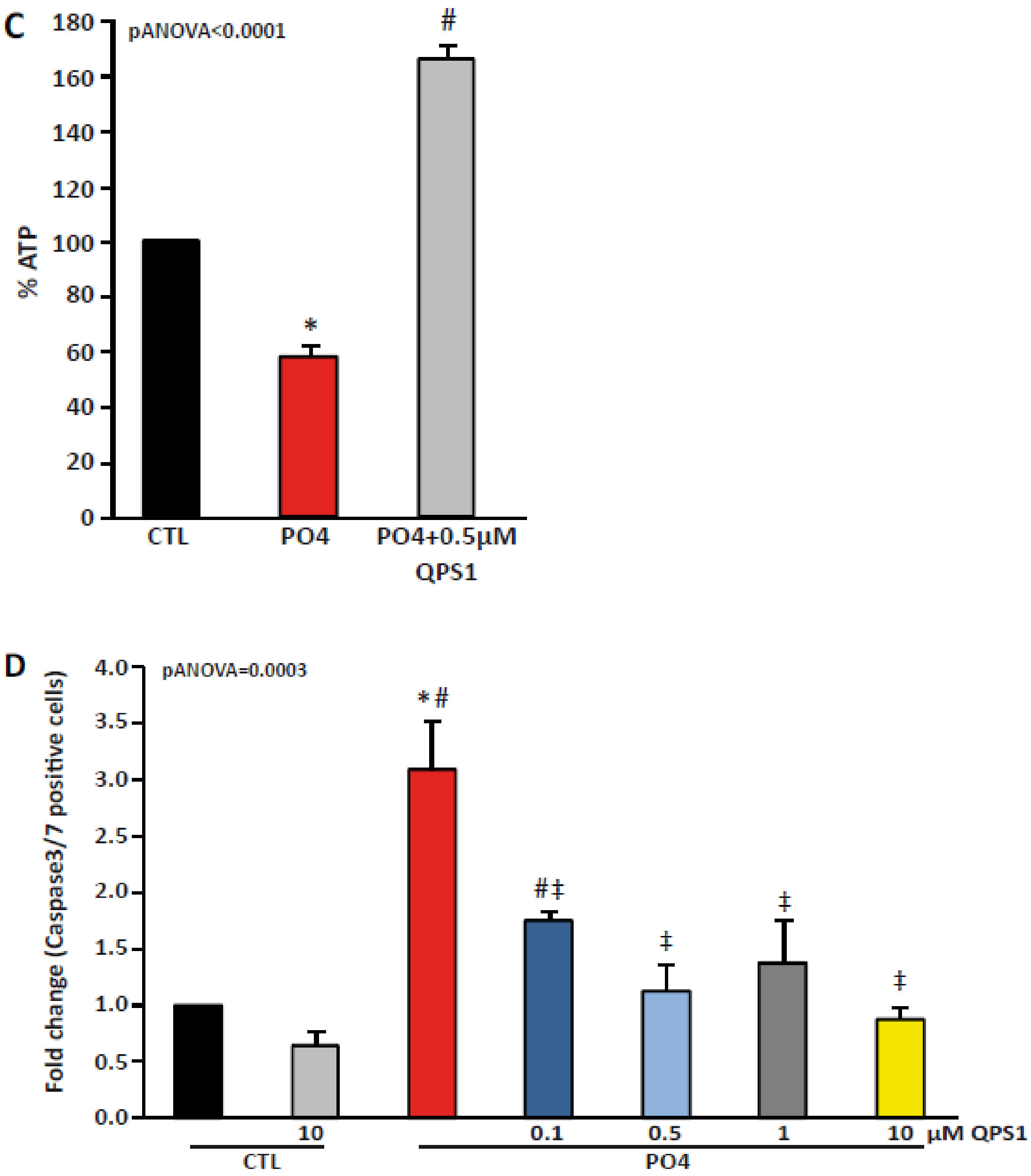
C
% ATP
pANOVA<0.0001
0
20
40
60
80
100
120
140
160
180
*
#
CTL
PO4
PO4+0.5µM QPS1
D
Fold change (Caspase3/7 positive cells)
pANOVA=0.0003
0.0
0.5
1.0
1.5
2.0
2.5
3.0
3.5
4.0
*#
#‡
‡
‡
‡
10
0.1
0.5
1
10 µM QPS1
CTL
PO4

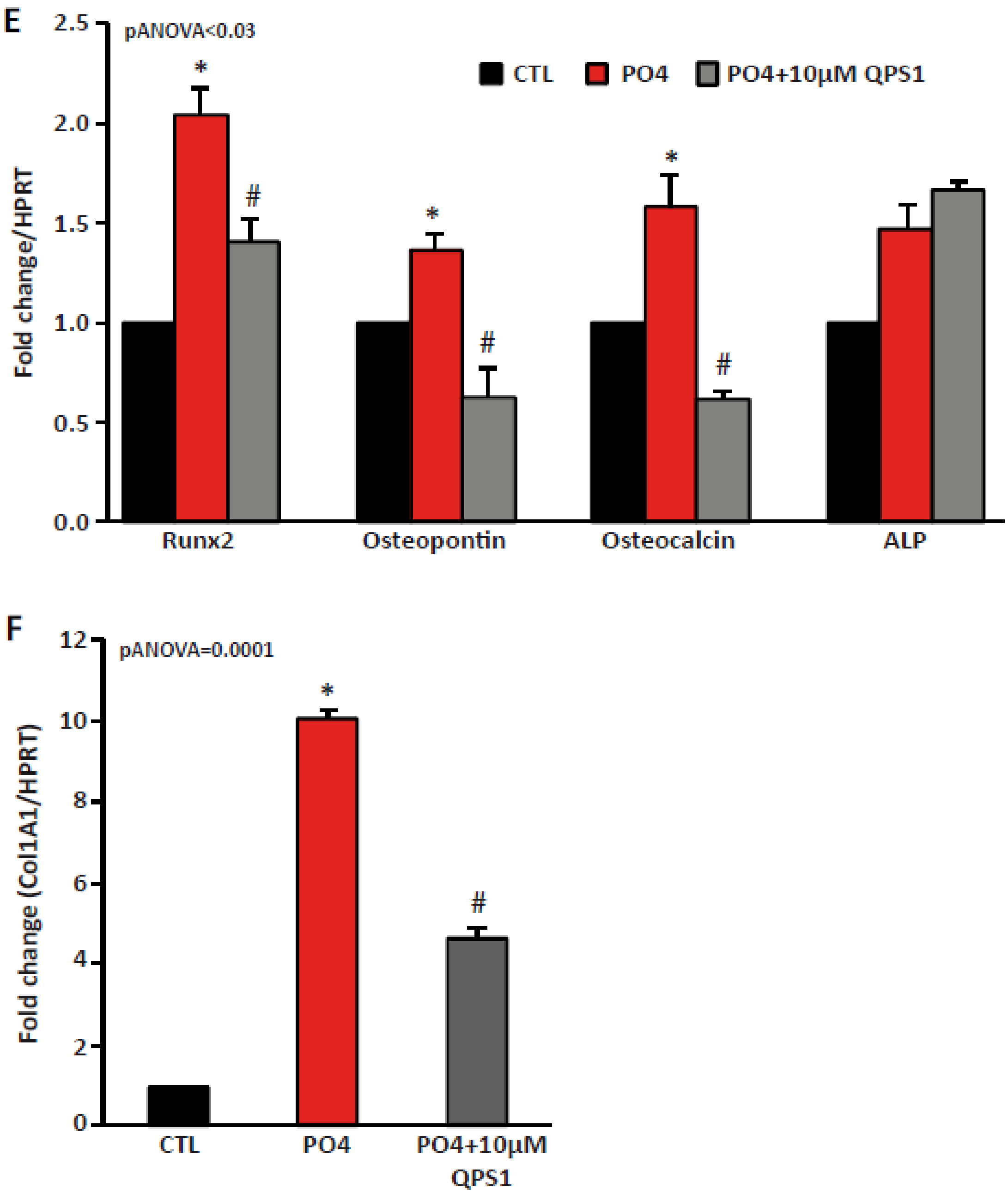
E
pANOVA<0.03
CTL
PO4
PO4+10µM QPS1
Fold change/HPRT
2.5
2.0
1.5
1.0
0.5
0.0
*
#
*
#
*
#
Runx2
Osteopontin
Osteocalcin
ALP
F
pANOVA=0.0001
Fold change (Col1A1/HPRT)
12
10
8
6
4
2
0
*
#
CTL
PO4
PO4+10µM QPS1

Supplementary information

General information

The following includes experimental procedures and spectroscopic information for the new compounds prepared. Thin-layer chromatography (TLC) analysis of reaction mixtures was performed using Silicyle silica gel 60 Å F254 TLC plates. Flash column chromatography was carried out on Silicycle Silica Gel 60 Å, 230 × 400 mesh. Nuclear magnetic resonance (NMR) spectra were recorded using Agilent DD2 500. ^{1}H and ^{13}C chemical shifts are reported in ppm downfield of tetramethylsilane and referenced to tetramethylsilane ($\delta = 0$ ppm) or residual chloroform peak ($\delta = 7.26$ ppm), methanol peak ($\delta = 3.31$ ppm) or dimethyl sulfoxide peak ($\delta = 2.50$ ppm). Coupling constants (*J*) are measured in hertz (Hz). Multiplicities are reported using the following abbreviations: s = singlet, d = doublet, t = triplet, q = quartet, m = multiplet, br = broad resonance. High-resolution mass spectra were obtained on a LC/MS-TOF Agilent 6210 using electrospray ionization (ESI). Infrared spectra were recorded using a Thermo Scientific Nicolet 380 FTIR spectrometer. Melting points were recorded on a Stanford Research Systems OptiMelt capillary melting point apparatus and are uncorrected. All the synthesized compounds (**1-10**, **QPS1-2**) have purity >95% (estimated by ^{1}H NMR).

Synthetic schemes

Scheme 1. Synthesis of QPS1[a]

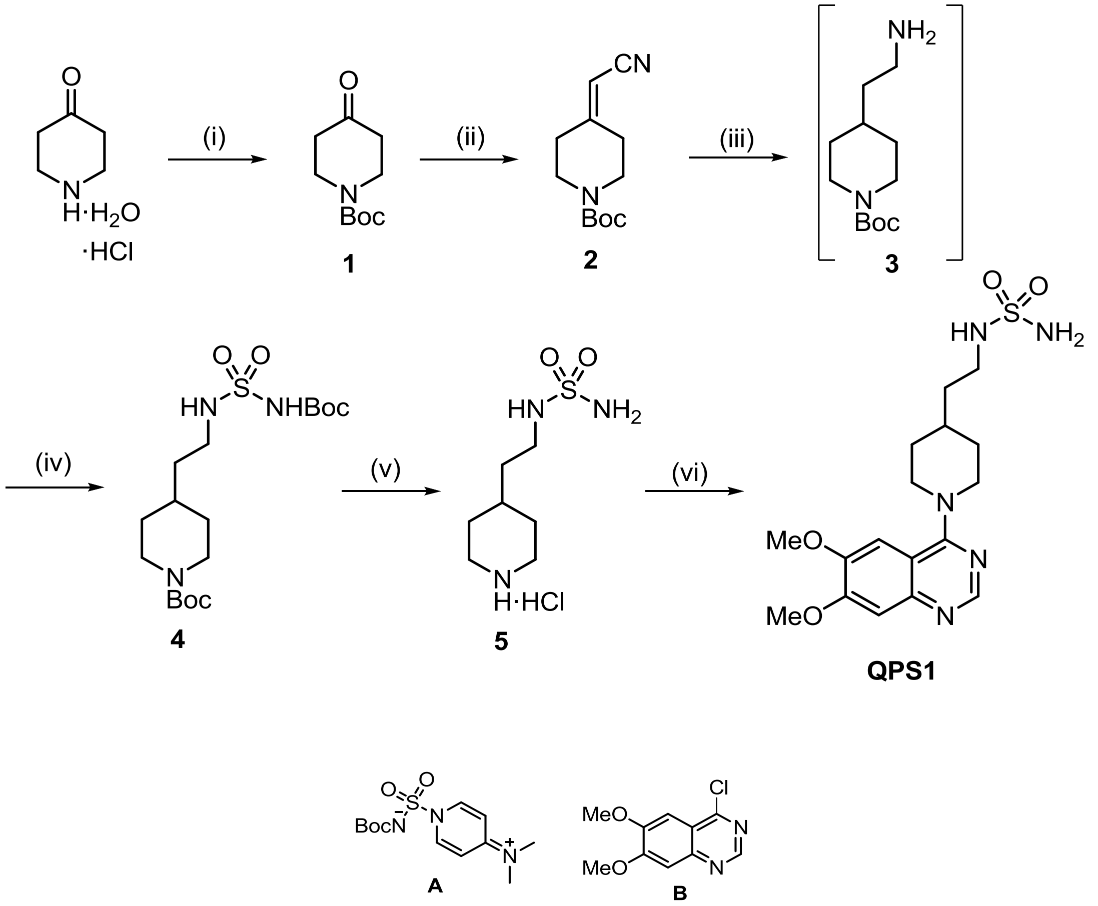
(i)
(ii)
(iii)
(iv)
(v)
(vi)
H·H2O ·HCl
Boc
1
2
3
4
5
H·HCl
QPS1
MeO
CN
NH2
NHBoc
BocN
A
B
Cl

[a] Conditions : (i) NaOH, Boc_2O, THF/H_2O, 16h (93%); (ii) diethyl (cyanomethyl)phosphonate, LiBr, Et_3N, THF, 16h (96%); (iii) H_2, Ni/Ra, $LiOH{\cdot}H_2O$, Pd/C, dioxane/H_2O; (iv) **A,** DIPEA, CH_2Cl_2 (61%); (v) 4M HCl/dioxane, 2h, quant.; (vi) **B**, K_2CO_3, CH_3CN, 90 °C (59%).

Scheme 2. Synthesis of QPS2[a]

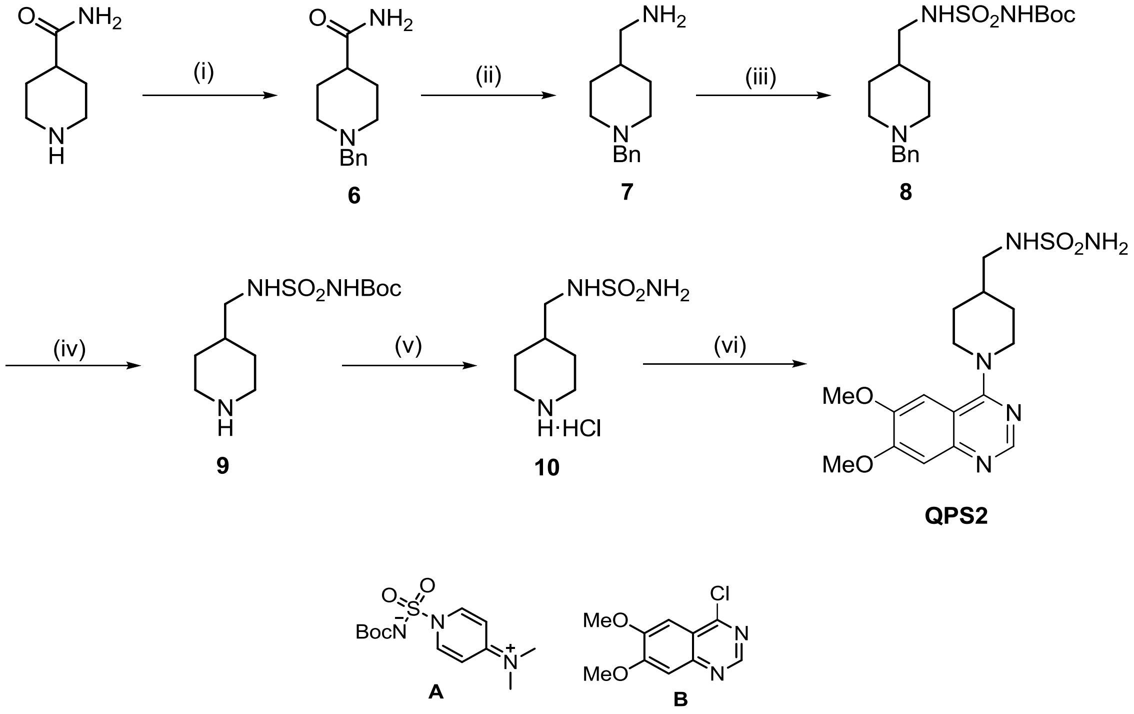
O
NH2
N
H
(i)
O
NH2
N
Bn
6
(ii)
NH2
N
Bn
7
(iii)
NHSO2NHBoc
N
Bn
8
(iv)
NHSO2NHBoc
N
H
9
(v)
NHSO2NH2
N
H·HCl
10
(vi)
NHSO2NH2
N
MeO
MeO
N
N
QPS2
O
O
S
BocN
N
N
A
Cl
MeO
MeO
N
N
B

[a] Conditions: (i) BnBr, K_2CO_3, EtOH, 16h (78%); (ii) $LiAlH_4$, THF, 6h, 70 °C (81%); (iii) **A,** DIPEA, CH_2Cl_2 (77%); (iv); H_2, Pd/C, $PdCl_2$, MeOH, 71% (v) 4M HCl/dioxane, 2h, quant.; (vi) **B**, K_2CO_3, *i*PrOH, 90 °C (78%).

Materials and methods

Synthetic route for QPS1

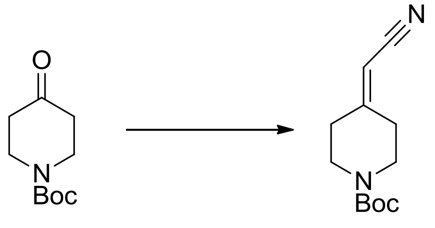

1 **2**

tert-Butyl 4-(cyanomethylene)piperidine-1-carboxylate (2)

Diethyl (cyanomethyl)phosphonate (4.56 mL, 28.2 mmol) and triethylamine (7.56 mL, 54.2 mmol) were added to a stirred solution of LiBr (2.82 g, 32.5 mmol) in THF (120 mL). *tert*-Butyl 4-oxopiperidine-1-carboxylate (**1**)[1] was added after 5 min and the mixture was stirred at ambient temperature overnight. If the reaction wasn't complete, LiBr was added. When the reaction was finished (TLC analysis), solvent was evaporated under vacuum and the mixture was dissolved in AcOEt. The organic layer was washed with $NaHCO_3$ and water. The aqueous layer was extracted with AcOEt and the organic layers were combined, dried over $MgSO_4$ and concentrated. Then the residue was chromatographed on silica gel eluting using 8/2 hexanes/AcOEt to give 5.78 g (96%) of *tert*-butyl 4-(cyanomethylene)piperidine-1-carboxylate (**2**) as a white solid. Mp: 115-118 °C; IR (ATR, ZnSe) = 3012, 2936, 2216, 1677, 1426, 1360, 1324, 827, 785 cm^{-1}; ^1H NMR ($CDCl_3$): δ (ppm) 5.20 (s, 1H), 3.51 (dt, *J* = 11.8 Hz, *J* = 5.7 Hz, 4H), 2.56 (t, *J* = 5.6 Hz, 2H), 2.33 (t, *J* = 5.3 Hz, 2H), 1.48 (s, 9H); ^{13}C NMR ($CDCl_3$): δ (ppm) 163.4, 154.2, 116.1, 94.3, 80.2, 44.1 (2C), 34.9, 32.5, 28.3; HRMS-ESI calcd for $C_{12}H_{18}N_2NaO_2$ $[M+Na]^+$ 245.1260 found 245.1258.

---

[1] Wang, Z.; Miller, E. J.; Scalia, S. J. *Org. Lett.* **2011**, 1*3*, 6540-6543.

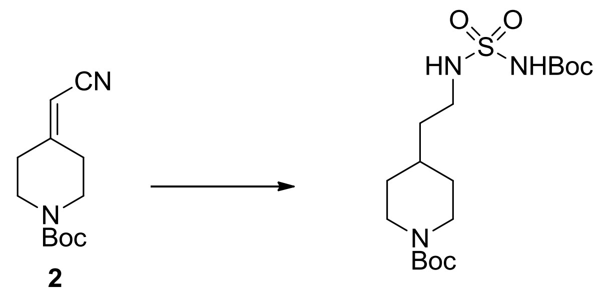

2 → **4**

tert-Butyl 4-(cyanomethylene)piperidine-1-carboxylate (4)

Acrylonitrile **2** (700 mg, 3.15 mmol) was dissolved in a mixture of dioxane (15 mL) and water (5 mL). Raney-Nickel (699 mg, 5.95 mmol) as a 50% suspension in water and 10% palladium of charcoal (210 mg, 0.197 mmol) were added with lithium hydroxide monohydrate (285 mg, 6.80 mmol), and the mixture was stirred under hydrogen atmosphere at ambient temperature overnight. The catalyst was filtered on celite, the solvents were removed under vacuum and the residue was used directly in the next step without further purification. The crude product, sulfamoylating agent **A**[2] (949 mg, 3.15 mmol) and DIPEA (0.82 mL, 4.73 mmol) were stirred 16 h, at room temperature in 60 mL of dichloromethane. Then the mixture was washed with NH_4Cl (2 ×) and brine. The organic layers were combined, dried over $MgSO_4$, concentrated, then the residue was chromatographed on silica gel, eluting using 7/3 hexanes/AcOEt to give *tert*-butyl 4-(cyanomethylene)piperidine-1-carboxylate **4** as a white solid (778 mg, 61% over 2 steps). Mp: 145-151 °C; IR (ATR, ZnSe) = 3307, 1722, 1659, 1478, 1211, 930, 785, 727 cm^{-1}; ^{1}H NMR ($CDCl_3$): δ (ppm) 7.46 (s, 1H, NH), 5.17 (t, *J* = 6.1 Hz, 1H, NH), 4.09 (br s, 2H), 3.13-3.09 (m, 2H), 2.68 (br s, 2H), 1.66 (d, *J* = 12.8 Hz, 2H), 1.54-1.48 (m, 12H), 1.46 (s, 9H), 1.14-1.06 (m, 2H); ^{13}C NMR ($CDCl_3$): δ (ppm) 154.8, 150.3, 83.8, 79.4, 43.8, 41.2, 35. 6, 33.1, 31.7, 28. 5, 28.0; HRMS-ESI calcd for $C_{17}H_{33}N_3NaO_6S$ $[M+Na]^+$ 430.1982 found 430.1982.

---

[2] Winum, J-Y.; Toupet, L.; Barragan, V.; Dewynter, G.; Montero, J-L. *Org. Lett.* **2001**, *3*, 2241-2243.

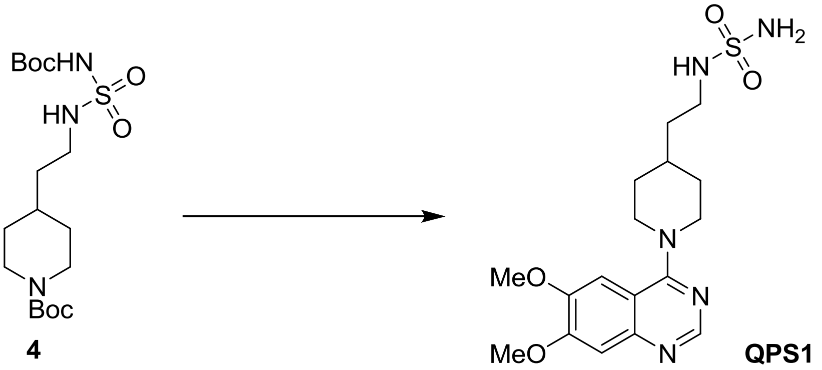

2-(1-(6,7-Dimethoxyquinazolin-4-yl)piperidin-4-yl)ethyl sulfamide (QPS1)

In a round-bottomed flask, 11.9 mL of HCl in dioxane (4 M) was added on sulfamide **4** (324 mg, 0.80 mmol). After 2 h, Boc deprotection was completed and solvent was evaporated under vacuum to give **5** in quantitative yield. The piperidine salt was dissolved in acetonitrile (12 mL) and stirred overnight at 90 °C. The solvent was removed under vacuum and the product was purified by flash column chromatography, eluting using 9/1 CH_2Cl_2/MeOH to give the desired product **QPS1** as a beige solid (170 mg, 59%). Mp: 156-160 °C; IR (ATR, ZnSe) = 3311, 2855, 1577, 1455, 1376, 1263, 861, 794 cm^{-1}; ^1H NMR (DMSO-d_6): δ (ppm) 8.51 (s, 1H), 7.20 (s, 1H), 7.10 (s, 1H), 6.50 (s, 2H), 4.14 (d, *J* = 13.1 Hz, 2H), 3.93 (s, 3H), 3.91 (s, 3H), 3.02 (t, *J* = 11.8 Hz, 2H), 2.96-2.94 (m, 2H), 1.81 (d, *J* = 10.9 Hz, 2H), 1.74–1.65 (m, 1H), 1.51-1.47 (m, 2H), 1.41-1.32 (m, 2H); ^{13}C NMR (MeOD-d_4): δ (ppm) 165.2, 156.5, 153.4, 150.1, 149.4, 112.3, 107.0, 105.0, 56.6, 56.5, 51.3, 41. 6, 37.2, 34.8, 33.2; HRMS-ESI calcd for $C_{17}H_{26}N_5O_4S$ $[M+H]^+$ 396.1700 found 396.1710.

Synthetic route for QPS2

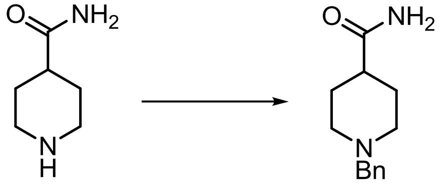

6

1-Benzylpiperidine-4-carboxamide (6)

To a stirred suspension of isonipectamide (5.0 g, 39 mmol) and K_2CO_3 (10.78 g, 78.02 mmol) in EtOH (210 mL) was added benzylbromide (5.10 mL, 42.90 mmol) and the mixture was heated under reflux overnight, cooled to room temperature and filtered. The filtrate was evaporated under vacuum and H_2O was added. The aqueous layer was extracted with dichloromethane (× 3), the organic layers combined and dried over $MgSO_4$ and filtrated. The solvent was evaporated under vacuum to give 1-benzylpiperidine-4-carboxamide (**6**) as a yellowish solid (6.66 g, 78%). Mp: 156-159 °C; IR (ATR, ZnSe) = 3329, 3151, 2922, 1627, 1494, 1432, 1390, 1148, 1129, 734, 698 cm^{-1}; ^1H NMR ($CDCl_3$): δ (ppm) 7.33-7.31 (m, 4H), 7.28-7.24 (m, 1H), 5.65 (br s, 1H), 5.52 (br s, 1H), 3.51 (s, 2H), 2.96-2.92 (m, 2H), 2.16 (tt, *J* = 11.8, 4.0 Hz, 1H), 2.01 (td, *J* = 11.7, 2.5 Hz, 2H), 1.89-1.84 (m, 2H), 1.80-1.71 (m, 2H); ^{13}C NMR ($CDCl_3$): δ (ppm) 178.2, 138.1, 129.1, 128.2, 127.0, 63.1, 53.0, 42.7, 28.8; HRMS-ESI calcd for $C_{13}H_{19}N_2O$ $[M+H]^+$ 219.1492 found 219.1493.

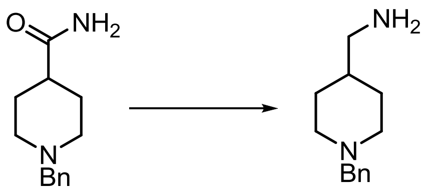

6 **7**

(1-Benzylpiperidin-4-yl)methanamine (7)

To a suspension of **6** (2.0 g, 9.2 mmol) in dry THF (24 mL) was added slowly to a solution of $LiAlH_4$ (0.52 g, 13.7 mmol) in dry THF (30 mL). The mixture was stirred under reflux and argon atmosphere for 6 h. After cooling, water was added at 0 °C, the precipitate was filtered and washed with Et_2O. The filtrate was extracted with Et_2O (× 2), dried over $MgSO_4$ and the solvent was evaporated under vacuum to give (1-benzylpiperidin-4-yl)methanamine (**7**) as an orange solid (1.52 g, 81%). Mp: 86-90 °C; IR (ATR, ZnSe) = 3344, 3024, 2933, 1579, 1476, 1230, 1029, 740, 698 cm^{-1}; ^{1}H NMR ($CDCl_3$): δ (ppm) 7.31-7.26 (m, 5H), 3.49 (s, 2H), 2.90 (d, *J* = 11.8 Hz, 2H), 2.57 (d, *J* = 5.9 Hz, 2H), 1.94 (t, *J* = 11.2 Hz, 2H), 1.70-1.67 (m, 2H), 1.29-1.21 (m, 3H); ^{13}C NMR ($CDCl_3$): δ (ppm) 138.6, 129.2, 128.1, 126.9, 63.5, 53. 7, 48.2, 39.4, 30.0; HRMS-ESI calcd for $C_{13}H_{21}N_2$ $[M+H]^+$ 205.1699 found 205.1699.

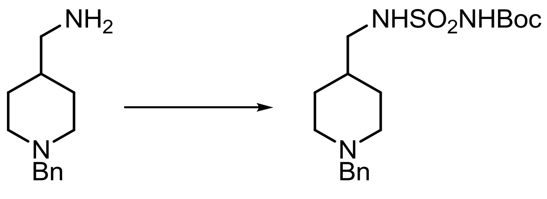

7 **8**

tert-Butyl N-((1-benzylpiperidin-4-yl)methyl)sulfamoylcarbamate (8)

Amine **7** (2.58 g, 12.6 mol), sulfamoylating agent **A**[1] (3.81 g, 12.6 mmol) and DIPEA (3.30 mL, 18.9 mmol) were stirred 16 h, at room temperature in dichloromethane (200 mL). Then the mixture was washed with NH_4Cl (× 2) and brine. The organic layers were combined, dried over $MgSO_4$, concentrated, then the residue was chromatographed on silica gel, eluting using 9/1 CH_2Cl_2/MeOH to give *tert*-butyl *N*-((1-benzylpiperidin-4-yl)methyl)sulfamoylcarbamate (**8**) as a white solid (3.74 g, 77%). Mp: 135 °C (dec.); IR (ATR, ZnSe) = 1644, 1494, 1457, 1294, 1150, 1135, 1088, 843, 770, 746, 696 cm^{-1}; ^1H NMR (DMSO-d_6): δ (ppm) 7.49 (Br s, 1H), 7.49-7.22 (m, 5H), 3.45 (s, 2H), 2.78-2.72 (m, 4H), 1.89 (t, *J* = 11.0 Hz, 2H), 1.64 (d, *J* = 11.9 Hz, 2H), 1.40 (s, 9H), 1.12-1.05 (m, 2H); ^{13}C NMR (MeOD-d_4): δ (ppm) 153.5, 134.9, 129. 8, 128.0, 127. 6, 80.4, 62.1, 52.4, 34.9, 28.4, 27.0; HRMS-ESI calcd for $C_{18}H_{30}N_3O_4S$ $[M+H]^+$ 384.1952 found 384.1962.

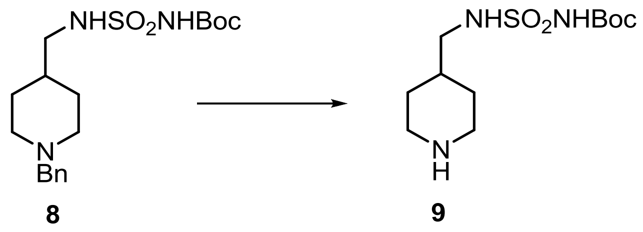

tert-Butyl *N*-(piperidin-4-ylmethyl)sulfamoylcarbamate (9)

10 % Pd on activated charcoal (57 mg, 0.54 mmol) and $PdCl_2$ (5 mg, 0.03 mmol) was added to **8** (207 mg, 0.54 mmol) in MeOH (15 mL). The mixture was hydrogenated under H_2 atmosphere overnight. After filtration through a pad of Celite, the filtrate was evaporated to give *tert*-butyl *N*-(piperidin-4-ylmethyl)sulfamoylcarbamate (**9**) (113 mg, 71%) as a white solid. Mp: 150 °C (dec.); IR (ATR, ZnSe) = 2928, 2492, 1652, 1283, 1141, 1087, 979, 910, 851, 795, 747 cm^{-1}; ^1H NMR (DMSO-d_6): δ (ppm) 3.20 (d, J = 12.3 Hz, 2H), 2.75 (t, J = 11.2 Hz, 2H), 2.62 (d, J = 6.6 Hz, 2H), 1.79 (d, J = 13.0 Hz, 2H), 1.65 (Br s, 1H), 1.36-1.21 (m, 5H); ^{13}C NMR δ (ppm) 155.1, 78.7, 67.3, 48.4, 43.2, 33.7, 31.7, 28.4, 26.6; HRMS-ESI calcd for $C_{11}H_{24}N_3O_4S$ $[M+H]^+$ 294.1482 found 294.1485.

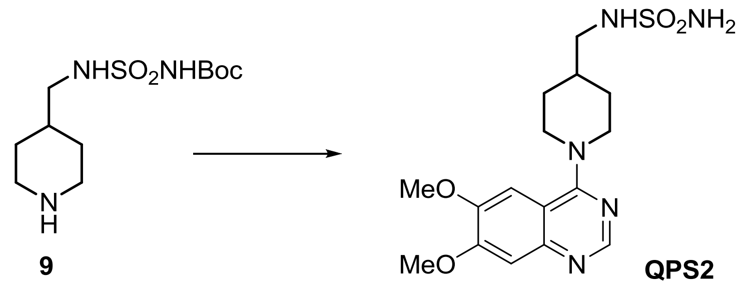

((1-(6,7-Dimethoxyquinazolin-4-yl)piperidin-4-yl)methyl)sulfamide (QPS2)

In a round-bottomed flask, 3 mL of HCl in dioxane (4 M) was added on sulfamide **9** (118 mg, 0.40 mmol). After 2 h, Boc deprotection was completed and solvent was evaporated under vacuum to give the amine hydrochloride **10** in quantitative yield. The piperidine salt was dissolved in isopropanol (25 mL) and stirred overnight under reflux. The solvent was removed under vacuum and the product was purified by flash column chromatography, eluting using 9/1 CH_2Cl_2/MeOH to give the desired product **QPS2** as a yellowish solid (120 mg, 78%). Mp: 95-100 °C; IR (ATR, ZnSe) = 3269, 2915, 1576, 1504, 1427, 1333, 1245, 1206, 991, 929, 852, 786 cm^{-1}; ^{1}H NMR (DMSO-d_6): δ (ppm) 8.50 (s, 1H), 7.19 (s, 1H), 7.10 (s, 1H), 6.59 (t, *J* = 6.1 Hz, 1H), 6.49 (s, 2H), 4.14 (d, *J* = 13.3 Hz, 2H), 3.92 (s, 3H), 3.90 (s, 3H), 3.02 (t, *J* = 12.0 Hz, 2H), 2.83 (t, *J* = 6.4 Hz, 2H), 1.86-1.79 (m, 3H), 1.39-1.33 (m, 2H); ^{13}C NMR (DMSO-d_6): δ (ppm) 163.6, 154.5, 152.9, 148.9, 148.4, 111.0, 107. 6, 103.8, 56.3, 56.0, 49.8, 48.5, 36.2, 30.0; HRMS-ESI calcd for $C_{16}H_{24}N_5O_4S$ $[M+H]^+$ 382.1544 found 382.1552.

NMR spectra of all the new compounds

Figure S1: ^{1}**H NMR spectrum of compound 2**

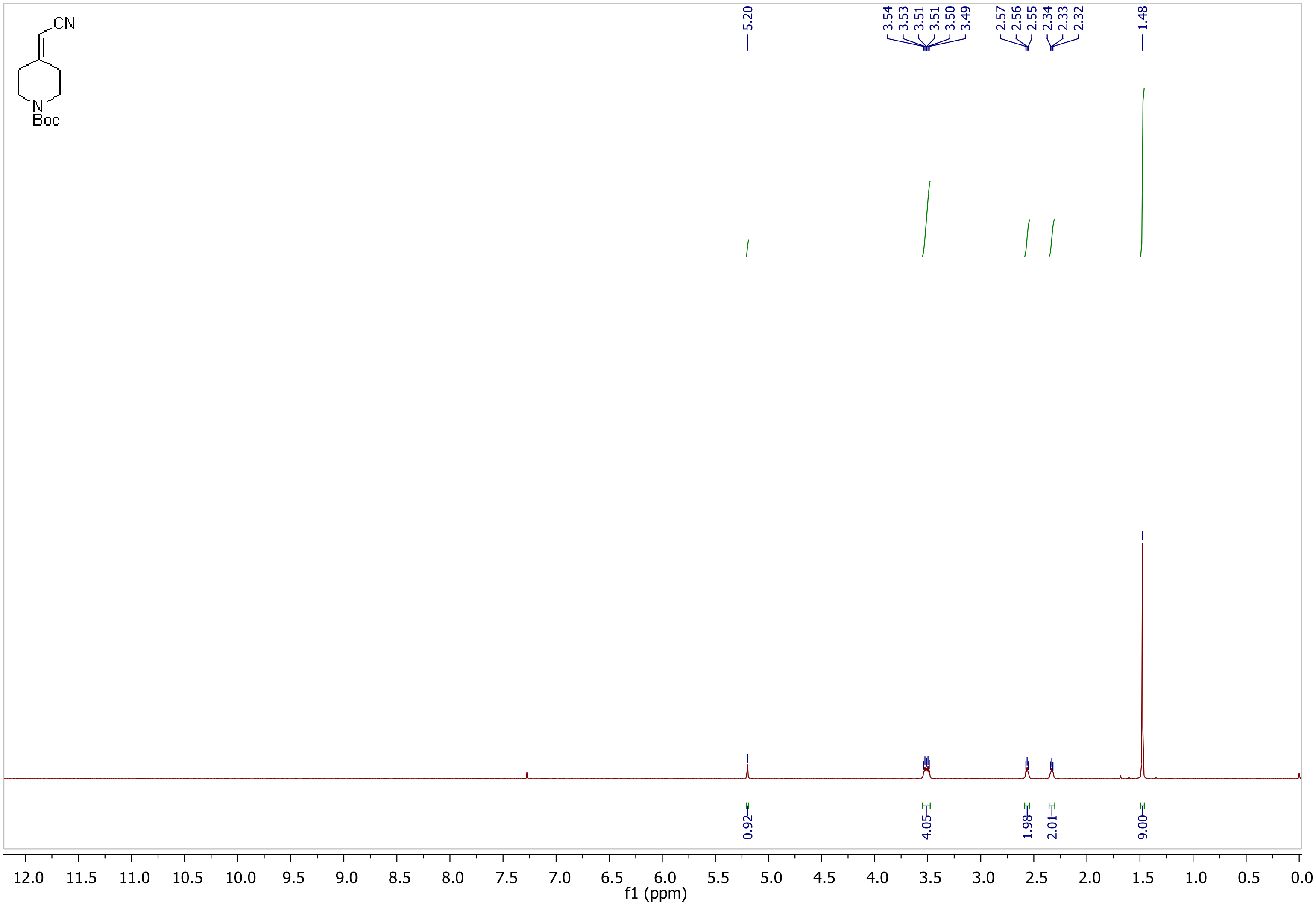

Figure S2: ^{13}**C NMR spectrum of compound 2**

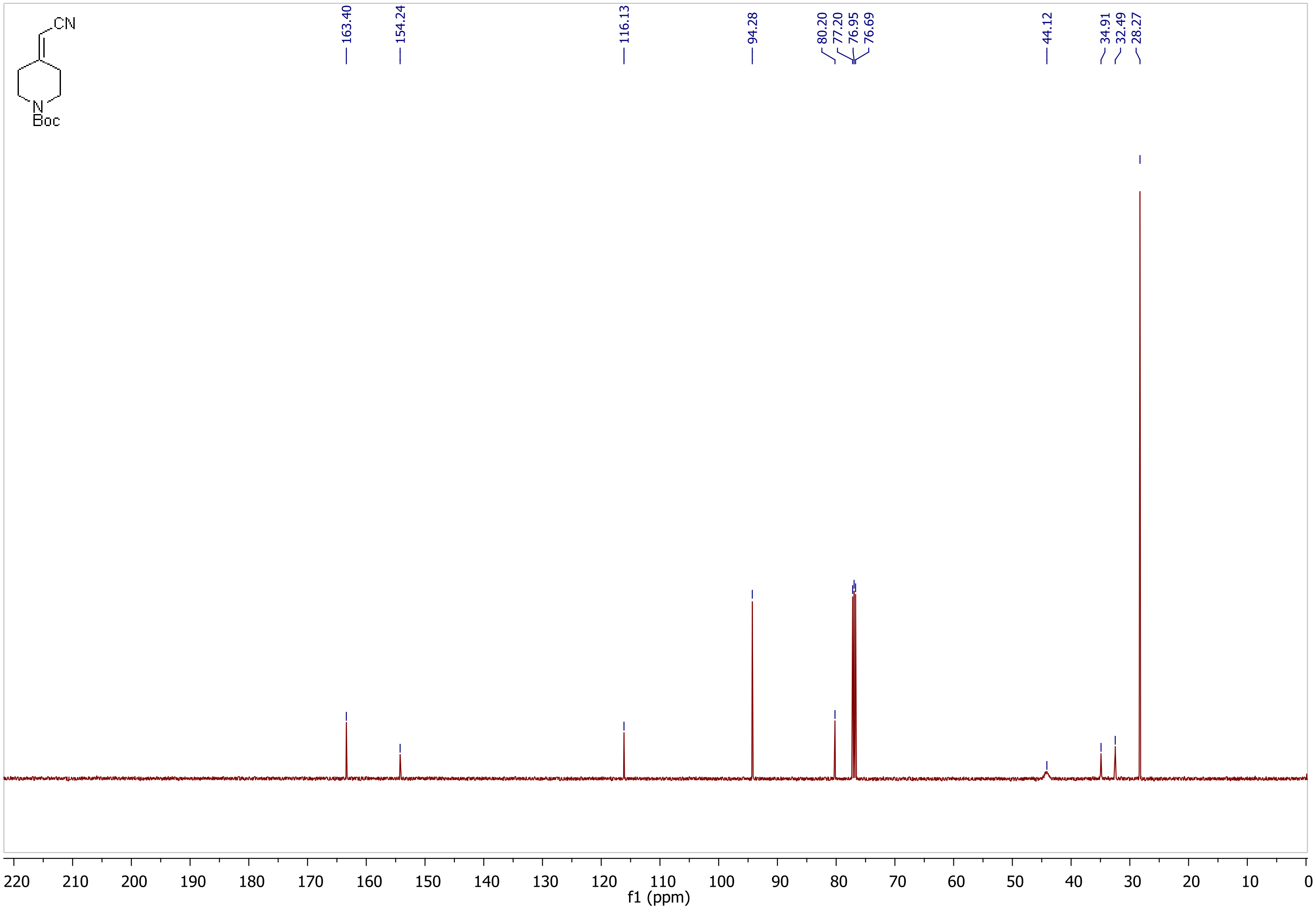

Figure S3: ^{1}**H NMR spectrum of compound 4**

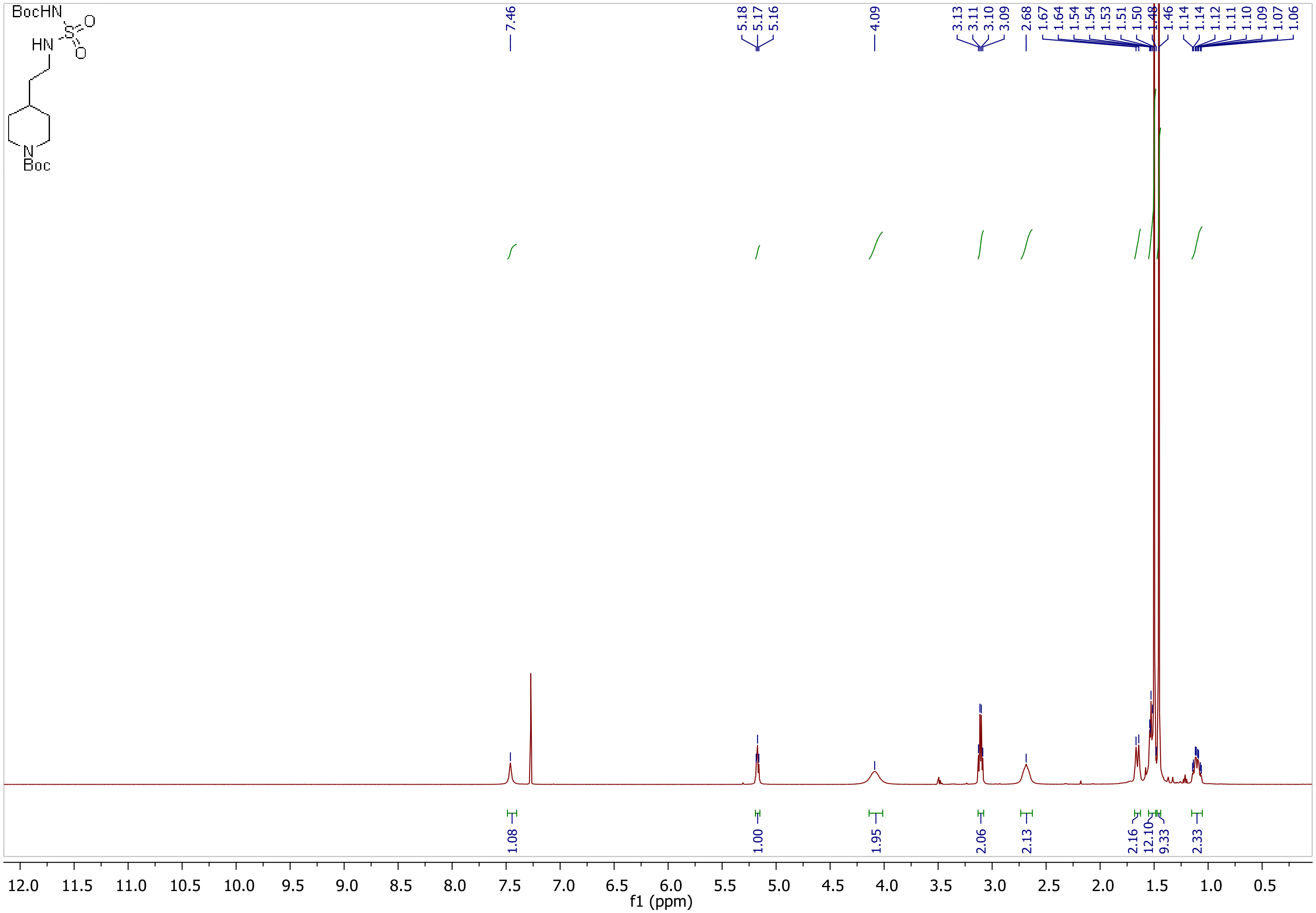

Figure S4: **^{13}C NMR spectrum of compound 4**

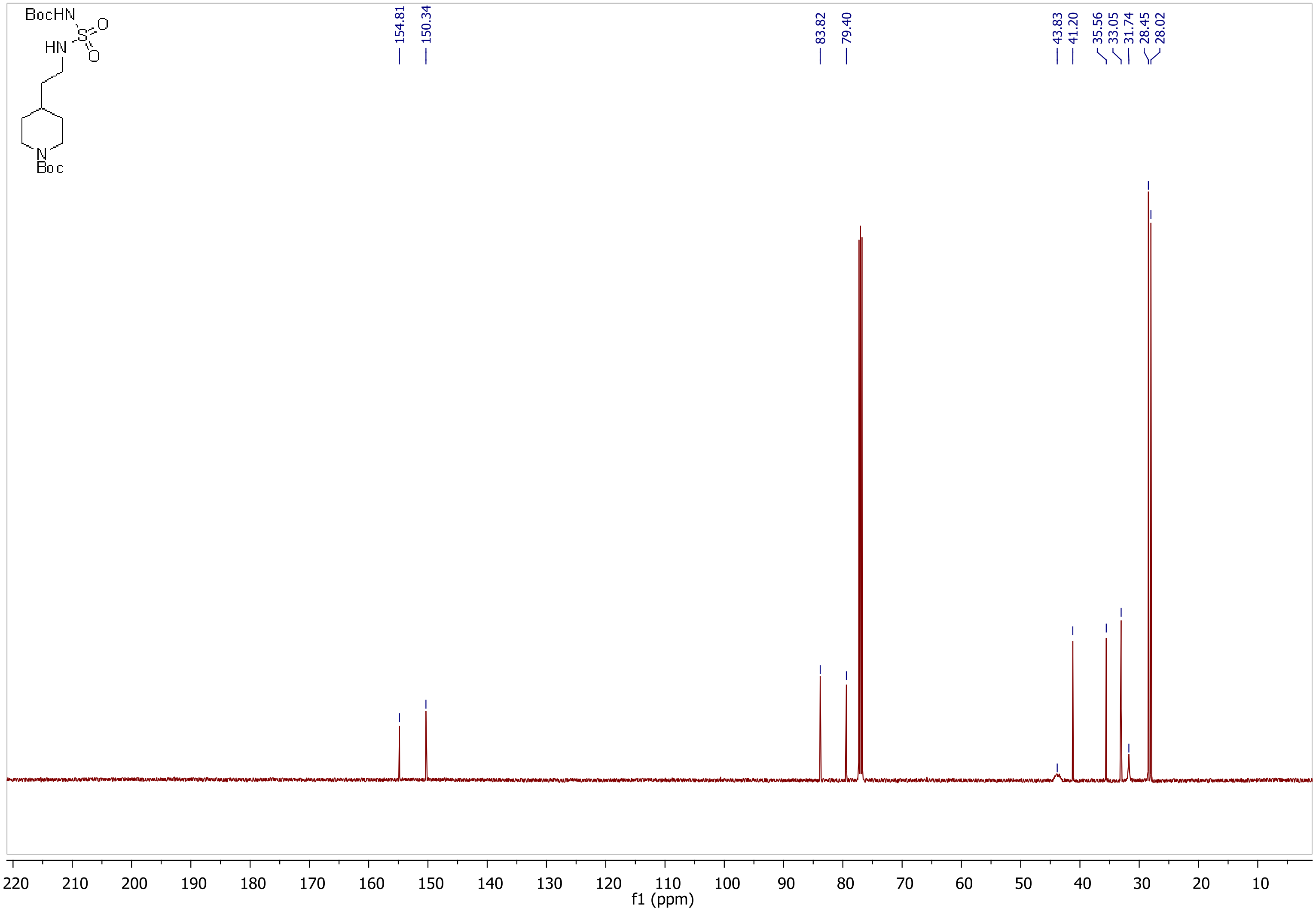

Figure S5: **^{1}H NMR spectrum of compound QPS1**

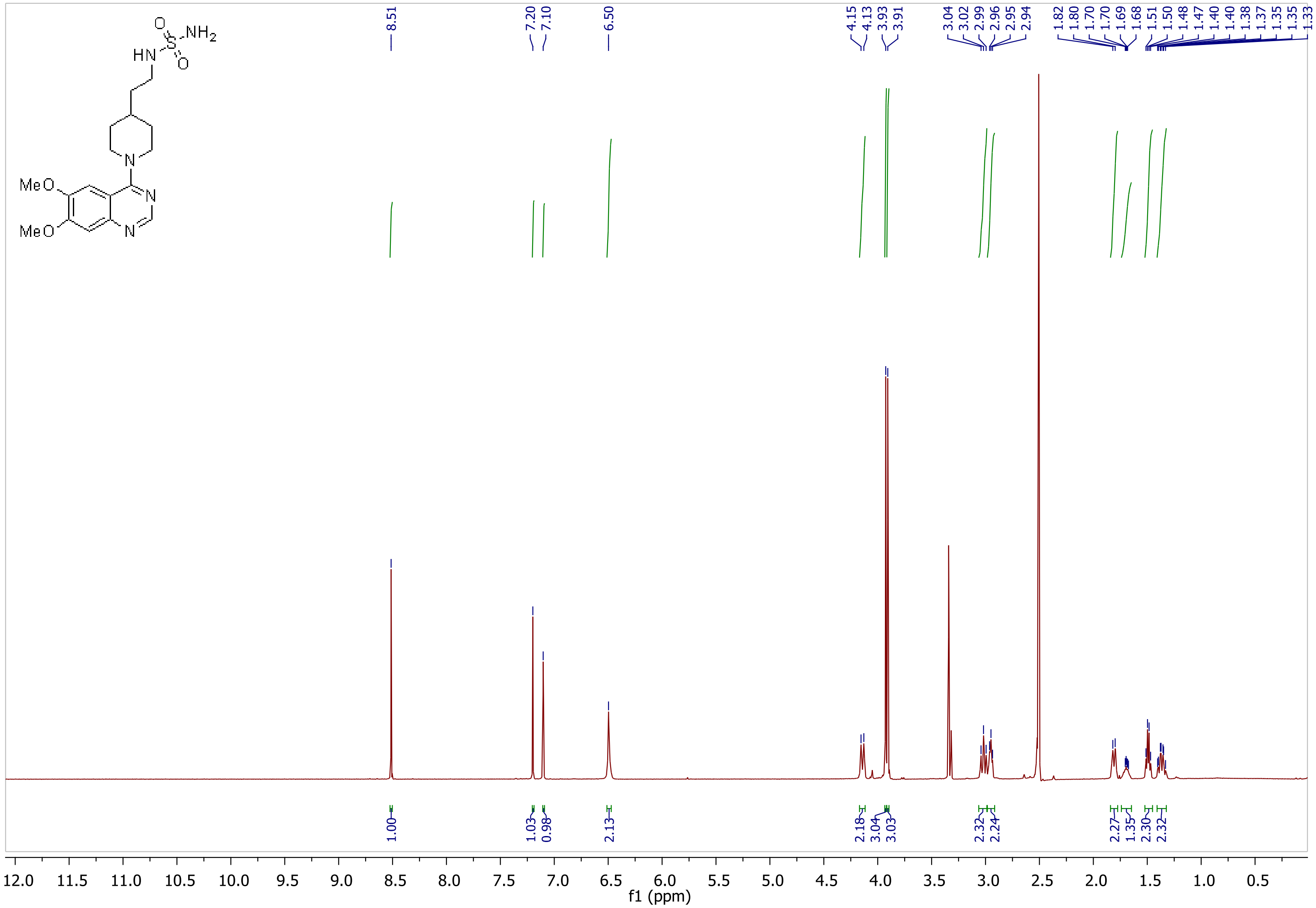

Figure S6: ^{13}C NMR spectrum of compound QPS1

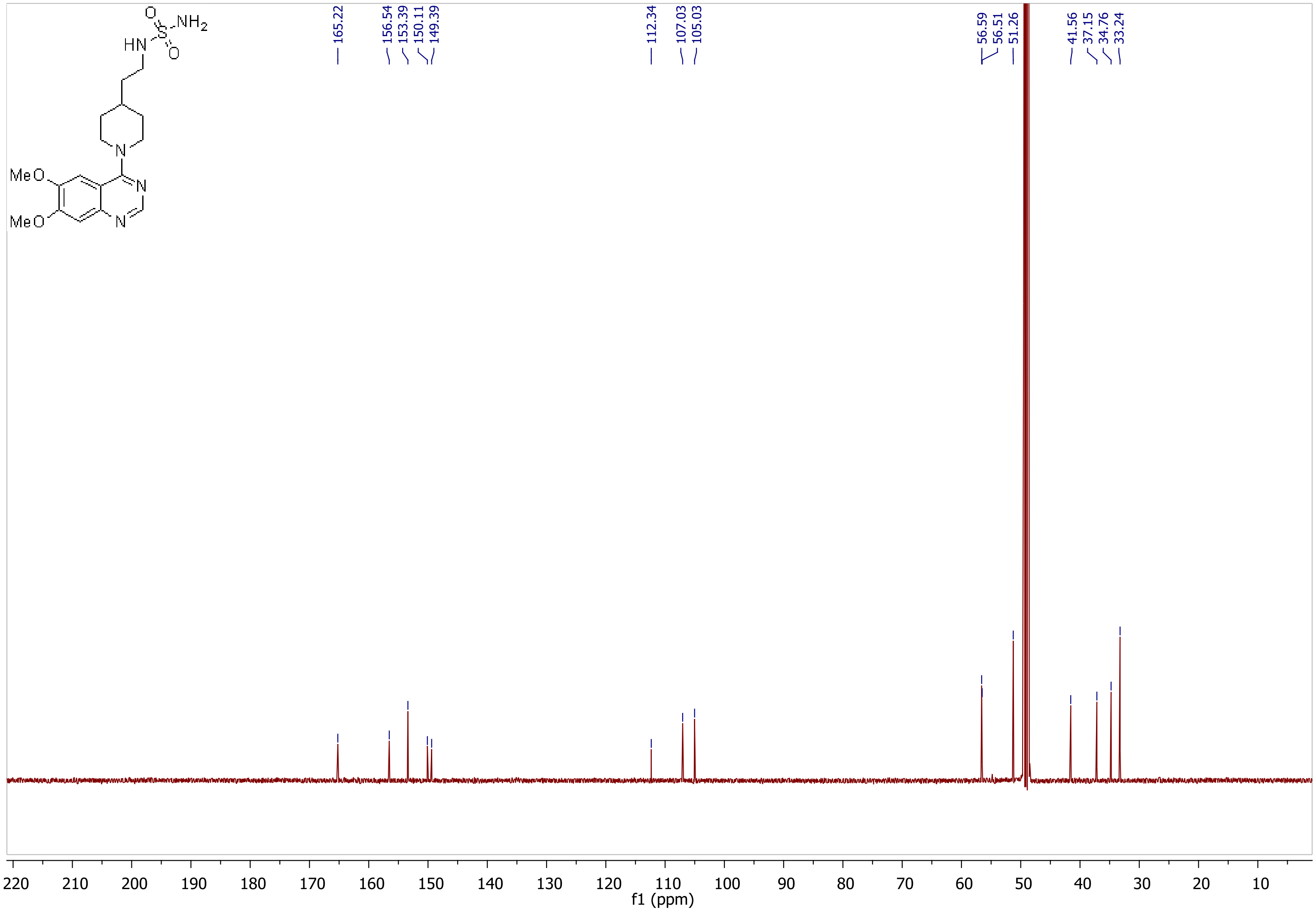

Figure S7: **^{1}H NMR spectrum of compound 6**

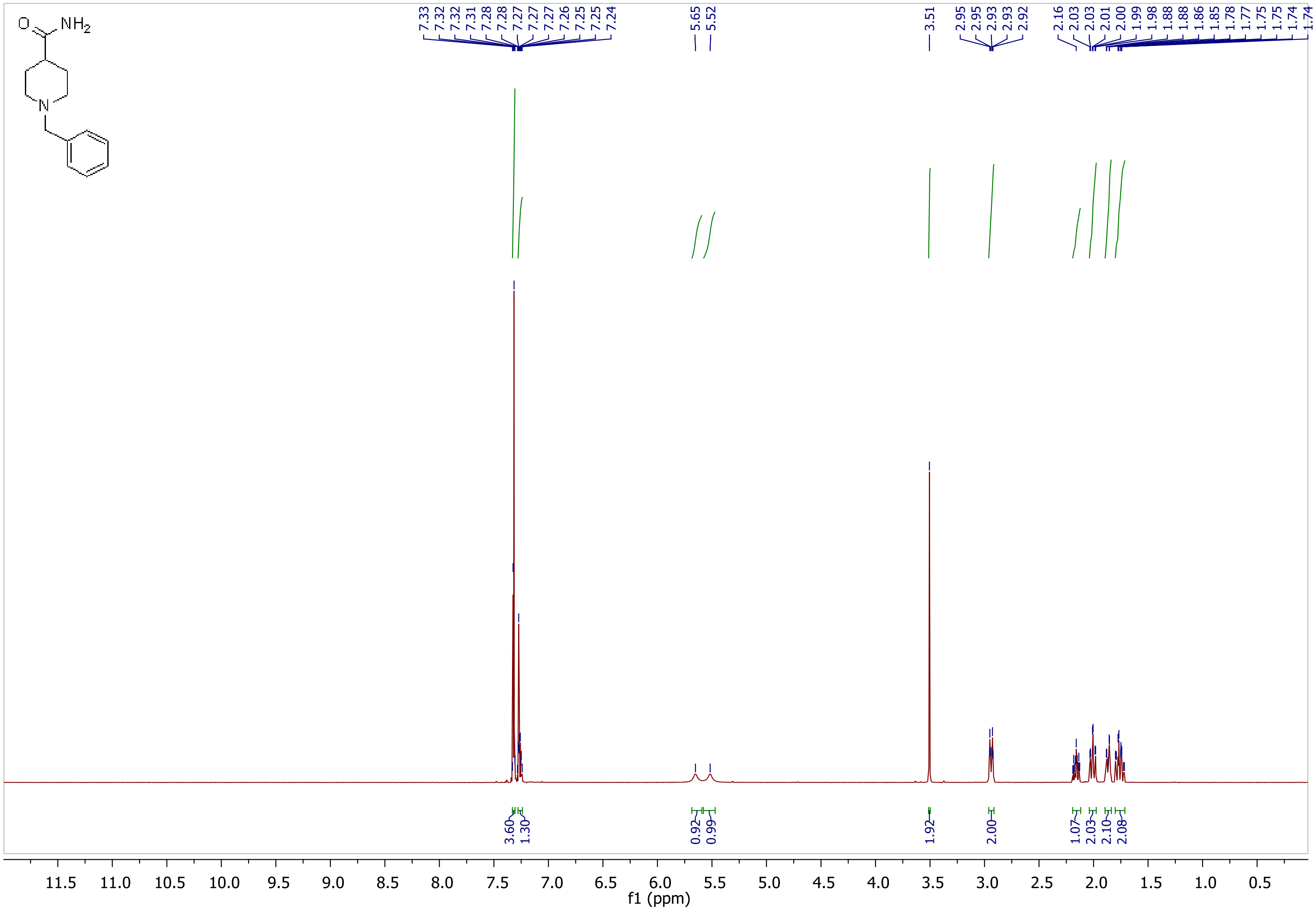

Figure S8: **^{13}C NMR spectrum of compound 6**

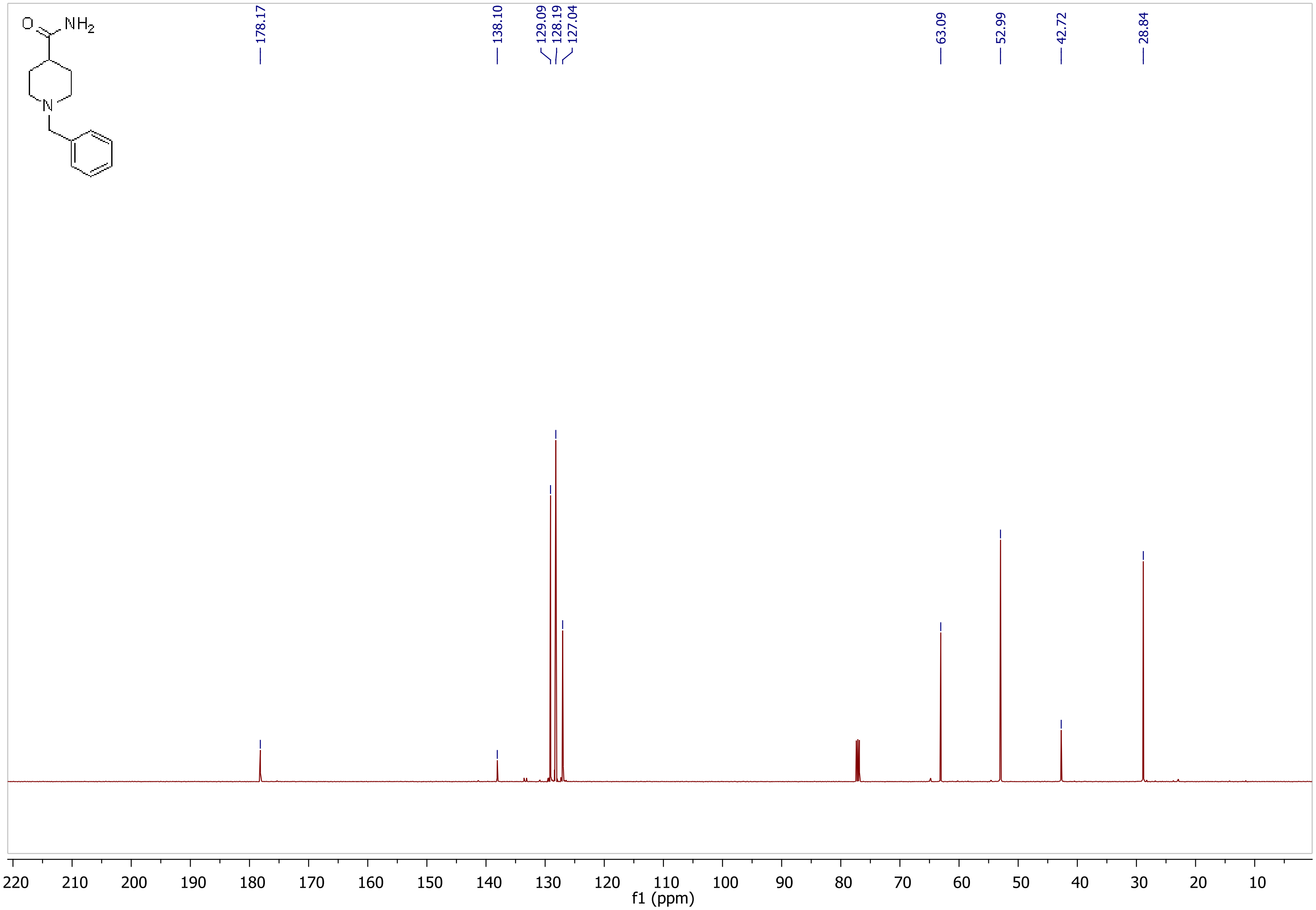

Figure S9: ^{1}**H NMR spectrum of compound 7**

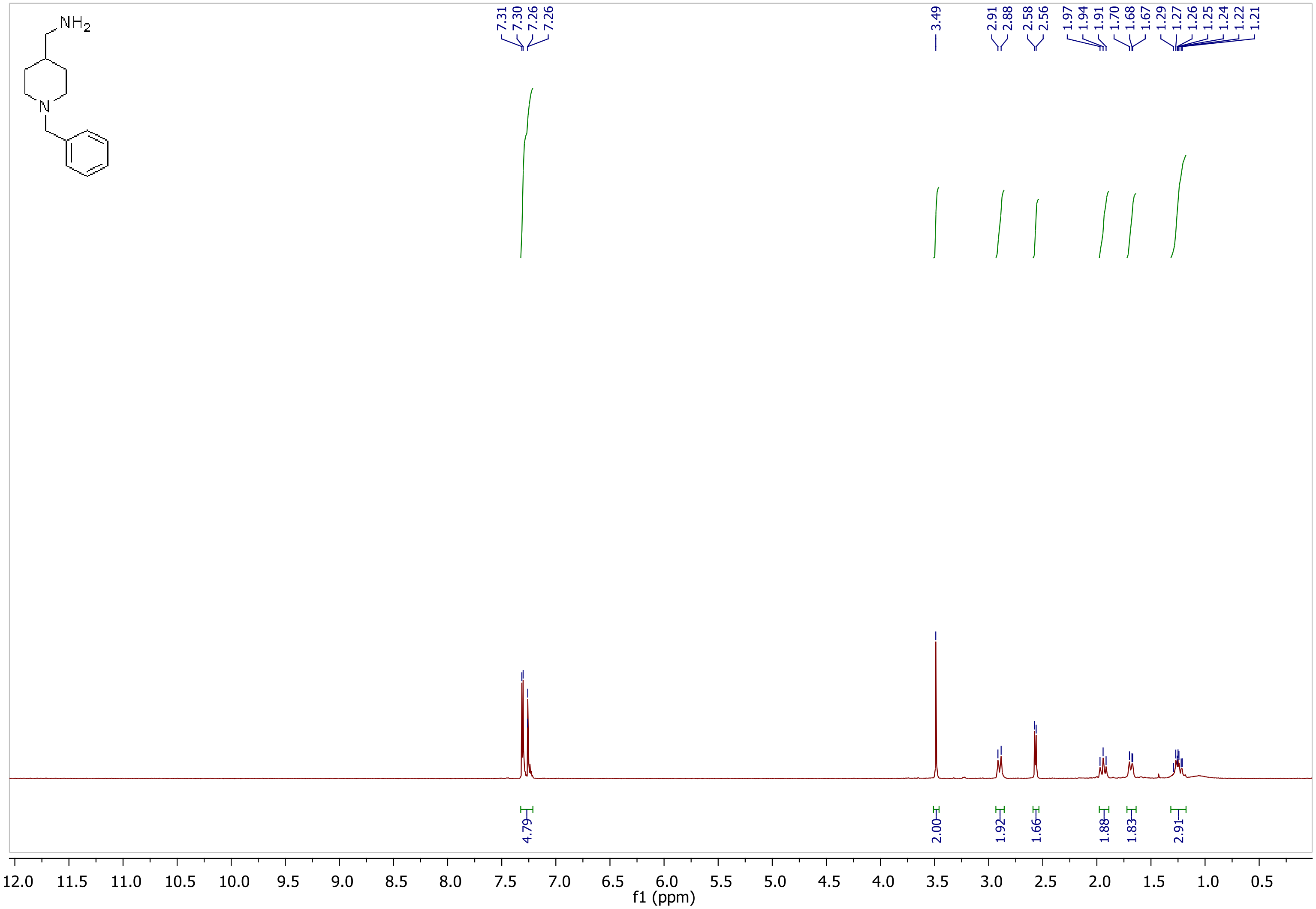

Figure S10: ^{13}**C NMR spectrum of compound 7**

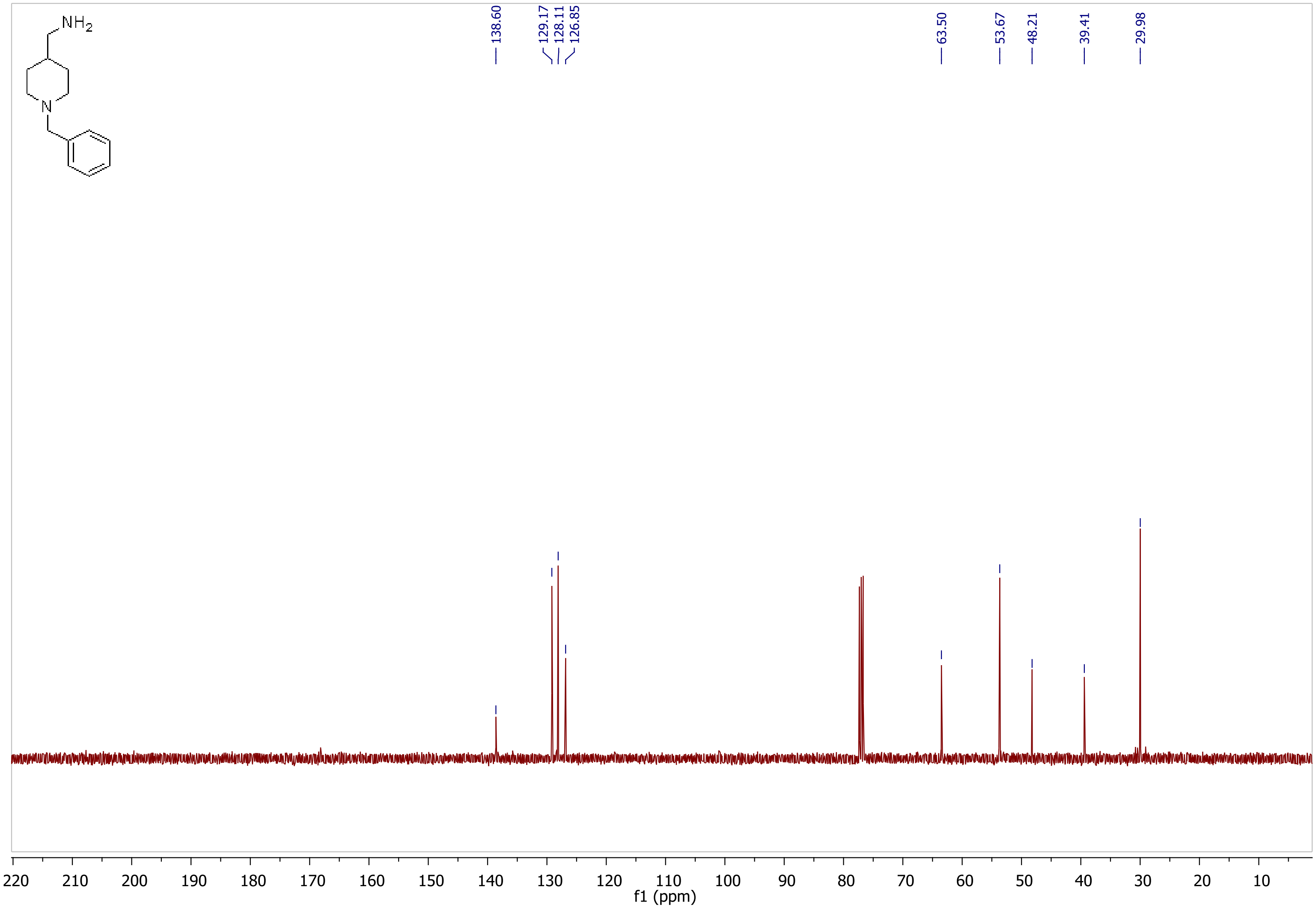

Figure S11: ^{1}**H NMR spectrum of compound 8**

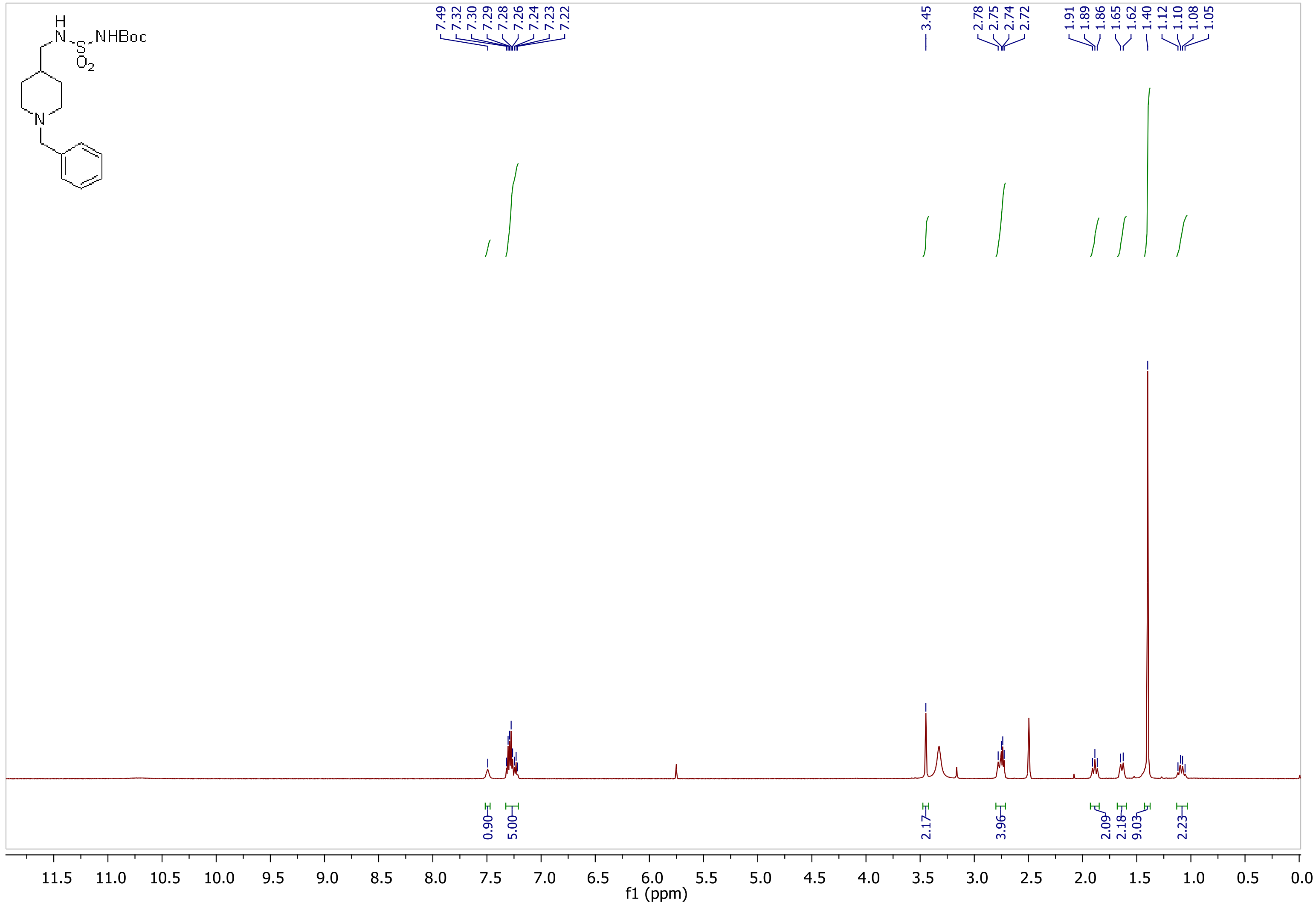

Figure S12: **^{13}C NMR spectrum of compound 8**

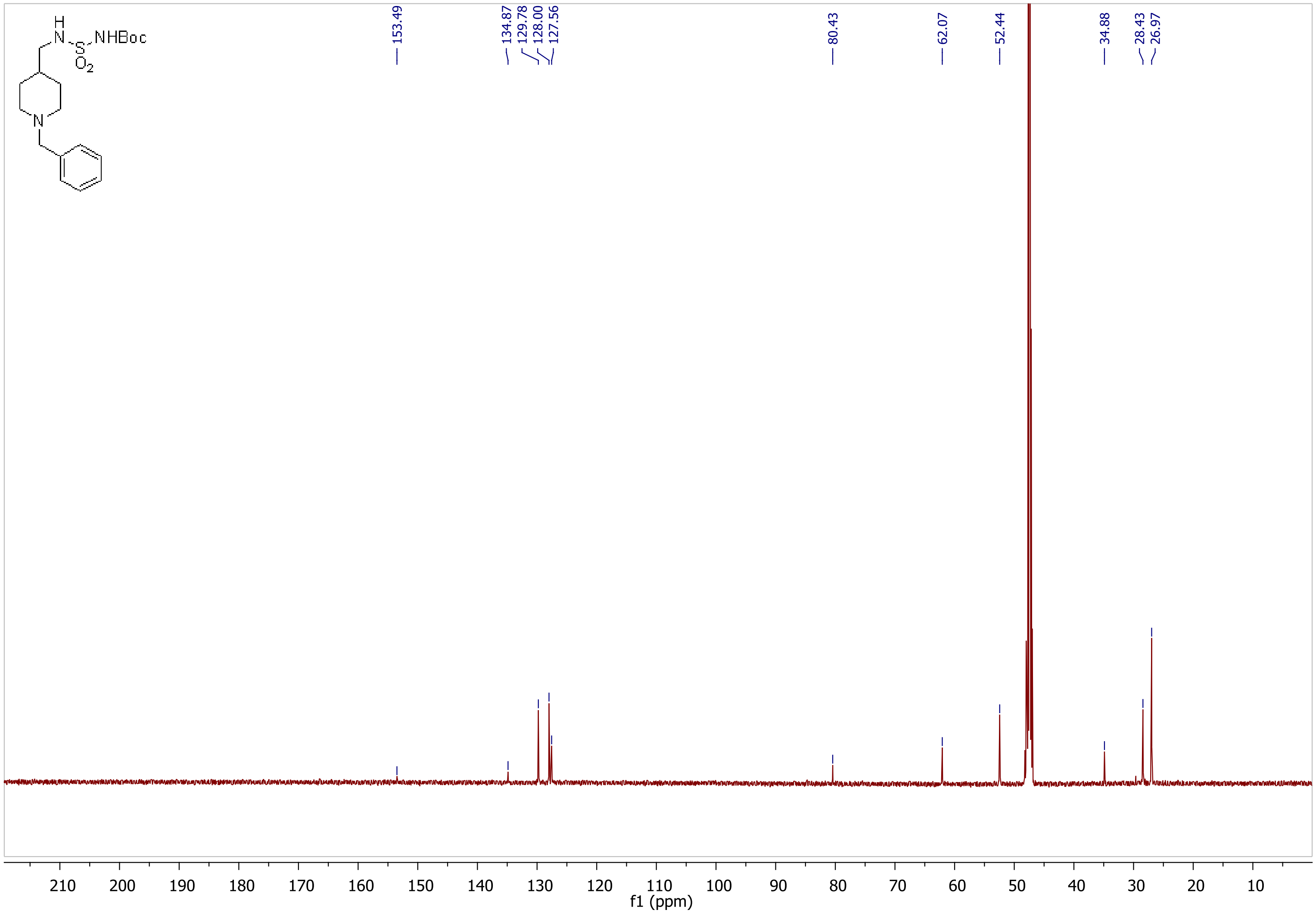

Figure S13: ^{1}**H NMR spectrum of compound 9**

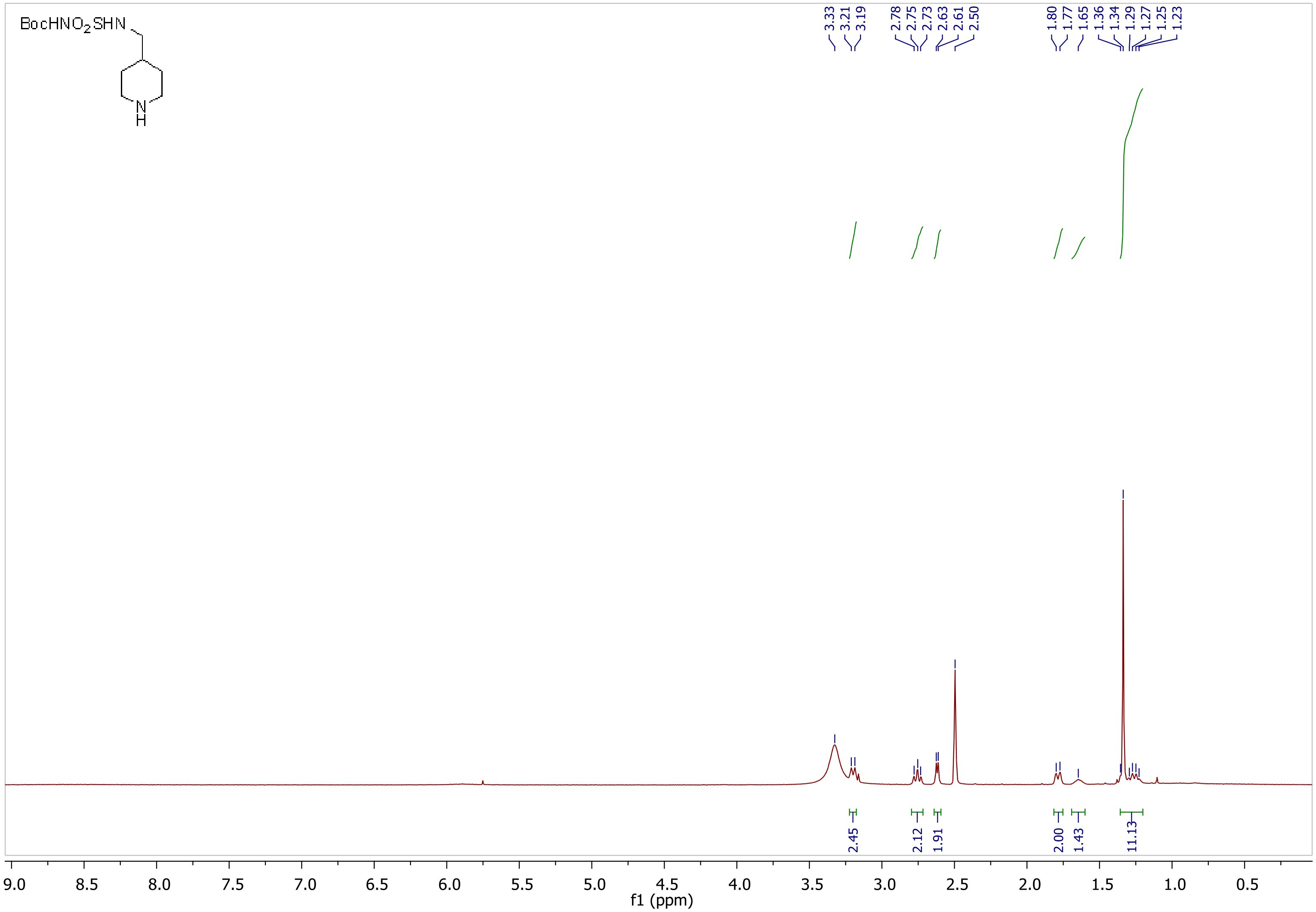

Figure S14: **^{13}C NMR spectrum of compound 9**

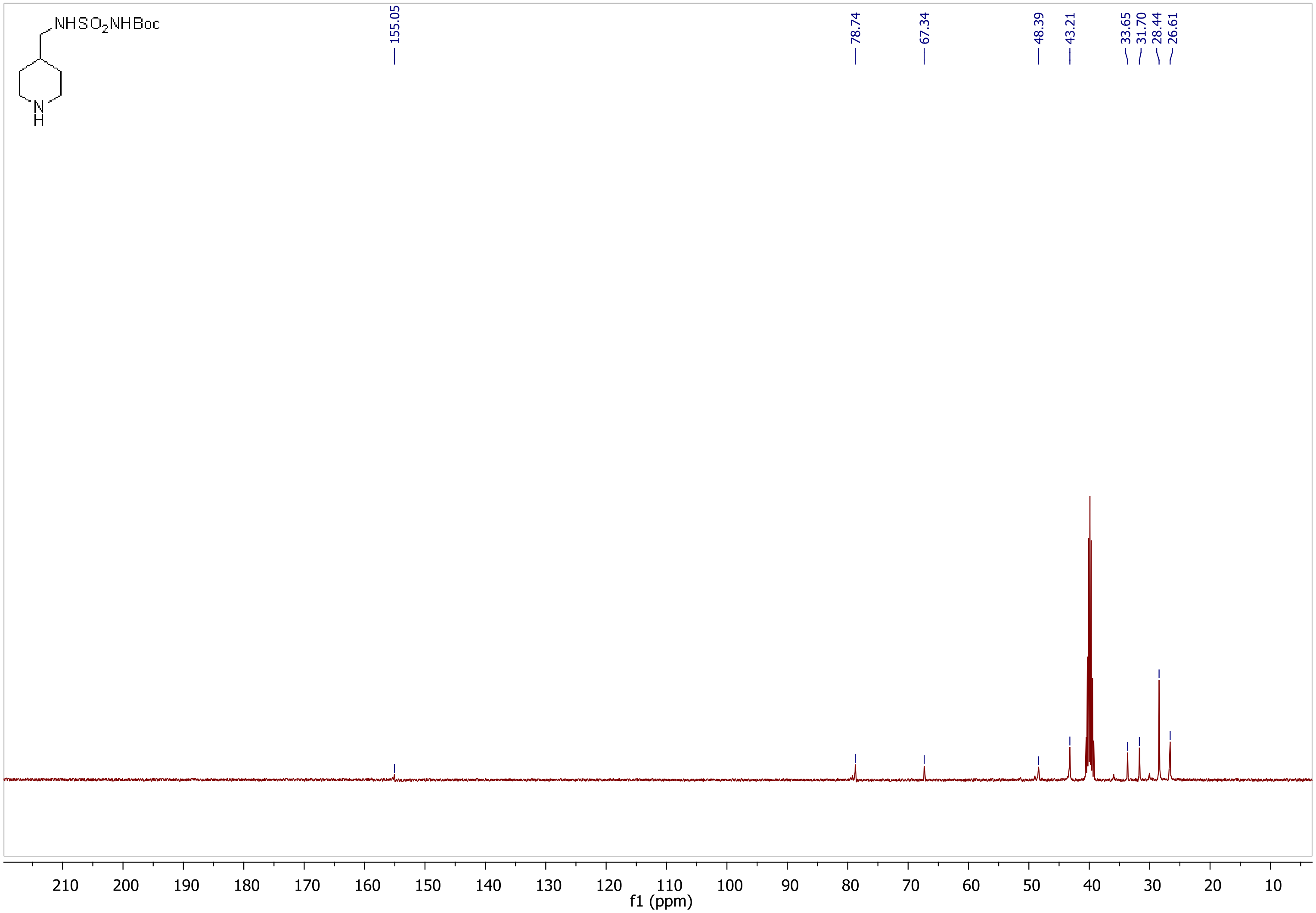

Figure S15: **^{1}H NMR spectrum of compound QPS2**

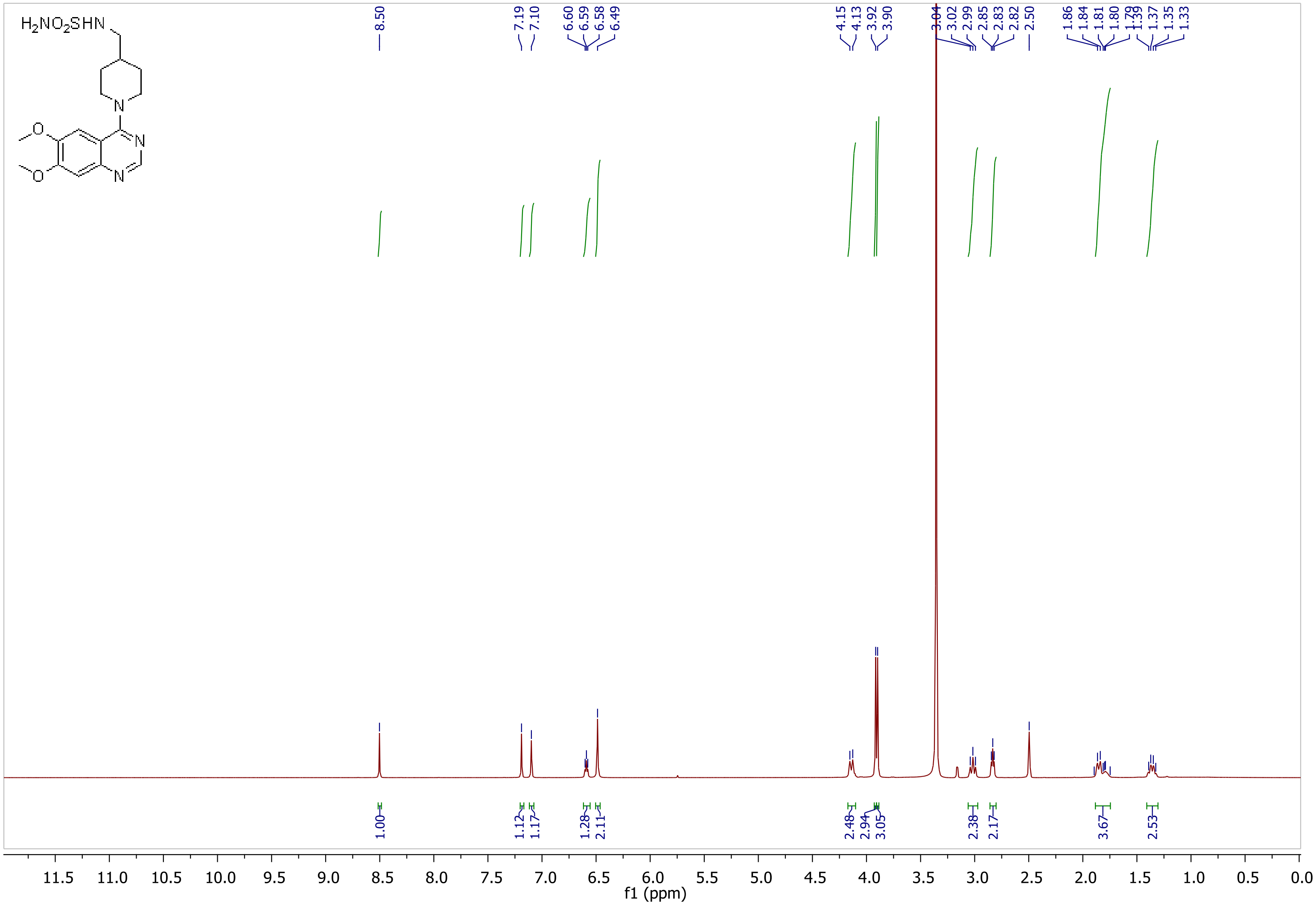

Figure S16: **^{13}C NMR spectrum of compound QPS2**

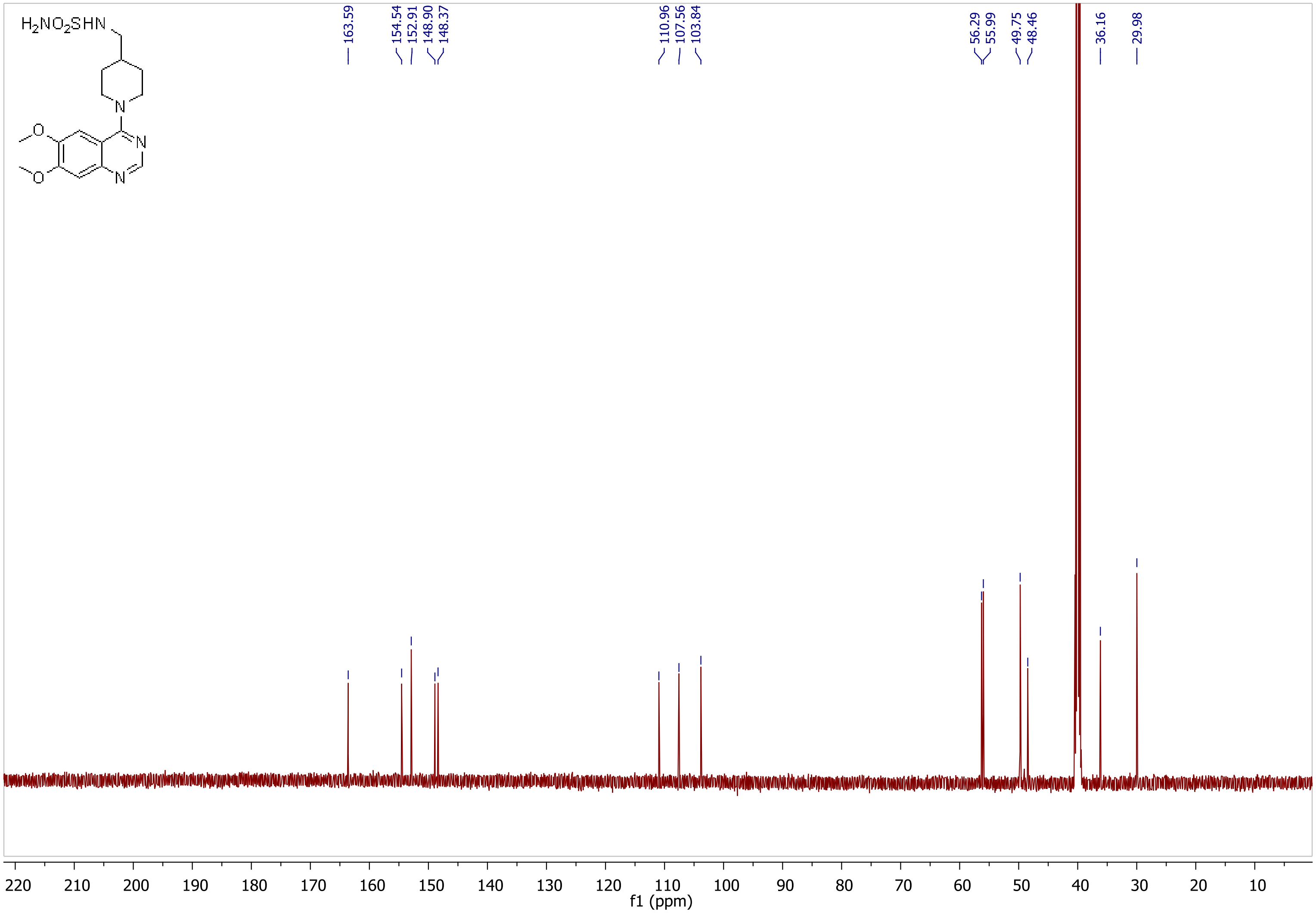

Chapter 3 Conclusions and discussions

Since the first detectable lesion to the final stage of calcific aortic valve disease where it requires surgical interventions, patients often suffer from poor quality of life due to the fact that there are no currently available pharmacological means that can prevent or slow disease progression [10]. In this study, we have shown in *in vitro* experiments that QPS1, in the low micromolar range, is able to prevent phosphate-induced mineralization of VICs by preventing phosphate-induced apoptosis and osteoblastic transition. By a series of enzyme-specific activity assays, we have demonstrated that QPS compounds are a class of potent, specific, and non-competitive inhibitors of human NPP1.

3.1 Potency, specificity, and non-competitivity of QPS 1

The most frequently used NPP1 inhibitor in cellular experiments, ARL67156, is a non-hydrolyzable competitive inhibitor of ectonucleotidases [89]. It inhibits NPP1 with a high potency (Ki 12 ± 3 μM); however, it also significantly inhibits other ectonucleotidases, especially NTPDase1 and NTPDase3. Different classes of ectonucleotidases are widely expressed by many types of cells where they play critical biological roles. Non-specific inhibition to these enzymes may result in a large off-target side-effect that could override the benefit exerted by the drug. For instance, NTPDase1 exerts control over platelet function and inhibition to this enzyme may produce deleterious effect on platelet aggregation [75, 76]. NTPDase3, on the other hand, regulates inflammation. Significant unnecessary inhibition to NTPDase3 may disturb inflammatory response [73, 74]. Other inhibitors of NPP1 like the derivatives of the 1,3,4-oxadiazole-2(3H)-thione have been shown to inhibit NPP1 with less potency (Ki 360 μM) [94].

We confirmed that QPS1 and QPS2 were potent inhibitors of NPP1 with Ki values of 70.2 nM and 187.2 nM, respectively. We also demonstrated that QPS1 was a specific inhibitor of NPP1 where in a series of ectonucleotidase-specific enzyme activity assays QPS1 did not inhibit NPP3, NTPDase1-3, NT5E, and ALP. The enzymatic activity assays also revealed that QPS1 and QPS2 were non-competitive inhibitors in which they do not compete for the binding pocket with the substrate. Non-competitivity is a preferred pharmaco-property for a drug in the case that the effectiveness of a drug is not manipulated by the substrate concentration.

3.2 Implications

To our knowledge, QPS1 is the first description of a compound that is both potent and specific to inhibit NPP1.

The specificity possessed by QPS1 can be used in complex biological systems to discriminate the role of NPP1 where different ectonucleotidases are present. It is worth to note that on any given type of cell surface, there are more than one ectonucleotidase enzymes present. They usually work in concert to regulate the levels of extracellular nucleotides and nucleosides. For instance on the membranes of VICs, there are NPP1, NPP2, NT5E, and ALP present at any given time [63]. Because there is currently no pharmacological mean that is specific to NPP1, it becomes difficult to study the role of NPP1 in biological systems. Concerning this, QPS1 can be used in future studies to elucidate the role of NPP1.

Over expression of NPP1 can promote tissue mineralization in two means and each has been implicated in several mineral-related human disorders. First, it promotes build-up of extracellular Pi which is the major component of hydroxyapatite crystals. By forming and enlarging the hydroxyapatite crystals, NPP1 has been shown to promote pathological mineralization of VICs which leads to calcification of aortic valve [35, 63], and meniscal cells which results in matrix calcification of the knee meniscal cartilage [60, 61]. NPP1 also promoted vascular mineralization of ApoE knockout mice [62]. Second, increased NPP1 can also promote mineralization in the form of calcium pyrophosphate dehydrate (CPPD) crystals which is formed by PPi production. Examples of which are chondrocalcinosis and osteoarthritis [95]. By a still controversial knowledge, overexpressed NPP1 has been shown to induce insulin resistance by interfering with the insulin receptor that impedes insulin signalling. In this case, K121Q gene variant of NPP1 is associated with type 2 diabete [96-99].

In our study, QPS1 was able to prevent mineralization in low nanomolar range by preventing phosphate-induced apoptosis and osteoblastic transitions of VICs. These findings suggest that QPS1 can be used to study the role of NPP1 in different disease models. Therefore, development of such a novel inhibitor of NPP1 that is potent, specific, and non-competitive may help shed light into the treatment of many human diseases.

Chapter 4 limitations and future perspectives

4.1 Impact on purinergic receptors

It is worth to note that ectonucleotidases are present in the cell population along with their corresponding purinergic receptors. Purinergic receptors are sensors of ectonucleotides and nucleosides. There are a total of 19 purinergic receptors with 4 families of ectonucleotidases [26, 52]. The combinations of these receptors and enzymes make up a complex biological system where they exert control over many biological events including cell survival, inflammation, mineralization, cell differentiation. We provided evidence that QPS1 was a potent and selective inhibitor of NPP1 and evaluated its effect on many other members of ectonucleotidase families. However, the effects of QPS1 on subsequent purinergic receptors were not evaluated. It is worth to be investigated in the future studies since the purinergic receptors play important roles in the complex of ectonucleotidase network by transmitting the signal within the cells. In this regard, excessive NPP1 expression and activity depletes extracellular ATP and reduces signalling through P2Y2 receptor that ultimately leads to apoptosis-mediated mineralization in VICs.

4.2 Interaction with hERG channel

The original description of QPS derivatives reported the binding of these derivatives with the human hERG potassium channel [95]. The human ether-a-go-go-related gene (hERG) responsible for the rapid delayed-rectifier K^+-current (I_{Kr}) is the main repolarizing current in ventricular cardiomyocytes of large mammals [100]. Inhibition of hERG causes reloplarization prolongation and it is the major cardiac safety concern in the development, approval and prescription of new drugs. The binding of QPS derivatives to hERG potassium channel is a major concern of using these drugs in *in vivo* experiments as it is reported that QPS1 is a potent ligand of hERG. Hence, further variations of QPS1 are needed to overcome this issue. Also, in the future development of these compounds requires cardiac-safety assays. We suggest that low-cost, high-throughput screens can be used in the early developmental stages. For example, drug-binding studies using radiolabeled I_{Kr}-blocker such as dofetilide can be used. In brief, the radioactive signal will be reduced if the test compound is able to displace the dofetilide that has affinity for the hERG protein. Besides, the fluorescent measurement of thallium flux through hERG channels by automated patch-clamp can also be used to assess the inhibition of hERG channel and it has be recently shown to have a fairly good correlation with hERG inhibition.

4.3 Pharmacokinetics

Although QPS derivatives demonstrated a high potency and specificity in enzyme-specific activity assays and were able to prevent phosphate-induced mineralization in *in vitro* experiments, the *in vivo* potency and specificity of these derivatives were not investigated in the current study and are to be elucidated in the future experiments. However, before conducting animal experiments, it is necessary to assess the pharmacokinetics of these derivatives. For example, the means of administrations, the sites of distributions, the rate of metabolism and excretion are among the most important pharmacokinetic properties of new drugs that are mandatory to be evaluated.

Besides, the off-target effects are necessary to be evaluated as well. Tissue mineralization is essentially important in terms of bone tissue whereas it is deleterious at ectopic sites such as the aortic valve and some cartilage. Blindly inhibiting all NPP1 activity may cause degeneration of bone tissue and lead to cons over pros effects. Therefore, QPS derivatives should be tested on bone mineralization as well.

Lastly, it is worth mentioning that the relationship between the mineralization and the level of NPP1 expression is U-shaped. Specifically, too many or too little NPP1 can both lead to mineralization of the tissue. Therefore, determining an optimal dose of QPS derivatives that prevents mineralization is a major concern when introducing these drugs in *in vivo* experiments.

Chapter 5 References

1. O'Brien, K.D., *Epidemiology and genetics of calcific aortic valve disease.* J Investig Med, 2007. **55**(6): p. 284-91.
2. Rajamannan, N.M., et al., *Calcific aortic valve disease: not simply a degenerative process: A review and agenda for research from the National Heart and Lung and Blood Institute Aortic Stenosis Working Group. Executive summary: Calcific aortic valve disease-2011 update.* Circulation, 2011. **124**(16): p. 1783-91.
3. Thaden, J.J., V.T. Nkomo, and M. Enriquez-Sarano, *The global burden of aortic stenosis.* Prog Cardiovasc Dis, 2014. **56**(6): p. 565-71.
4. Yutzey, K.E., et al., *Calcific aortic valve disease: a consensus summary from the Alliance of Investigators on Calcific Aortic Valve Disease.* Arterioscler Thromb Vasc Biol, 2014. **34**(11): p. 2387-93.
5. Freeman, R.V. and C.M. Otto, *Spectrum of calcific aortic valve disease: pathogenesis, disease progression, and treatment strategies.* Circulation, 2005. **111**(24): p. 3316-26.
6. Cosmi, J.E., et al., *The risk of the development of aortic stenosis in patients with "benign" aortic valve thickening.* Arch Intern Med, 2002. **162**(20): p. 2345-7.
7. Stewart, B.F., et al., *Clinical factors associated with calcific aortic valve disease. Cardiovascular Health Study.* J Am Coll Cardiol, 1997. **29**(3): p. 630-4.
8. Bosse, Y., P. Mathieu, and P. Pibarot, *Genomics: the next step to elucidate the etiology of calcific aortic valve stenosis.* J Am Coll Cardiol, 2008. **51**(14): p. 1327-36.
9. Thanassoulis, G., et al., *Genetic associations with valvular calcification and aortic stenosis.* N Engl J Med, 2013. **368**(6): p. 503-12.
10. Hutcheson, J.D., E. Aikawa, and W.D. Merryman, *Potential drug targets for calcific aortic valve disease.* Nat Rev Cardiol, 2014. **11**(4): p. 218-31.
11. Yip, C.Y. and C.A. Simmons, *The aortic valve microenvironment and its role in calcific aortic valve disease.* Cardiovasc Pathol, 2011. **20**(3): p. 177-82.
12. El-Hamamsy, I., et al., *Endothelium-dependent regulation of the mechanical properties of aortic valve cusps.* J Am Coll Cardiol, 2009. **53**(16): p. 1448-55.
13. Simmons, C.A., *Aortic valve mechanics: an emerging role for the endothelium.* J Am Coll Cardiol, 2009. **53**(16): p. 1456-8.
14. Balachandran, K., et al., *Cyclic strain induces dual-mode endothelial-mesenchymal transformation of the cardiac valve.* Proc Natl Acad Sci U S A, 2011. **108**(50): p. 19943-8.
15. Bischoff, J. and E. Aikawa, *Progenitor cells confer plasticity to cardiac valve endothelium.* J Cardiovasc Transl Res, 2011. **4**(6): p. 710-9.
16. Olsson, M., J. Thyberg, and J. Nilsson, *Presence of oxidized low density lipoprotein in nonrheumatic stenotic aortic valves.* Arterioscler Thromb Vasc Biol, 1999. **19**(5): p. 1218-22.
17. Aronow, W.S., et al., *Association of coronary risk factors and use of statins with progression of mild valvular aortic stenosis in older persons.* Am J Cardiol, 2001. **88**(6): p. 693-5.

18. Moura, L.M., et al., *Rosuvastatin affecting aortic valve endothelium to slow the progression of aortic stenosis.* J Am Coll Cardiol, 2007. **49**(5): p. 554-61.
19. Novaro, G.M., et al., *Effect of hydroxymethylglutaryl coenzyme a reductase inhibitors on the progression of calcific aortic stenosis.* Circulation, 2001. **104**(18): p. 2205-9.
20. Bellamy, M.F., et al., *Association of cholesterol levels, hydroxymethylglutaryl coenzyme-A reductase inhibitor treatment, and progression of aortic stenosis in the community.* J Am Coll Cardiol, 2002. **40**(10): p. 1723-30.
21. Cowell, S.J., et al., *A randomized trial of intensive lipid-lowering therapy in calcific aortic stenosis.* N Engl J Med, 2005. **352**(23): p. 2389-97.
22. Rossebo, A.B., et al., *Intensive lipid lowering with simvastatin and ezetimibe in aortic stenosis.* N Engl J Med, 2008. **359**(13): p. 1343-56.
23. Chan, K.L., et al., *Effect of Lipid lowering with rosuvastatin on progression of aortic stenosis: results of the aortic stenosis progression observation: measuring effects of rosuvastatin (ASTRONOMER) trial.* Circulation, 2010. **121**(2): p. 306-14.
24. Gerdts, E., et al., *Impact of baseline severity of aortic valve stenosis on effect of intensive lipid lowering therapy (from the SEAS study).* Am J Cardiol, 2010. **106**(11): p. 1634-9.
25. Mathieu, P. and M.C. Boulanger, *Basic mechanisms of calcific aortic valve disease.* Can J Cardiol, 2014. **30**(9): p. 982-93.
26. Mathieu, P., M.C. Boulanger, and R. Bouchareb, *Molecular biology of calcific aortic valve disease: towards new pharmacological therapies.* Expert Rev Cardiovasc Ther, 2014. **12**(7): p. 851-62.
27. Capoulade, R., et al., *Impact of metabolic syndrome on progression of aortic stenosis: influence of age and statin therapy.* J Am Coll Cardiol, 2012. **60**(3): p. 216-23.
28. Mohty, D., et al., *Association between plasma LDL particle size, valvular accumulation of oxidized LDL, and inflammation in patients with aortic stenosis.* Arterioscler Thromb Vasc Biol, 2008. **28**(1): p. 187-93.
29. Mahmut, A., et al., *Elevated expression of lipoprotein-associated phospholipase A2 in calcific aortic valve disease: implications for valve mineralization.* J Am Coll Cardiol, 2014. **63**(5): p. 460-9.
30. O'Brien, K.D., et al., *Apolipoproteins B, (a), and E accumulate in the morphologically early lesion of 'degenerative' valvular aortic stenosis.* Arterioscler Thromb Vasc Biol, 1996. **16**(4): p. 523-32.
31. Otto, C.M., et al., *Characterization of the early lesion of 'degenerative' valvular aortic stenosis. Histological and immunohistochemical studies.* Circulation, 1994. **90**(2): p. 844-53.
32. Bosse, Y., et al., *Refining molecular pathways leading to calcific aortic valve stenosis by studying gene expression profile of normal and calcified stenotic human aortic valves.* Circ Cardiovasc Genet, 2009. **2**(5): p. 489-98.
33. Jamaluddin, M., et al., *TNF-alpha-induced NF-kappaB/RelA Ser(276) phosphorylation and enhanceosome formation is mediated by an ROS-dependent PKAc pathway.* Cell Signal, 2007. **19**(7): p. 1419-33.

34. Branchetti, E., et al., *Antioxidant enzymes reduce DNA damage and early activation of valvular interstitial cells in aortic valve sclerosis.* Arterioscler Thromb Vasc Biol, 2013. **33**(2): p. e66-74.
35. El Husseini, D., et al., *High expression of the Pi-transporter SLC20A1/Pit1 in calcific aortic valve disease promotes mineralization through regulation of Akt-1.* PLoS One, 2013. **8**(1): p. e53393.
36. El Husseini, D., et al., *P2Y2 receptor represses IL-6 expression by valve interstitial cells through Akt: implication for calcific aortic valve disease.* J Mol Cell Cardiol, 2014. **72**: p. 146-56.
37. Yu, Z., et al., *Tumor necrosis factor-alpha accelerates the calcification of human aortic valve interstitial cells obtained from patients with calcific aortic valve stenosis via the BMP2-Dlx5 pathway.* J Pharmacol Exp Ther, 2011. **337**(1): p. 16-23.
38. Kaden, J.J., et al., *Tumor necrosis factor alpha promotes an osteoblast-like phenotype in human aortic valve myofibroblasts: a potential regulatory mechanism of valvular calcification.* Int J Mol Med, 2005. **16**(5): p. 869-72.
39. Mohler, E.R., 3rd, et al., *Bone formation and inflammation in cardiac valves.* Circulation, 2001. **103**(11): p. 1522-8.
40. Rajamannan, N.M., et al., *Human aortic valve calcification is associated with an osteoblast phenotype.* Circulation, 2003. **107**(17): p. 2181-4.
41. O'Brien, K.D., et al., *Osteopontin is expressed in human aortic valvular lesions.* Circulation, 1995. **92**(8): p. 2163-8.
42. O'Brien, K.D., *Pathogenesis of calcific aortic valve disease: a disease process comes of age (and a good deal more).* Arterioscler Thromb Vasc Biol, 2006. **26**(8): p. 1721-8.
43. Kaden, J.J., et al., *Expression of bone sialoprotein and bone morphogenetic protein-2 in calcific aortic stenosis.* J Heart Valve Dis, 2004. **13**(4): p. 560-6.
44. Rajamannan, N.M., et al., *Atorvastatin inhibits hypercholesterolemia-induced calcification in the aortic valves via the Lrp5 receptor pathway.* Circulation, 2005. **112**(9 Suppl): p. I229-34.
45. Guruharsha, K.G., M.W. Kankel, and S. Artavanis-Tsakonas, *The Notch signalling system: recent insights into the complexity of a conserved pathway.* Nat Rev Genet, 2012. **13**(9): p. 654-66.
46. Linefsky, J.P., et al., *Association of serum phosphate levels with aortic valve sclerosis and annular calcification: the cardiovascular health study.* J Am Coll Cardiol, 2011. **58**(3): p. 291-7.
47. Martola, L., P. Barany, and P. Stenvinkel, *Why do dialysis patients develop a heart of stone and bone of china?* Blood Purif, 2005. **23**(3): p. 203-10.
48. Ketteler, M., et al., *Association of low fetuin-A (AHSG) concentrations in serum with cardiovascular mortality in patients on dialysis: a cross-sectional study.* Lancet, 2003. **361**(9360): p. 827-33.
49. Doyon, M., P. Mathieu, and P. Moreau, *Decreased expression of gamma-carboxylase in diabetes-associated arterial stiffness: impact on matrix Gla protein.* Cardiovasc Res, 2013. **97**(2): p. 331-8.
50. Capoulade, R., et al., *Circulating levels of matrix gla protein and progression of aortic stenosis: a substudy of the Aortic Stenosis Progression Observation:*

Measuring Effects of rosuvastatin (ASTRONOMER) trial. Can J Cardiol, 2014. **30**(9): p. 1088-95.

51. Goding, J.W., *Ecto-enzymes: physiology meets pathology.* J Leukoc Biol, 2000. **67**(3): p. 285-311.
52. Mathieu, P., *Pharmacology of ectonucleotidases: relevance for the treatment of cardiovascular disorders.* Eur J Pharmacol, 2012. **696**(1-3): p. 1-4.
53. Stefan, C., S. Jansen, and M. Bollen, *NPP-type ectophosphodiesterases: unity in diversity.* Trends Biochem Sci, 2005. **30**(10): p. 542-50.
54. Okawa, A., et al., *Mutation in Npps in a mouse model of ossification of the posterior longitudinal ligament of the spine.* Nat Genet, 1998. **19**(3): p. 271-3.
55. Johnson, K., et al., *Matrix vesicle plasma cell membrane glycoprotein-1 regulates mineralization by murine osteoblastic MC3T3 cells.* J Bone Miner Res, 1999. **14**(6): p. 883-92.
56. Koshizuka, Y., et al., *Nucleotide pyrophosphatase gene polymorphism associated with ossification of the posterior longitudinal ligament of the spine.* J Bone Miner Res, 2002. **17**(1): p. 138-44.
57. Rutsch, F., et al., *Mutations in ENPP1 are associated with 'idiopathic' infantile arterial calcification.* Nat Genet, 2003. **34**(4): p. 379-81.
58. Lorenz-Depiereux, B., et al., *Loss-of-function ENPP1 mutations cause both generalized arterial calcification of infancy and autosomal-recessive hypophosphatemic rickets.* Am J Hum Genet, 2010. **86**(2): p. 267-72.
59. Nitschke, Y., et al., *Generalized arterial calcification of infancy and pseudoxanthoma elasticum can be caused by mutations in either ENPP1 or ABCC6.* Am J Hum Genet, 2012. **90**(1): p. 25-39.
60. Johnson, K., et al., *Up-regulated expression of the phosphodiesterase nucleotide pyrophosphatase family member PC-1 is a marker and pathogenic factor for knee meniscal cartilage matrix calcification.* Arthritis Rheum, 2001. **44**(5): p. 1071-81.
61. Johnson, K., et al., *The nucleoside triphosphate pyrophosphohydrolase isozyme PC-1 directly promotes cartilage calcification through chondrocyte apoptosis and increased calcium precipitation by mineralizing vesicles.* J Rheumatol, 2001. **28**(12): p. 2681-91.
62. Nitschke, Y., et al., *Npp1 promotes atherosclerosis in ApoE knockout mice.* J Cell Mol Med, 2011. **15**(11): p. 2273-83.
63. Cote, N., et al., *ATP acts as a survival signal and prevents the mineralization of aortic valve.* J Mol Cell Cardiol, 2012. **52**(5): p. 1191-202.
64. Mahmut, A., et al., *Adenosine derived from ecto-nucleotidases in calcific aortic valve disease promotes mineralization through A2a adenosine receptor.* Cardiovasc Res, 2015.
65. Leblanc, R. and O. Peyruchaud, *New insights into the autotaxin/LPA axis in cancer development and metastasis.* Exp Cell Res, 2014.
66. van Meeteren, L.A. and W.H. Moolenaar, *Regulation and biological activities of the autotaxin-LPA axis.* Prog Lipid Res, 2007. **46**(2): p. 145-60.
67. Tania, M., et al., *Autotaxin: a protein with two faces.* Biochem Biophys Res Commun, 2010. **401**(4): p. 493-7.
68. Ikeda, H. and Y. Yatomi, *Autotaxin in liver fibrosis.* Clin Chim Acta, 2012. **413**(23-24): p. 1817-21.

69. Moolenaar, W.H., et al., *Autotaxin in embryonic development.* Biochim Biophys Acta, 2013. **1831**(1): p. 13-9.
70. Bouchareb, R., et al., *Autotaxin Derived From Lipoprotein(a) and Valve Interstitial Cells Promotes Inflammation and Mineralization of the Aortic Valve.* Circulation, 2015. **132**(8): p. 677-90.
71. Buhring, H.J., A. Streble, and P. Valent, *The basophil-specific ectoenzyme E-NPP3 (CD203c) as a marker for cell activation and allergy diagnosis.* Int Arch Allergy Immunol, 2004. **133**(4): p. 317-29.
72. Erdmann, S.M., et al., *Regarding Ebo DG, Hagendorens MM, Bridts CH, Schuerwegh AJ, De Clerck LS & Stevens WJ. In vitro allergy diagnosis: should we follow the flow? Clin Exp Allergy 2004; 34:332-9.* Clin Exp Allergy, 2004. **34**(9): p. 1498-9; author reply 1499-500.
73. Robson, S.C., J. Sevigny, and H. Zimmermann, *The E-NTPDase family of ectonucleotidases: Structure function relationships and pathophysiological significance.* Purinergic Signal, 2006. **2**(2): p. 409-30.
74. Kukulski, F., et al., *Comparative hydrolysis of P2 receptor agonists by NTPDases 1, 2, 3 and 8.* Purinergic Signal, 2005. **1**(2): p. 193-204.
75. Kauffenstein, G., et al., *NTPDase1 (CD39) controls nucleotide-dependent vasoconstriction in mouse.* Cardiovasc Res, 2010. **85**(1): p. 204-13.
76. Sevigny, J., et al., *Differential catalytic properties and vascular topography of murine nucleoside triphosphate diphosphohydrolase 1 (NTPDase1) and NTPDase2 have implications for thromboregulation.* Blood, 2002. **99**(8): p. 2801-9.
77. Yegutkin, G.G., *Nucleotide- and nucleoside-converting ectoenzymes: Important modulators of purinergic signalling cascade.* Biochim Biophys Acta, 2008. **1783**(5): p. 673-94.
78. Hunsucker, S.A., B.S. Mitchell, and J. Spychala, *The 5'-nucleotidases as regulators of nucleotide and drug metabolism.* Pharmacol Ther, 2005. **107**(1): p. 1-30.
79. Mahmut, A., et al., *Adenosine derived from ecto-nucleotidases in calcific aortic valve disease promotes mineralization through A2a adenosine receptor.* Cardiovasc Res, 2015. **106**(1): p. 109-20.
80. Hessle, L., et al., *Tissue-nonspecific alkaline phosphatase and plasma cell membrane glycoprotein-1 are central antagonistic regulators of bone mineralization.* Proc Natl Acad Sci U S A, 2002. **99**(14): p. 9445-9.
81. Mathieu, P., et al., *Calcification of human valve interstitial cells is dependent on alkaline phosphatase activity.* J Heart Valve Dis, 2005. **14**(3): p. 353-7.
82. Ma, H.W., *[Rickets-like genetic diseases].* Zhongguo Dang Dai Er Ke Za Zhi, 2013. **15**(11): p. 923-7.
83. Alonso, G., M. Varsavsky, and M. Munoz-Torres, *[Hypophosphatasia: new therapeutic approaches].* Med Clin (Barc), 2009. **132**(3): p. 108-11.
84. Waymire, K.G., et al., *Mice lacking tissue non-specific alkaline phosphatase die from seizures due to defective metabolism of vitamin B-6.* Nat Genet, 1995. **11**(1): p. 45-51.
85. Narisawa, S., N. Frohlander, and J.L. Millan, *Inactivation of two mouse alkaline phosphatase genes and establishment of a model of infantile hypophosphatasia.* Dev Dyn, 1997. **208**(3): p. 432-46.

86. Beck, G.R., Jr., *Inorganic phosphate as a signaling molecule in osteoblast differentiation.* J Cell Biochem, 2003. **90**(2): p. 234-43.
87. Cote, N., et al., *Inhibition of ectonucleotidase with ARL67156 prevents the development of calcific aortic valve disease in warfarin-treated rats.* Eur J Pharmacol, 2012. **689**(1-3): p. 139-46.
88. Crack, B.E., et al., *Pharmacological and biochemical analysis of FPL 67156, a novel, selective inhibitor of ecto-ATPase.* Br J Pharmacol, 1995. **114**(2): p. 475-81.
89. Levesque, S.A., et al., *Specificity of the ecto-ATPase inhibitor ARL 67156 on human and mouse ectonucleotidases.* Br J Pharmacol, 2007. **152**(1): p. 141-50.
90. Ramaprasad, G.C., et al., *Synthesis and biological property of some novel 1,3,4-oxadiazoles.* Eur J Med Chem, 2010. **45**(10): p. 4587-93.
91. Khanum, S.A., et al., *Synthesis and antimicrobial study of novel heterocyclic compounds from hydroxybenzophenones.* Eur J Med Chem, 2005. **40**(11): p. 1156-62.
92. Kalsi, R., et al., *Anti-inflammatory and analgesic activities of 5-(4-[aryl(aryl azo)methyleneamino]phenyl)-1,3,4-oxadiazole-2(3H)-thiones.* Pharmacology, 1989. **39**(2): p. 103-8.
93. Loetchutinat, C., F. Chau, and S. Mankhetkorn, *Synthesis and evaluation of 5-Aryl-3-(4-hydroxyphenyl)-1,3,4-oxadiazole-2-(3H)-thiones as P-glycoprotein inhibitors.* Chem Pharm Bull (Tokyo), 2003. **51**(6): p. 728-30.
94. Khan, K.M., et al., *1,3,4-Oxadiazole-2(3H)-thione and its analogues: a new class of non-competitive nucleotide pyrophosphatases/phosphodiesterases 1 inhibitors.* Bioorg Med Chem, 2009. **17**(22): p. 7816-22.
95. Patel, S.D., et al., *Quinazolin-4-piperidin-4-methyl sulfamide PC-1 inhibitors: alleviating hERG interactions through structure based design.* Bioorg Med Chem Lett, 2009. **19**(12): p. 3339-43.
96. Bacci, S., et al., *Joint effect of insulin signaling genes on cardiovascular events and on whole body and endothelial insulin resistance.* Atherosclerosis, 2013. **226**(1): p. 140-5.
97. Kang, J.Y., et al., *Impact of ENPP1 K121Q on change of insulin resistance after web-based intervention in Korean men with diabetes and impaired fasting glucose.* J Korean Med Sci, 2014. **29**(10): p. 1353-9.
98. Pan, W., M. Chandalia, and N. Abate, *New Insights into the Role of ENPP1 in Insulin Resistance.* J Metabonomics Metab, 2012. **1**(1).
99. Prakash, J., et al., *K121Q ENPP1/PC-1 gene polymorphism is associated with insulin resistance in a North Indian population.* J Genet, 2013. **92**(3): p. 571-6.
100. Heijman, J., et al., *Cardiac safety assays.* Curr Opin Pharmacol, 2014. **15**: p. 16-21.

Appendix Enzyme Inhibitor Kinetics

Types of inhibitors

As in general, there are two categories of enzyme inhibitors based on whether it modifies enzyme activity permanently or non-permanently. Irreversible inhibitors covalently bound to the targeting enzyme and modify enzyme structure permanently so that the enzyme activity is permanently reduced. In contrast, reversible inhibitors bind to enzymes non-covalently and removing the inhibitors from the system restores enzyme activity. This type of inhibitors reaches equilibrium as shown:

$$EI \leftrightarrow E + S + I \leftrightarrow ES$$

Reversible inhibitors are then subcategorized into three types: competitive, non-competitive, and uncompetitive.

1) Competitive inhibitor

In competitive inhibition, the inhibitor and the substrate bind the enzyme mutually exclusively. In another word, the competitive inhibitor binds only to the free enzyme and competes with substrate for the binding to the active site of the enzyme. If V_{max} (maximum velocity) is the rate of reaction under the condition where there are enough substrates to completely saturate the active sites of the enzymes, there will be a requirement for a higher concentration of substrate to reach V_{max} when competitive inhibitors are added in the system. Therefore, Km, the substrate concentration required to reach 1/2 V_{max}, is higher.

2) Non-competitive inhibitor

Non-competitive inhibitors bind to a site of an enzyme that is different from its active site. Therefore, it can bind to both free enzyme and enzyme-substrate complex with equal affinity. As the name applies, this type of inhibitors does not compete with substrates for binding to the enzyme. In this case, increasing substrate concentration does not reduce the inhibition. Therefore, Km is unchanged while V_{max} is reduced.

3) Uncompetitive inhibitor

Uncompetitive inhibitor is a rare class of inhibitors that the binding of the inhibitor to an enzyme results in enhanced enzyme affinity to its substrate. However, the enzyme-inhibitor-substrate complex now has a reduced activity. Therefore, kinetically, both the Km and V_{max} are reduced.

Dixon plot

In this current study, we have determined the mode of inhibition and the potency of QPS derivatives by plotting 1/V (y-axis) against concentration of inhibitor at each concentration of substrate (x-axis), the Dixon plot. Ki is the concentration of inhibitor required to half the maximum inhibition. In the case of competitive inhibitor, the lines intersect above the x-axis and the x-axis value ([inhibitor]) of intersected point is the Ki, which is an indicative of the potency of an inhibitor. The smaller the Ki value, the more potent the inhibitor is. The non-competitive inhibition gives a graph where the lines intersect on the x-axis.

A. Competitive

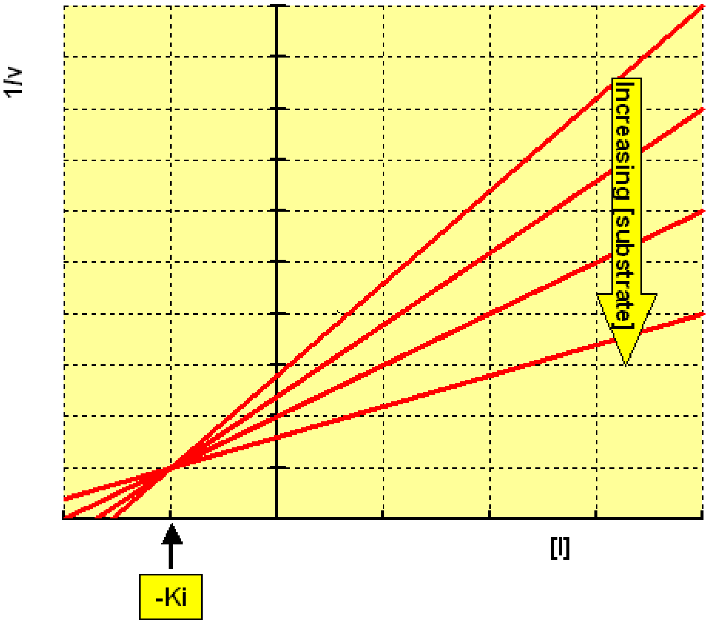

B. Non-competitive

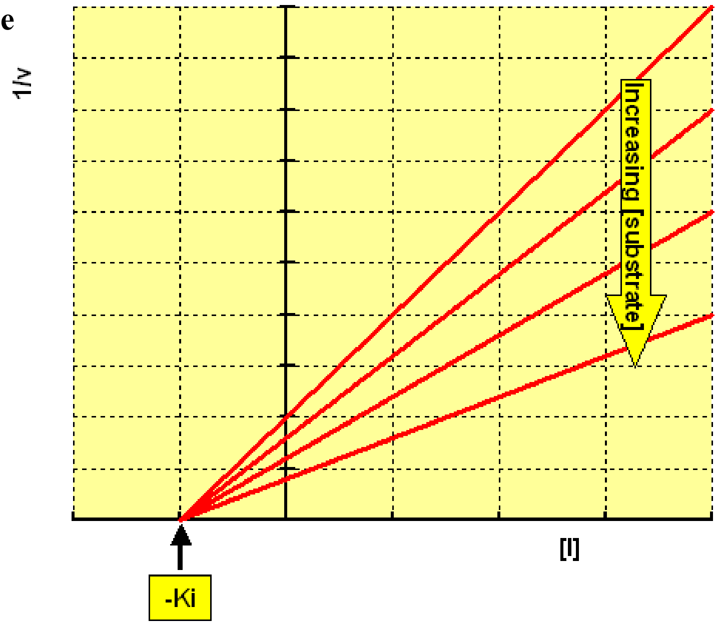

Figure 1. A) Dixon plot for competitive inhibition. B) Dixon plot for non-competitive inhibition. Source: http://www.ucl.ac.uk/~ucbcdab/enzass/inhibition.htm#nci.